

*Superoxide dismutase 1 is a multifunctional protein that can act as  
transcriptional regulator in Arabidopsis*

Dissertation

zur Erlangung des

Doktorgrades der Naturwissenschaften (Dr. rer. nat.)

der

Naturwissenschaftlichen Fakultät I

- Biowissenschaften -

der Martin-Luther-Universität Halle-Wittenberg

vorgelegt

von Herrn **Bernd Heinrich Dreyer**

geboren am 22.06.1994 in Haren (Ems)

Gutachter:

1. Prof. Dr. Thomas Altmann
2. Prof. Dr. Klaus Humbeck
3. Prof. Dr. Joost T. van Dongen

Arbeit eingereicht am: 18.07.2022

Datum der öffentlichen Verteidigung: 01.06.2023

# I. TABLE OF CONTENTS

<b>I.</b>	<b>TABLE OF CONTENTS</b> .....	<b>1</b>
<b>II.</b>	<b>LIST OF FIGURES</b> .....	<b>4</b>
<b>III.</b>	<b>LIST OF TABLES</b> .....	<b>6</b>
<b>IV.</b>	<b>ACKNOWLEDGEMENTS</b> .....	<b>7</b>
<b>V.</b>	<b>PREFACE</b> .....	<b>8</b>
<b>VI.</b>	<b>ABBREVIATIONS</b> .....	<b>9</b>
<b>1</b>	<b>INTRODUCTION</b> .....	<b>11</b>
1.1	Superoxide dismutases (SODs) and ROS.....	11
1.2	Distinct SOD isoforms and subcellular distribution in plants .....	12
1.3	Regulation and role of CSDs during plant stress response.....	13
1.4	SODs might control ROS gradients during plant development .....	17
1.5	SOD1/CSD1 – More than just an Enzyme? .....	18
1.6	Heavy-metal associated isoprenylated plant proteins (HIPPI) .....	21
1.7	N-terminal acetylation .....	22
1.8	Moonlighting .....	24
1.9	Scope of this thesis .....	25
<b>2</b>	<b>MATERIAL AND METHODS</b> .....	<b>27</b>
2.1	Arabidopsis lines .....	27
2.2	Bacterial and yeast strains .....	27
2.3	Plant growth conditions .....	28
2.3.1	<i>Arabidopsis thaliana</i> cultivation on soil.....	28
2.3.2	<i>In-vitro</i> cultivation of <i>Arabidopsis thaliana</i> .....	28
2.4	Transfection of Arabidopsis mesophyll protoplasts .....	28
2.5	Transfection of <i>Oryza sativa</i> stem cell protoplasts.....	29
2.6	Nuclear localisation .....	29
2.7	Fluorescence recovery after photobleaching (FRAP) .....	29
2.8	Nuclear enrichment of the CSD1 protein .....	30
2.9	Salt tolerance experiment .....	30
2.10	Transcriptional profiling by RNA-seq.....	31
2.11	Transcriptional profiling by RT-qPCR.....	32
2.12	SELEX.....	33

---

2.13	DAP-seq .....	34
2.14	ChIP-seq .....	34
2.15	EMSA .....	35
2.16	Hydrogen peroxide treatment of CSD1 .....	37
2.17	SOD activity assay .....	37
2.18	Transactivation assay.....	37
2.19	Gal4-based transactivation assay.....	38
2.20	Bimolecular fluorescence complementation (BiFC).....	38
2.21	Yeast Two-hybrid (Y2H) .....	39
2.22	Extraction of total soluble protein extracts.....	39
2.23	SDS-PAGE and Western blot.....	40
2.24	Immunoprecipitation .....	40
2.25	Mass spectrometry analysis.....	41
2.26	Statistical analysis .....	42
<b>3</b>	<b>RESULTS.....</b>	<b>43</b>
3.1	Chapter 1: CSD1 translocates to the nucleus upon salt stress and regulates the expression of salt-responsive genes.....	43
3.1.1	CSD1 translocates to the nucleus upon salt stress.....	43
3.1.2	CSD1 is required for the salt stress response in Arabidopsis.....	46
3.1.3	Transgenic <i>35S:FLAG-CSD1</i> plants indicate role of CSD1 in developmental processes.....	48
3.1.4	CSD1 affects the early transcriptional salt stress response in Arabidopsis.....	50
3.1.5	CSD1 binds DNA in a sequence-specific manner.....	54
3.1.6	CSD1 binds to the promoter of salt-stress responsive genes.....	57
3.1.7	CSD1 regulates the transcriptional activity of salt-stress responsive genes.....	61
3.1.8	Summary.....	64
3.2	Chapter 2: CSD1-interacting protein HIPP20 is member of a novel class of transcriptional activators .....	65
3.2.1	HIPP20 and homologs are nuclear localised proteins in Arabidopsis.....	66
3.2.2	HIPP20 protein levels do not impact vegetative growth of Arabidopsis .....	68
3.2.3	Nuclear interaction between CSD1 and HIPP20 in Arabidopsis and <i>Oryza sativa</i> .....	69
3.2.4	HIPP proteins are a novel class of transcriptional activators .....	71
3.2.5	Summary.....	73

3.3	Chapter 3: Co-IP reveals novel PTM of CSD1 and temporal and stress-dependent interactome of CSD1 and CSD2.....	74
3.3.1	The CSD1 protein receives an NTA in Arabidopsis .....	75
3.3.2	<i>In-silico</i> analysis suggests N-terminal acetylation of several SOD proteins.....	77
3.3.3	Co-IP of CSD1 and CSD2 from total protein extracts of Arabidopsis identified a plethora of interactors.....	79
3.3.4	Complex formation of CSD1 and CSD2 depends on the timing rather than the stress	84
3.3.5	The complex formation of CSD1 and CSD2 is time- and stress-specific .....	87
3.3.6	Summary.....	91
<b>4</b>	<b>DISCUSSION.....</b>	<b>92</b>
4.1	Chapter 1: CSD1 acts as a transcriptional regulator in the early salt stress response ..	92
4.2	Chapter 2: CSD1-interacting protein HIP20 belongs to a novel class of transcriptional co-activators .....	98
4.3	Chapter 3: Co-IP reveals novel PTM of CSD1 and temporal and stress-dependent interactome of CSD1 and CSD2.....	101
<b>5</b>	<b>SUMMARY .....</b>	<b>106</b>
<b>6</b>	<b>ZUSAMMENFASSUNG.....</b>	<b>108</b>
<b>7</b>	<b>REFERENCES .....</b>	<b>110</b>
<b>8</b>	<b>CURRICULUM VITAE .....</b>	<b>135</b>
<b>9</b>	<b>EIDESTATTLICHE ERKLÄRUNG/ DECLARATION UNDER OATH .....</b>	<b>136</b>
<b>10</b>	<b>APPENDIX .....</b>	<b>137</b>
10.1	Supplemental figures for Chapter 1 .....	137
10.2	Supplemental figures for Chapter 2.....	143
10.3	Supplementary data .....	145

## II. LIST OF FIGURES

Figure 1: Localization of CSD1 in Arabidopsis and <i>Oryza sativa</i> protoplasts. ....	44
Figure 2: CSD1 translocate to the nucleus upon salt stress. ....	45
Figure 3: CSD1 is required for salt stress tolerance in Arabidopsis. ....	47
Figure 4: Overexpression of FLAG-CSD1 in Arabidopsis results in severe knock-down phenotype. ....	49
Figure 5: Differential expressed genes (DEGs) in Col-0, <i>csd1-3</i> and <i>OxCS1</i> Arabidopsis seedlings after 30 minutes of 150 mM NaCl treatment determined by RNA-seq analysis. ....	51
Figure 6: Expression of ten salt-stress related genes after 30 minutes of 150 mM NaCl treatment in Arabidopsis seedlings. ....	52
Figure 7: CSD1 associates with specific genomic regions in Arabidopsis <i>in-vivo</i> . ....	56
Figure 8: CSD1 associates with the promoter of <i>SPL2</i> . ....	57
Figure 9: CSD1 binds specific sequences in the <i>NCED3</i> and <i>ZAT7</i> promoter. ....	59
Figure 10: Dilution series and H <sub>2</sub> O <sub>2</sub> treatment of CSD1 affects the binding to the <i>ZAT7</i> promoter. ....	60
Figure 11: EMSA confirms the binding of CSD1 to DNA-sequences in the promoter of <i>HSFA6B</i> , <i>TAT3</i> and <i>RNS1</i> . ....	61
Figure 12: CSD1 activates the transcription of the <i>NCED3</i> promoter. ....	62
Figure 13: CSD1 activates the transcription of the <i>HSFA6B</i> and <i>TAT3</i> promoter. ....	63
Figure 14: Predicted interaction partners of CSD1. ....	65
Figure 15: Nuclear localization of HIPP20, HIPP21 and HIPP22 in Arabidopsis. ....	67
Figure 16: Growth phenotype of <i>hipp20-1</i> and <i>35S:HIPP20-GFP</i> Arabidopsis plants. ....	68
Figure 17: CSD1 interacts with HIPP20 and its homologs. ....	70
Figure 18: HIPP proteins are transcriptional activators. ....	72
Figure 19: Reported interaction partners of CSD1/SOD1 proteins. ....	75
Figure 20: CSD1 receives an N-terminal acetylation <i>in-vivo</i> . ....	76
Figure 21: <i>In-silico</i> analysis suggests that most SOD proteins undergo N-terminal acetylation. .....	78
Figure 22: CSD1 and CSD2 pulldown from total protein extracts of Arabidopsis. ....	79
Figure 23: Identification of a plethora of CSD1/CSD2 interaction partners. ....	81
Figure 24: CSD interactome showed dynamics. ....	83

---

Figure 25: Ribosomal proteins are the largest fraction of identified interactions partners.....	84
Figure 26: CSD complex formation depends on the stress condition and the timepoint. ....	85
Figure 27: CSD1 and CSD2 interaction partners show stress and timepoint specific enrichment dynamics.....	88
Figure 28: Complex formation with ribosomal proteins is partially time- and stress-specific.	90
Figure 29: Growth phenotype of transgenic CSD1 plants grown under short day conditions. .....	137
Figure 30: T-DNA insertion in genomic locus of AT1G08830 - CSD1.....	138
Figure 31: Overview of the systematic evolution of ligands by exponential enrichment (SELEX) experiment. ....	139
Figure 32: DNA-affinity purification sequencing (DAP-seq) and ChIP-qPCR confirmation experiment. ....	140
Figure 33: ChIP-seq analysis of untreated and treated (30 minutes, 150 mM NaCl) samples. .....	141
Figure 34: CSD1 binds to a sequence in the <i>CIF1</i> and <i>MDAR4</i> promoter. ....	142
Figure 35: Subcellular localization and NLS of HIPP20, HIPP21 and HIPP22. ....	143
Figure 36: Phylogenetic tree of the HIPP protein family in Arabidopsis (A) and <i>Oryza sativa</i> (B).....	144

### III. LIST OF TABLES

Table 1: Used abbreviations in this thesis.....	9
Table 2: List of primers used for the gene expression analysis. ....	32
Table 3: EMSA probes used in this study.....	36
Table 4: Primers used in this study to amplify promoter sequences for the transactivation assays. .....	38
Table 5: The 32 hits identified in all conditions (untreated and treated) are shown. ....	82
Table 6: The 27 hits overlapping at the 5-minute timepoint between the H <sub>2</sub> O <sub>2</sub> , MV and NaCl treatment are shown.....	86
Table 7: The 41 hits overlapping at the 30-minute timepoint between the H <sub>2</sub> O <sub>2</sub> , MV and NaCl treatment are shown.....	87

## IV. ACKNOWLEDGEMENTS

First, I thank Prof. Dr. Thomas Altmann, Prof. Dr. Klaus Humbeck for being my first and second referee and their scientific support. Furthermore, I thank Prof. Dr. Joost van Dongen for being my third referee and his supervision, guidance, and support in the early stage of the project.

I would like to express my deepest gratefulness to my long-lasting supervisor, Dr. Jos Schippers, who developed me to be a scientist. Through all the good and tough times, I always knew that the project will be a success because of our constant teamwork and your consistent confidence. I perceive our long work relationship also as a friendship.

Furthermore, I would like to thank the whole seed development group of the IPK. The atmosphere and support within our group made every workday enjoyable. Especially, the PhD evenings with good food or the coffee breaks helped to sustain a good mood during experimentally challenging times.

Also, I would like to thank the collaborations partners that helped to develop the project scientifically: Prof. Dr. Iris Finkemeier and Dr. Jürgen Eirich (WWU Münster), Prof. Dr. Joseph Ecker and Dr. Carol Huang and Dr. Anna Bartlett (Salk Institute, USA), Prof. Dr. Udo Conrad and Isolde Tillack (IPK Gatersleben).

Finally, I thank my parents, Elisabeth und Heiner, and my girlfriend, Geeisy, for always loving me and supporting me, being my constant pillar of strength and their unconditional support throughout my life.



## V. PREFACE

Prior to this thesis, a review article about CuZnSODs in plants was published in the Annual Plant Reviews Online 2019:

**Dreyer, B.H. and Schippers, J.H.M.** (2019). Copper-Zinc Superoxide Dismutases in Plants: Evolution, Enzymatic Properties, and Beyond. In Annual Plant Reviews online, J.A. Roberts (Ed.). <https://doi.org/10.1002/9781119312994.apr0705>

I, Bernd Heinrich Dreyer, am the first author and one of the corresponding authors and wrote >90% of the manuscript. Text from the manuscript will only be used to introduce the research topic. All used sections are cited appropriately at the beginning and end of a relevant section.

## VI. ABBREVIATIONS

Table 1: Used abbreviations in this thesis.

Abbreviation	Name
3-AT	3-Amino-triazole
ALS	amyotrophic lateral sclerosis
UAS	<i>Upstream activating sequence</i>
BiFC	Bimolecular fluorescence complementation
ChIP-seq	Chromatin immunoprecipitation sequencing
<i>Col-0</i>	<i>Columbia-0</i>
CSD1	COPPER/ZINC SUPEROXIDE DISMUTASE 1
DNA	Deoxyribonucleic acid
DAPI	4',6-Diamidin-2-phenylindol
DAP-seq	DNA affinity purification sequencing
DBD	DNA-binding domain
DEG	Differentially expressed gene
EMSA	Electrophoretic mobility shift assay
ERAD	ER-associated degradation
FC	Fold change
<i>fLUC</i>	Firefly luciferase
FRAP	Fluorescence recovery after photobleaching
GFP	Green fluorescence protein
HIPP	Heavy metal-associated isoprenylated plant protein
HMA	Heavy-metal associated domain
HRP	Horseradish peroxidase
MES	2-(N-morpholino) ethanesulfonic acid
NAT	N-terminal acetyltransferases
NLS	Nuclear localisation signal
NTA	N-terminal acetylation
PCR	Polymerase chain reaction
PTM	Post-translational modification
PTS	Peroxisomal targeting signal
<i>RnLUC</i>	Renilla luciferase
ROS	Reactive oxygen species
SAM	Shoot apical meristem
SELEX	Systematic evolution of ligands by exponential enrichment

---

SOD	Superoxide dismutase
TA	Transactivation assay
TSS	Transcriptional start site
Y2H	Yeast Two-Hybrid
YFP	Yellow fluorescence protein

---

# 1 INTRODUCTION

**The following text is cited from my published review article (Dreyer & Schippers, 2019):**

“Superoxide dismutase (SOD) is a primary antioxidant enzyme that can be found in organisms from all kingdoms of life. Its date of origin indicates a pivotal role in the evolution of life on our planet. [...] SODs were initially appreciated for their antioxidant properties and potential to improve plant stress tolerance. However, recent findings indicate a role for SODs in maintaining reactive oxygen species (ROS) gradients to guide plant developmental processes. Moreover, after nearly 50 years of research on SODs, these enzymes still hold many surprises as evidenced by the recent finding that SOD in yeast acts as a transcriptional regulator.”<sup>1</sup>

**End of citation (Dreyer & Schippers, 2019)**

## 1.1 Superoxide dismutases (SODs) and ROS

**The following text is cited from my published review article (Dreyer & Schippers, 2019):**

“The discovery of superoxide dismutases (SOD) resulted in the superoxide theory of oxygen toxicity and the realisation that oxygen radicals are important biological products (McCord et al., 1971; Fridovich, 1978; Foyer and Noctor, 2005). SODs catalyse the dismutation of superoxide ( $O_2^-$ ) while producing hydrogen peroxide ( $H_2O_2$ ) and molecular oxygen. SODs appear to be essential for survival in many organisms and especially in the field of medicine, their malfunctioning is linked to diverse diseases. Considering that these enzymes belong to the oldest and best-conserved proteins between all kingdoms of life, they must have a pivotal role in the evolution of life on earth. SODs were initially only recognised for their enzymatic function and role in the protection against oxidative stress. Major breakthroughs in the field of radical biology led to an adjustment of the one-sided view on reactive oxygen species (ROS). First of all, it was found that ROS are produced specifically by cells upon pathogen infection (Babior et al., 1973; Doke, 1983). These observations indicated that cells do not simply scavenge away all ROS but that they maintain them at a level that is needed for cellular

---

<sup>1</sup> pp. 1, Dreyer & Schippers (2019)

functioning. With the advent of transcriptome tools, it was found that each ROS provokes a specific transcriptional response, indicating that they can act as specific signalling molecules (Schmidt and Schippers, 2015). Thus any component involved in the formation or removal of ROS can have an important impact on ROS signalling. SODs are in this case especially interesting as they scavenge  $O_2^-$ , but release  $H_2O_2$ , a general accepted second messenger in all fields of biology. The realisation that there is a need for ROS is also reflected in new studies, whereby ROS participates in cell proliferation and differentiation processes, cell growth and stress signalling. It is likely that SODs evolved as enzymes with a single purpose, but due to the integration of ROS signals with cellular homeostasis and development also these enzymes might have adapted additional novel functions.”<sup>2</sup>

**End of citation (Dreyer & Schippers, 2019)**

## **1.2 Distinct SOD isoforms and subcellular distribution in plants**

All SODs are metalloenzymes that contain within their active site a redox-active metal. During evolution, different SOD enzymes appeared that are classified into different subgroups based on the metal they use in their active site. The SODs are classified into iron superoxide dismutases (FeSODs), manganese superoxide dismutases (MnSODs) and copper-zinc superoxide dismutases (CuZnSODs).

**The following text is cited from my published review article (Dreyer & Schippers, 2019):**

“Plants feature all three SOD families and their subcellular localisation can be generally described as MnSODs are mitochondrial, FeSODs are plastidial and CuZnSODs are more broadly localised (Bowler et al., 1992). In rice, one MnSOD isoform was shown to localise to the Golgi apparatus and plastids which indicate that there might be some differences in the viridiplantae kingdom (Shiraya et al., 2015). In Arabidopsis, the three CuZnSOD isoforms (CSD1, CSD2, and CSD3) localise specifically to different cellular compartments. The first isoform CSD1 localises to the cytosol and the nucleus (Xu et al., 2010; Huang et al., 2012). CSD2 features an N-terminal chloroplast targeting peptide (CTP) and localises to the

---

<sup>2</sup> pp. 1-2, Dreyer & Schippers (2019)

chloroplast. The third isoform CSD3 harbours a C-terminal ALK peroxisomal targeting peptide and localises to the peroxisome (Huang et al., 2012). Huang et al. (2012) also showed that the deletion of the CTP or the C-terminal PTS signal leads to mislocalisation of the individual isoforms. Interestingly, several reports conducted in different plant species indicate that a CuZnSOD isoform localises to the extracellular space (Streller and Wingsle, 1994; Ogawa et al., 1996; Kasai et al., 2006).”<sup>3</sup>

**End of citation (Dreyer & Schippers, 2019)**

Several developmental processes like cell extension and the formation of the casparian strip propose the involvement of an extracellular SOD protein (Janku et al., 2019; Rojas-Murcia et al., 2020; Fujita, 2021), however the SOD isoform still needs to be experimentally confirmed.

**The following text is cited from my published review article (Dreyer & Schippers, 2019):**

“Distinct subcellular localisation of the individual CuZnSOD isoforms indicates the necessity of superoxide removal within specialised cellular compartments and allows the differential regulation of individual isoforms upon changing environmental conditions which might have been an evolutionary advantage. Unfortunately, our subcellular distribution picture of SODs is incomplete and needs further assessment to understand the role of each SOD and if they fulfil the same function in each cellular compartment to which they are localised.”<sup>4</sup>

**End of citation (Dreyer & Schippers, 2019)**

### **1.3 Regulation and role of CSDs during plant stress response**

**The following text is cited from my published review article (Dreyer & Schippers, 2019):**

“Responses of plants to stress involves three fundamental steps: sensing of the external stress, signalling through cellular messengers, and ultimately a transcriptional response that results in adaptation towards the external stress. A common cellular feature upon being exposed to stress is the formation of ROS: produced either due to disruption of metabolic activities or actively produced in the form of an oxidative burst for signalling purposes during stress responses

---

<sup>3</sup> pp. 10-11, Dreyer & Schippers (2019)

<sup>4</sup> pp. 11, Dreyer & Schippers (2019)

(Choudhury et al., 2017). Therefore, plants need to adapt their antioxidant system in response to abiotic and biotic stress. As part of the antioxidant system the expression of CSD proteins is modified to effectively scavenge  $O_2^-$ , often the first product of disrupted metabolic reactions or actively produced by NADPH oxidases as a signalling molecule. SOD proteins are regulated during many plant stress responses which were in part reviewed by Wang et al. (2016a). Here, we give a specific overview on how plant CSD proteins are controlled during plant stress responses.

The exposure of plants to drought or salinity stress results mainly in cellular dehydration, which further leads to osmotic stress and altered cytosolic and vacuolar volumes, and the production of ROS species by a disruption of metabolism (Bartels and Sunkar, 2005; Choudhury et al., 2017). As drought, osmotic, and salinity stress have these cellular effects in common, they share similar early response mechanisms. In general, abiotic stress results in the generation of ROS. So, one common mechanism of plants is the adaptation to increased ROS by altering the expression of components of their antioxidant system. The expression of *CSD* genes, mainly *CSD1* and *CSD2*, was studied in *Arabidopsis* as well as several crop species during abiotic and biotic stress. Upon salt stress, the expression of *CSD1* is increased in *Arabidopsis* (Jia et al., 2009; Shafi et al., 2015), in wheat (Sairam et al., 2005), in tomato (Feng et al., 2016a), in cucumber (Zhou et al., 2017), and especially in the salt-sensitive species rice (Nounjan et al., 2012; Ozfidan-Konakci et al., 2014; Rossatto et al., 2017). The comparison of two mosses, the drought-tolerant *Tortula ruralis* and the drought-sensitive *Cratoneuron filicinum*, revealed that reduced lipid peroxidation in the drought-tolerant species correlates with increased CuZnSOD enzyme activity (Dhindsa and Matowe, 1981). PEG-induced drought stress in *Caragana* resulted in enhanced gene expression of all three *CSD* genes (Zhang et al., 2014). In maize, cytosolic *CSDs* were significantly increased after paraquat treatment (Matters and Scandalios, 1986). Also, drought and photooxidative herbicide tolerances were both correlated with high levels of CuZnSODs and glutathione reductase activities in maize (Malan et al., 1990). During high light stress, the expression of *CSD1* and *CSD2* is increased to overcome metabolic ROS (Xing et al., 2013). Also, acute ozone stress in rice or low nitrogen stress in soybean roots increases the expression of *CSD1* (Ueda et al., 2013; Wang et al., 2016b). The transcription of *CSD1* and *CSD2* was increased upon arsenic stress in *Arabidopsis* (Abercrombie et al., 2008). Furthermore, both genes are also upregulated by oxidative stress and it is linked to regulation by miR398 (Sunkar et al., 2006). Differential expression of *CSD* genes upon cold, heat, drought,

and salt stress in *Musa acuminata* was observed (Feng et al., 2015). In addition, copper nanoparticles induced expression of *CSD* genes in cucumber (Mosa et al., 2018). In upland cotton (*Gossypium hirsutum*), the expression of *CSD1* and *CSD2* is upregulated during heat stress within the first 24 hours and downregulated within the first 24 hours during salt stress, indicating species-specific regulations of *CSD* genes (Wang et al., 2017). In tomato *CSD2* is upregulated, while *CSD3* is downregulated and *CSD1* expression remained constant upon drought stress, whereas upon salt stress *CSD1* is upregulated, *CSD2* is downregulated and *CSD3* expression remains constant (Feng et al., 2016). Expressional studies in cucumber upon heat, cold, and salt stress further indicate species-specific regulations and add spatio-temporal information to the expression patterns (Zhou et al., 2017). Differential expression of *CSDs* was also observed in biotic interactions. In *Arabidopsis*, the expression of *CSD1* and *CSD2*, as well as their protein abundance, is enhanced after treatment with salicylic acid (SA) analogues that are considered pathogen-associated signals (Kliebenstein et al., 1999). Also, reduced *CSD* accumulation is linked to increased levels of cell death during infection with virulent and avirulent *Peronospora parasitica* (Kliebenstein et al., 1999). Upon infestation with aphids, *CSD1* was upregulated in *Arabidopsis* (Moran et al., 2002). The *CSD1* gene was also upregulated in leaves of maize and cotton infested by aphids (Sytykiewicz, 2014). The barley *CSD1* (*HvCSD1*) is also upregulated in the interaction of barley and the hemibiotrophic pathogen *Pyrenophora teres f. teres*, especially during the subsequent resistance response (Lightfoot et al., 2017). Gene expression profiles in response to aphid feeding are proposed to be similar to wounding and pathogen response (Moran et al., 2002); therefore, we can expect that *CSD1* is differentially regulated in other plant-pathogen interactions. As stresses provoke an imbalance in cellular ROS homeostasis, it is not only surprising that SODs in general but also specifically *CSDs* are regulated during these stress responses. So far, little is known about the mechanisms regulating the expression of *CSDs* during all of these stress responses.

During high light stress, the expressional upregulation of *CSD1* and *CSD2* is facilitated by MKK5 (Xing et al., 2013). Furthermore, the AtANAC069 transcription factor negatively regulates the expression of *CSDs* and other antioxidative enzymes (He et al., 2017). Consequently, the overexpression of *ANAC069* results in decreased salt and osmotic stress tolerance. However, the direct binding of *ANAC069* to the promoters of *CSD* genes was not shown (He et al., 2017). These are the first reports that indicate mechanisms controlling the expression of *CSD* genes upon stress. Nearly all the mentioned studies only focus on *CSD*



transcript levels and not protein abundance. Two decades ago, plant SODs were ‘hot’ candidates for increasing plant stress tolerance. In theory, the overexpression of enzymes like SODs or catalases may help plants to adapt to individual stress scenarios. SODs were of special interest as they scavenge  $O_2^-$  which is generated under various stress conditions. The benefit of manipulating one module to increase the tolerance of a plant to various stress conditions lead to a plurality of overexpression studies. Transgenic tobacco plants that overexpress the *CSD2* gene from pea have been subjected to methyl viologen, chilling temperatures, moderate, and high light intensity (Gupta et al., 1993). The authors observed that *CSD2* overexpressing plants retained higher photosynthesis rates and showed reduced levels of light-mediated cellular damage concluding that transgenic expression of *CSD2* can improve stress tolerance (Gupta et al., 1993). Similar results were observed for the integration of *CSD1* and *CSD2* of tomato into potato tuber disc by *Agrobacterium* (Perl et al., 1993). Pea cytosolic *CSD* overexpression in tobacco plants resulted in increased resistance towards acute doses of ozone (Pitcher and Zilinskas, 1996). Tobacco plants overexpressing *CSD2* from *Kandelia candel* showed enhanced salt tolerance (Jing et al., 2015). Rice plants overexpressing *CSD2* are more tolerant to salt and saline-sodic stress (Guan et al., 2017). Furthermore, the *CSD2*-overexpressing rice lines performed better than nontransformed plants in terms of germination rate, SOD activity, fresh weight, root length, and height. Arabidopsis plants expressing the *CSD2* gene from *Sedum alfredii*, a cadmium hyperaccumulator of the Crassulaceae, had enhanced antioxidative defence capacity (Li et al., 2017). Furthermore, a coexpression network based on microarray data indicated oxidative regulation after Cd-induced oxidative stress in Arabidopsis suggesting that *SaCSD2* may participate in this network. Plum plants that overexpress *CSD1* were found to be more tolerant towards salt stress (Diaz-Vivancos et al., 2013). In contrast, the overexpression of chloroplastic SOD (*CSD2*) from petunia in tobacco and tomato led to a 50-fold and a 2–4 fold increases of SOD levels respectively, however, these plants did not exhibit increased resistance to paraquat, high light, low temperature or low  $CO_2$  stress (Tepperman and Dunsmuir, 1990). It may well be that increased hydrogen peroxide scavenging capacity is also required to improve the plant to combat oxidative stress more efficiently (Foyer et al., 1994). Therefore, dual transgenic approaches were performed. In *Manihot esculenta* transgenic expression of *CSD* and ascorbate peroxidase (*APX*) increased cold stress tolerance (Xu et al., 2014). Enhanced antioxidative defence capabilities were also observed in transgenic tall fescue plants overexpressing *CSD2* and *APX* in response to hydrogen peroxide, methyl viologen, and heavy metal exposure (Lee et al., 2007). Transgenic coexpression of *CSD1* and *APX* in tobacco

resulted, to some extent, to the alleviation of water stress symptoms (Faize et al., 2011). Overexpression of *CSD2* and a catalase gene from maize in chloroplasts of Chinese cabbage enhanced tolerance to sulfur dioxide and salt stress (Tseng et al., 2007). Taken together, these studies demonstrated a measurable effect of SOD overexpression on plant stress tolerance, although the effect itself was not that large. In addition, overexpression of SODs was shown in *Arabidopsis* to result in developmental defects, including growth arrests (Zeng et al., 2017), indicating that constitutive activation of SODs might interfere with its dual roles in stress responses and the regulation of plant growth.”<sup>5</sup>

#### **End of citation (Dreyer & Schippers, 2019)**

Future experiments need to focus on CSD protein abundance as the translation of CSD is controlled by miR398 (Bonnet et al., 2004). Furthermore, it is also important to understand the regulation of CSD on the protein level in regard to its stability and turn-over rate. CSD proteins might still be high-impact targets for breeding, but as the fundamental knowledge about the regulation and function seems to be incomplete, the lack of information needs to be tackled first.

## **1.4 SODs might control ROS gradients during plant development**

**The following text is cited from my published review article (Dreyer & Schippers, 2019):**

“Within the last ten years, the idea of oxidative signalling has become a valid explanation for how ROS may regulate plant development and stress responses. Accumulation of  $O_2^-$  is proposed to be an important factor for stem cell maintenance in plant and animals’ cells (Dunand et al., 2007; Sarsour et al., 2008; Owusu-Ansah and Banerjee, 2009; Zeng et al., 2017). Furthermore, the accumulation of  $O_2^-$  is required for cell proliferation, whereas elevated  $H_2O_2$  concentrations promote cellular differentiation (Tsukagoshi et al., 2010; Mittler, 2017; Zeng et al., 2017). These findings suggest that  $O_2^-$  gradients are linked to maintaining stem-ness while  $H_2O_2$  accumulation promotes cell differentiation. SODs as  $O_2^-$  scavengers or  $H_2O_2$  producers may be key players in regulating ROS gradients. Interestingly, a few studies describe the role of SODs and especially CuZnSODs in plant development. Two studies strongly indicate an

---

<sup>5</sup> pp. 18-21, Dreyer & Schippers (2019)

important role of CuZnSODs in developmental processes and highlight gaps in our knowledge. In 2012, a comprehensive analysis of tobacco pollen tube growth identified that CSD1 is among the central regulators of pollen-tube tip growth (Hafidh et al., 2012). Tobacco CSD1 knockdown plants showed severe pollen-tube growth defects and occasionally abnormal tip morphology. It is well established that ROS are involved in the regulation of polarised cell growth in pollen tube or root hair elongation in plants (Lee and Yang, 2008; Kanaoka and Torii, 2010); however, the ROS type is unknown. We may now speculate that H<sub>2</sub>O<sub>2</sub> might be the ROS molecule that is involved in polar cell growth, at least it is in line with the need of NADPH oxidases as endogenous O<sub>2</sub><sup>-</sup> source and the severe phenotype observed in a tobacco CSD1 knockdown. Furthermore, SODs are involved in the complex ROS-mediated control of plant stem cell fate (Zeng et al., 2017). A balance between O<sub>2</sub><sup>-</sup> and H<sub>2</sub>O<sub>2</sub> controls stem cell maintenance and differentiation. O<sub>2</sub><sup>-</sup> is enriched in the central zone of the SAM to promote stemness, whereas H<sub>2</sub>O<sub>2</sub> is more abundant in the differentiating peripheral zone to initiate stem cell differentiation (Zeng et al., 2017). To allow an accumulation of O<sub>2</sub><sup>-</sup> inside the stem cell niche, SODs are repressed in plant stem cells. In line, peroxidases are activated to reduce the spontaneous accumulation of H<sub>2</sub>O<sub>2</sub> in the stem cell niche (Zeng et al., 2017). Also, ectopic expression of several SOD proteins including CSD1 and CSD2 under the *CLV3* or *UBQ10* promoter leads to a *wus*-like phenotype with terminated stem cells (Zeng et al., 2017). Both studies indicate the importance of understanding the complex interplay between endogenous and exogenous ROS and how individual plant cell types are influenced by these different kinds of ROS. We expect that these recent studies are the first of many more that will investigate the complex interplay between ROS signalling, ROS scavenging enzymes and development.”<sup>6</sup>

End of citation (Dreyer & Schippers, 2019)

## 1.5 SOD1/CSD1 – More than just an Enzyme?

The following text is cited from my published review article (Dreyer & Schippers, 2019):

“The protein family superoxide dismutase has been scrutinised for more than 50 years and plenty of research studies have been published regarding its function throughout life (McCord

---

<sup>6</sup> pp. 22-23, Dreyer & Schippers (2019)

and Fridovich, 2014), still, these proteins hold up surprises with unexpected, radical, novel discoveries. Even with these recent remarkable findings, we expect that research on this family is far from complete, especially in plants. In yeast, the unexpected finding that SOD1 is involved in repression of respiration in a single circuit with oxygen, glucose, and ROS through two casein kinases resulted in a re-evaluation of SOD1s cellular function and provoked future studies (Reddi and Culotta, 2013). In 2014, Tsang et al. explored an astonishing novel function of SOD1 in *S. cerevisiae*. SOD1 relocates into the nucleus upon oxidative stress (Tsang et al., 2014). The ROS-dependent signalling that initiates nuclear relocalisation of SOD1 is mediated by Mec1/ATM and its effector kinase Dun1/Cds1. Dun1 interacts with SOD1 and phosphorylates SOD1 at S60 and S99. In the nucleus, SOD1 associates with the promoters of oxidative resistance and repair genes. The authors indicate that the SOD1 protein can act as an enzyme and as a transcription factor. Of special interest is the role of H<sub>2</sub>O<sub>2</sub> in this mechanism as it is the product of SOD1s enzymatic reaction and likely also the signalling molecule that activates the Mec1/ATM upstream kinase of this signalling pathway. Therefore, this study provides further evidence for the role of H<sub>2</sub>O<sub>2</sub> as second messenger of ROS signalling and provoked a revision of SOD1s cellular significance. In 2018, Tsang et al. explored that SOD1 is also a conserved effector of mTORC1 signalling in yeast and human cells (Tsang et al., 2018). mTOR-dependent phosphorylation of SOD1 at S39 in yeast and T40 in humans in response to sufficient nutrient supply restrains SOD1 activity. In contrast, starvation stimulates SOD1 activity to prevent oxidative damage. These studies highlight the complexity of SOD1 proteins throughout life and that they catalyse the crucial scavenging of superoxide and act as transcriptional regulators to adapt to certain stressful situations. However, it needs to be elucidated if this additional function as a transcriptional regulator is yeast-specific or a common feature of SOD. In humans, SOD1 is studied to a great extent due to its pathogenic role in amyotrophic lateral sclerosis (ALS) which is a fatal neurodegenerative disease characterised by gradual loss of motor neurons (Redler and Dokholyan, 2012). SOD protein aggregates have been discovered in patients with sporadic or familial ALS (Shibata et al., 1994, 1996). Recent studies refine the idea of nonnative SOD1 oligomers as the toxic species involved in ALS instead of large protein aggregates (Luchinat et al., 2014; Proctor et al., 2016). ALS-related amino acid mutations and several post-translational modifications (PTMs) affect the stability of the SOD1 dimer towards enhanced dimer dissociation, subsequently resulting in large amounts of oligomers and aggregates (Redler et al., 2014; Broom et al., 2016). Interestingly, environmental factors that induce PTMs significantly influence the disease progression

(Pasinelli and Brown, 2006; Barber and Shaw, 2010; Chattopadhyay et al., 2015). Several PTMs are described (Wilcox et al., 2009; Coelho et al., 2014) and are linked to increased concentrations of nonnative disease-related oligomers (Redler et al., 2011; Coelho et al., 2014). Recently, Fay and coworkers discovered a phosphomimetic mutation, T2D, that stabilises the SOD1 proteins and rescues ALS-associated effects in cellular assays (Fay et al., 2016). The authors speculate that the stabilisation of SOD1 in its native conformation might offer a reasonable pharmaceutical strategy against incurable ALS. Interestingly, the SOD1 protein in humans cannot only be phosphorylated at threonine-2 but also at Thr-58 or Ser-59 (Wilcox et al., 2009). Furthermore, it is glutathionylated at Cys-111 which strongly promotes dimer dissociation. Protein glutathionylation is linked to redox regulation in human and plants (Dalle-Donne et al., 2009); however, so far only a model exists in humans in which increased oxidative stress promotes SOD1 monomer formation and subsequently SOD1 aggregation (Wilcox et al., 2009). The Cys-111 is not strictly conserved between humans and Arabidopsis; however, CSD1 contains a Cys at position 101 that is not present in human SOD1. The T58/S59 phosphorylation site is also of interest as this amino-acid sequence is shared in nearly all SOD1 proteins throughout life and it was shown that this site is phosphorylated in yeast and results together with S99 phosphorylation in relocalisation of SOD1 into the nucleus (Tsang et al., 2014). Several of these PTM sites are also conserved in plants; however, in plants, we lack information about putative PTMs on CSD1. For example, Ser-58 and Thr-59 are conserved. Thus, these are promising candidates for PTMs in plants. A study in mice identified another PTM site of particular interest where the Ser-98 within a solvent-exposed beta-sheet of SOD1 was phosphorylated (Banks et al., 2017). This site is also involved in the regulation of SOD1's role in transcription in yeast (Tsang et al., 2014) and is conserved in plants. Another interesting aspect is the phenotype of SOD1/CSD1 loss in higher eukaryotes. Two studies explored that loss of SOD1 is lethal in human cell lines (Inoue et al., 2010; Banks et al., 2017). In yeast, SOD1 knockout results in increased sensitivity towards redox agents and hyperoxia (Culotta, 2000). Furthermore, it also results in an increase in spontaneous DNA mutations when cells are grown in the air (Gralla and Valentine, 1991). In mice, SOD1 deficiency is not lethal, however, results in many different phenotypes that resemble aging caused by elevated ROS (Elchuri et

al., 2005; Iuchi et al., 2007; Hashizume et al., 2008). An in-depth phenotypic analysis in plants is still missing that shows a true null mutant of CSD1 and the phenotypic result of it.”<sup>7</sup>

#### **End of citation (Dreyer & Schippers, 2019)**

The amino acid sequence of SOD1/CSD1 is largely conserved between *Arabidopsis*, *Saccharomyces cerevisiae* and *Homo sapiens*, however it remains so far elusive if the novel roles for SOD1 are also present in CSD1 of plants. Considering the importance of ROS signalling in the development and the adaptation responses of plants, it is vital to elucidate if CSD1 shares the novel molecular functions of SOD1 as this might represent an important target for future breeding approaches.

## **1.6 Heavy-metal associated isoprenylated plant proteins (HIPP)**

HIPP proteins have a specific two domain structure consisting of a heavy metal associated (HMA) domain and a C-terminal isoprenylation motif (Tehseen et al., 2010). Sequence analyses in the model plant *Arabidopsis* revealed 44 genes encoding proteins containing the two characteristic domains. That said, some HIPP family members contain more than one HMA domain. HMA domains (pfam 00403.6) exhibit a core sequence (M/L/IxCxxC) with two characteristic cysteines that are implicated in heavy metal binding (Hung et al., 1998; Barth et al., 2009). In general, HMA containing proteins are predicted to function in heavy metal transport and heavy metal homeostasis (Lin et al., 1997). In addition to the HMA domain, HIPP proteins contain an isoprenylation motif (CaaX-motif). Isoprenylation is a post-translational modification that involves the formation of a covalent thioether bond between a cysteine and farnesyl- or geranylgeranyl residues (Raju, 2019). The lipid modification of the protein creates a hydrophobic anchor that is important for interaction of the protein with membranes or other proteins (Yalovsky et al., 1999). In general, prenylated proteins play important regulatory roles in cell cycle control, signal transduction, cytoskeletal organisation or intracellular vesicle transport (Crowell, 2000). Recently, several HIPPs were linked to distinct stress responses. For example, HIPP26 interacts with the zinc finger homeodomain transcription factor ATHB29, which together regulate drought stress responses in *Arabidopsis* (Barth *et al.*, 2009). In

---

<sup>7</sup> pp. 23-25, Dreyer & Schippers (2019)

*Nicotiana benthamiana*, HIP26 interacts with the movement protein of the potato mop-top virus that negates or reverses lipidation of HIP26, thus releasing membrane-associated HIP26, thereby activating a drought stress response and facilitating virus long-distance movement (Cowan et al., 2018). HIP3 as novel zinc-binding protein is reported to be an upstream regulator of the salicylate-dependent pathway and involved in biotic and abiotic stress responses (Zschiesche et al., 2015). HIP27 was identified as susceptibility gene for the beet cyst nematode *Heterodera schachtii* as loss-of-function Arabidopsis *hipp27* mutants exhibited severely reduced susceptibility (Radakovic et al., 2018).

A recent report suggests that HIP proteins represent a novel functional component of the plant ER-associated protein degradation (ERAD) by interaction with cytokinin-degrading CKX proteins and regulation of the ERAD of CKX proteins (Guo et al., 2021). Summarising the recent findings, HIP proteins are involved in abiotic and/or biotic stress response pathways. Still, the exact molecular mechanism of HIP proteins has not been identified. As HIP proteins are reported to be involved in stress adaptation processes, characterisation of HIP family members might provide clues on increasing crop resistance against biotic and abiotic stresses.

## 1.7 N-terminal acetylation

Post-translational and co-translational modifications of proteins represent an important mechanistic tool for organisms to control protein function and fate. A pervasive protein modification of which many scientists are unaware, even though most of the proteins of prokaryotes and multicellular organisms receive it, is the N-terminal  $\alpha$ -acetylation (NTA). NTA is regarded as the irreversible enzymatic co- and post-translational addition of an acetate moiety onto protein N- $\alpha$ -amino groups (Gigliione & Meinel, 2021). NTAs are found in all organisms. Interestingly, the percentage of proteins that receive an NTA is increasing with organism complexity. About 1-2 % of proteins in bacteria (Bienvenut et al., 2015; Ouidir et al., 2015), 10-45% in Archaea, 60% in fungi, and >80% of the cytosolic proteome in multicellular eukaryotes are receiving an NTA (Aksnes et al., 2016; Breiman et al., 2016). The NTA is catalysed by N-terminal acetyltransferases (NATs) which transfer the acetyl group from acetyl-CoA to the free  $\alpha$ -amino groups of the protein N termini. In plants, several cytosolic/membrane NATs with distinct substrate specificity have been identified (Aksnes et al., 2016). NTAs are

facilitated by NatA/B/C/E complexes that consist of distinct catalytic subunits. The catalytic subunits associate with auxiliary subunits to improve catalytic performance, target specificity and ribosome binding (Aksnes et al., 2016). The different Nat complexes contain different substrate specificities and cover together a range of amino acids that receive an NTA. An NTA to the  $\alpha$ -amino acid alanine through the NatA complex is the most common acetylation in Arabidopsis (Giglione & Meinnel, 2021).

NatA was the first NAT complex that was identified in plants (Linster et al., 2015; Xu et al., 2015). The core of this complex consists of a catalytically active subunit (AtNAA10) and an auxiliary subunit AtNAA15. In Arabidopsis, NAA10 and NAA15, subunits of NatA, are classified as embryo defective genes (Devic, 2008) and T-DNA insertion lines confirmed the loss of both subunits arrests embryo development (Feng et al., 2016b; Feng & Ma, 2016). Arabidopsis plants expressing an artificial miRNA (ami) for AtNAA10 or AtNAA15 showed altered development in combination with growth retardation (Linster et al., 2015) indicating that both subunits are important for NatA activity. The amiNAA10 and amiNAA15 lines showed increased tolerance to drought and it was proposed that NTA by NatA is a hormone-controlled dynamic process that regulates cellular stress responses to drought (Linster et al., 2015; Giglione & Meinnel, 2021). Furthermore, the proteasome machinery was upregulated in the *amiNAA10* and *amiNAA15* lines suggesting that the NatA complex might control cellular proteostasis (Linster et al., 2015). A recent study showed the proteome of Arabidopsis plants is imprinted with acetylation marks to coordinate proteome stability (Linster et al., 2022). The absence of NTAs results in protein destabilisation by a novel nonAc/N-degron in plants. That NTAs control the stability of proteins was known before, the number of proteins that are controlled by NTAs surprised. However, NTAs not only control the stability of proteins, but they also regulate the folding, complex formation or membrane targeting. In Arabidopsis, the mechanistic role for the NTA was shown for the SUPPRESSOR of NPR1 CONSTITUTIVE 1 (SNC1) where the reception of the NTA serves as degradation signal (Xu et al., 2015). So far, only a few examples of a mechanistic function for the NTA are known, but with further research more examples can be expected.

Inside a plant cell, considering space and time, the pool of proteins of one single protein may feature both unmodified (free) and N-acetylation termini resulting in partial *in vivo* NTA. The acetylation yield ( $\text{NTAed}/(\text{free} + \text{NTAed})$ ) describes the relationship between the NTAed and free fraction of the protein ranging from 0 to 100% (Aksnes et al., 2016). As the NTA regulates



different aspects from stability to complex formation, the acetylation yield might represent a cellular mechanism to fine-tune the molecular function of target proteins. NTAs represent a PTM of high importance considering the control of the stability of a protein pool. The identification of target proteins might allow for specific fine-tuning of adaptation responses and developmental processes and therefore be a novel target for future breeding strategies.

## 1.8 Moonlighting

Before the establishment of the industrial law people in the USA had long daily working hours. The sudden establishment in 1938 gave people more daily time on their hands, and to fill that newly gained free time many people started an extra (part time) job. The extra job often came at night when the moonlight is shining. Therefore, it was named moonlighting to follow a second job part time in the evening to earn additional money. Nowadays, holding a second job is generally called moonlighting, sometimes also referred to illegal employment. In a biological context, the phenomenon by which a protein can perform more than one function is called protein moonlighting (Jeffrey, 2003). In 1999, Constance Jeffrey was the first to draw the similarity between proteins with a second function and people with a second job, generating a new scientific term (Jeffrey, 1999; Huberts & van der Klei, 2010). Moonlighting proteins presumably possessed a single function and gained the additional through evolution. A moonlighting protein performs its dual function through the same domain which is different from multifunctional proteins which contain multiple domains (Sriram et al., 2005). Many of today's known moonlighting proteins are involved in highly conserved processes like for example glycolysis and tricarboxylic acid (TCA) cycle. Especially those proteins possessing fundamental enzymatic functions are often highly conserved and found throughout the different kingdoms of life, are also the best candidates to gain a second function (Huberts & van der Klei, 2010). The HEXOKINASE 1 (HXK1) is one of the identified moonlighting proteins in Arabidopsis. HXK1 is a glucose sensor that integrates nutrient and hormone signals to govern gene expression and plant growth in response to environmental cues (Moore et al., 2003). Cho et al. suggested that nuclear HXK1 forms a glucose signaling complex with novel nuclear interaction partners to directly modulate specific target gene transcription independent of glucose metabolism (Cho et al., 2006). Another moonlighting protein is the enzyme aconitase which catalyzes the isomerisation of citrate to isocitrate as part of the TCA cycle (Hirling et al.,

1994). In animals, under conditions that lead to low iron concentrations the cytosolic aconitase loses its iron-cluster, consequently its enzymatic function and becomes an RNA binding protein binding to iron-responsive elements in untranslated regions of mRNAs (Hentze & Kühn, 1996). Here, the moonlighting cytosolic aconitase is also renamed to iron regulatory protein 1 (IRP1). In plants, aconitase binds to the untranslated region of the chloroplastic CSD2 mRNA, thus regulating its translation and playing a role in mediating oxidative stress (Moeder et al., 2007). Only a handful of moonlighting proteins are characterised for both individual functions in plants and other organisms (Jeffrey, 2014). However, increasing evidence suggests that especially cytosolic enzymes of the central metabolism might be moonlighting proteins by taking over new tasks to connect energy metabolism to adaptive stress responses and maintain redox homeostasis (Jethva et al., 2022). The concept of moonlighting is also extended to plant kinases by creating specific signaling niches (Turek & Irving, 2021). Two classes of moonlighting proteins, trigger enzymes and intracellular/surface moonlighting proteins (Jeffrey, 2019), are arising. To understand the complex signaling during development, abiotic/biotic stress signaling and the additional crosstalk between these, it is of paramount importance to identify and characterise moonlighting proteins and their hidden functions.

## 1.9 Scope of this thesis

Recent advances in developmental and stress response biology indicate the importance of ROS homeostasis to guide and regulate these physiological processes. In this light, new hypotheses were established for the role of cellular regulators of ROS homeostasis, like SODs. This resulted in several new discoveries regarding SOD1 as transcriptional regulator during oxidative stress (Tsang et al., 2014) and as a regulator in nutrient sensing (Tsang et al., 2018), thus changing the textbook view on SOD1. Furthermore, the efforts to understand the role of SOD1 in the development of ALS resulted in the identification of a plethora of PTMs that SOD1 receives in human cells (Banks & Andersen, 2019). On top, SOD1 is reported to interact with several other proteins (<https://thebiogrid.org>, Stark et al., 2006), suggesting that it acts in different protein complexes through-out the cell. These recent advances have been made in yeast and human cells and indicate a more diverse molecular function of SOD1. This work here tackles the question if the textbook view on the conserved SOD1 protein in plants, CSD1, also needs to be altered towards a multifunctional and moonlighting protein. This was addressed by three main

research questions: (1) Is CSD1 a transcriptional regulator in plants? (2) Is CSD1 post-translationally regulated in plants? (3) In which protein complexes does CSD1 act in plants?

The main aim of the study is determining if CSD1 is a moonlighting protein in Arabidopsis by acting as a transcriptional regulator. Here, a combination of molecular, biochemical and physiological experiments was used to tackle this question. To shed further light on the molecular function of CSD1 as ROS and transcriptional regulator, post-translational modifications and potential interactors were assessed. Therefore, novel experimental approaches using a CSD1-specific antibody were undertaken to gain knowledge in the wild type Arabidopsis background.

Taken together the experimental approach taken here will fill the knowledge gap about the regulation and function of CSD1 in Arabidopsis. This will alter the current simplistic view on CSD1 and might give leads for a novel approach for future breeding to directly address the protein structure, stability and turn-over rate instead of gene expression.

## 2 MATERIAL AND METHODS

### 2.1 Arabidopsis lines

The T-DNA insertion lines used in this study were obtained from the Nottingham Arabidopsis Stock Centre (NASC). Homozygous T-DNA insertion was confirmed using the following primers: *csd1-3* (SALK\_024857; LP 5'-3' GTC ATT ACC CTT TCC GAG GTC; RP 5'-3' AAC AGT TTC TGG CCT TAA GCC), *hipp20-1* (SALK\_048115; LP 5'-3' AGG TGA AGA TCG ACT GTG ACG; RP 5'-3' ATA TGT TGC GTT GCT TCT CAC), *hipp21-1* (SALK\_131715.53.60; LP 5'-3' TCCATGGAAAAATGTGATTGG; RP 5'-3' AAAAGAGAATGGGTGCATTTG), *hipp22-1* (SALK\_204024; LP 5'-3' CCGGGATTTGTATTCTTCTCG; RP 5'-3' CGCATTGAAGCTTTCTTCAC).

In this study constructs for generating transgenic lines have been made by using a Gateway expression vector and *Agrobacterium tumefaciens* (*GV3101*) to transform Arabidopsis plants following the floral dip protocol (Clough & Bent, 1998). The transgenic lines *35S:HIPP20-GFP*, *35S:CSD1-GFP* and *35S:GFP* were generated by recombining the *pENTR* donor vectors with the *pK7FGW2* destination vector (Karimi et al., 2007). The transgenic lines *35S:CSD1* (*OxCSD1*) and *35S:FLAG-CSD1* (*OxFLAGCSD1*) were generated by recombining the *pENTR* donor vectors with the *pK7GW2* destination vector (Karimi et al., 2007). All transgenic lines were screened on kanamycin to establish stable non-segregating lines.

### 2.2 Bacterial and yeast strains

Several bacterial and yeast strains have been used in this study. The bacterial strains *DB3.1* (ThermoFisher), *TOP10* (ThermoFisher) and *DH5 $\alpha$*  (ThermoFisher) were used for the cloning approaches to acquire and propagate plasmids. The yeast strain *PJ69-4a* was used for the Y2H experiment and the *Agrobacterium tumefaciens* strain *GV3101* was used to generate transgenic Arabidopsis plants using the floral dip method (Clough & Bent, 1998).

## 2.3 Plant growth conditions

### 2.3.1 *Arabidopsis thaliana* cultivation on soil

*Arabidopsis* seeds were sown on soil (Einheitserde VM, Gebrüder Patzer, Sinnthal-Jossa, Germany) that was mixed with nematodes to prevent fly infestation. Stratification of seeds was performed at 4° C for 48 hours and then grown under long-day conditions (16 h light period at 21° C, 8 h darkness at 16° C) at 60% relative humidity and a light intensity of 120  $\mu\text{mol s}^{-1} \text{m}^{-2}$ . A light cycle of 8 h light at 22° C, 16 h darkness at 20° C with a relative humidity of 60% and a light intensity of 100  $\mu\text{mol s}^{-1} \text{m}^{-2}$  was used as short-day conditions. *Arabidopsis* plants grown under short-day conditions were used for the isolation of protoplasts.

### 2.3.2 *In-vitro* cultivation of *Arabidopsis thaliana*

For selection, sterile transgenic *Arabidopsis* seeds were grown on ½ MS medium (0.05% MES, 0.5% Sucrose) containing kanamycin. To sterilise *Arabidopsis* seeds, seeds were treated with 1 ml of sodium hypochlorite (1% v/v) for 5 minutes at room temperature. Afterwards, the sodium hypochlorite was decanted under sterile conditions and seeds were washed 5-times with 1 ml of sterile dH<sub>2</sub>O and sown to the plates. These plates were stratified for two days at 4° C in the cold room before being transferred to the long-day Percival.

For RNA-seq, CHIP-seq or pulldown experiments, sterile *Arabidopsis* seeds were sown directly in liquid ½ MS medium (0.05% MES, 0.5% Sucrose) in a 100-ml Erlenmeyer flask. These flasks were directly transferred into a Percival with long-day conditions.

## 2.4 Transfection of *Arabidopsis* mesophyll protoplasts

Transfection of *Arabidopsis* protoplasts was performed via the “Tape-Sandwich” protocol (Wu et al., 2009). For all transfections of *Arabidopsis* protoplasts to study protein localisations, 10  $\mu\text{g}$  of plasmid was used. In BiFC experiments, 5  $\mu\text{g}$  of plasmid was used. In transactivation assays, 5  $\mu\text{g}$  of the promoter and effector plasmid was used and 1.5  $\mu\text{g}$  of the reference plasmid.

## 2.5 Transfection of *Oryza sativa* stem cell protoplasts

For transfection of *Oryza sativa* stem cell protoplasts, *O. sativa* stems were cut with a razor blade into fine strips. Protoplasts were then generated and transfected following the tape-sandwich protocol (Wu et al., 2009), except using Onozuka RS cellulase (Duchefa) instead of Onozuka R-10 (Duchefa). Furthermore, the centrifugation steps were performed at 240 x g instead of 100 x g.

## 2.6 Nuclear localisation

Arabidopsis mesophyll protoplasts were isolated via the “tape-sandwich” method (Wu et al., 2009) and transfected with the *p2GWY7,0-CSD1* construct that is expressing the CSD1-YFP protein via a *35S* promoter. To study the localisation of the HIPP20 protein, the *p2FGW7,0-HIPP20* construct was used. For the HIPP21 and HIPP22 localisation, the *p2GWY7,0-HIPP21* and *p2GWY7,0-HIPP22* construct was used to transfect Arabidopsis mesophyll protoplasts. These gateway vectors were used from Karimi et al., 2007.

After the transfection, the protoplasts were kept in the dark overnight and examined using the confocal laser scanning microscope (Leica, SP8) at the following day. The 4',6-Diamidin-2-phenylindol (DAPI) was used to confirm the nuclear localisation and shortly before imaging.

Stable transgenic Arabidopsis plants expressing the *35S:HIPP20-GFP* or *35S:CSD1-GFP* were generated with the *pK7GWF7,0-HIPP20* or *pK7GWF7,0-CSD1* construct and the floral dip method (Clough & Bent, 1998). The plants were selected into the T<sub>2</sub> generation and afterwards examined using the confocal laser scanning microscope (Leica, SP8).

## 2.7 Fluorescence recovery after photobleaching (FRAP)

Transgenic Col-0 plants carrying a *35S:CSD1-GFP* or a *35S:GFP* construct were sowed out on ½ MS medium (0.05% MES, 0.5% Sucrose) and grown in a Percival for 2 weeks. The roots of seedlings were imaged under control (dH<sub>2</sub>O) and treated (NaCl) conditions by immersion in the indicated solution under a cover glass on an objective slide using a confocal laser scanning

microscope (SP8; Leica Microsystems). The following FRAP protocol was used to bleach the nuclei and measure the fluorescence recovery: (1) pre-bleach (2 iterations; t/iteration 3 seconds), (2) bleach (80% laser intensity, 4 seconds), (3) post-bleach 1 (60 iterations, t/iteration 3 seconds), (4) post-bleach 2 (20 iterations, t/iteration 6 seconds). For each individual condition, at least five individual measurements were performed. The standard deviation is displayed in the graphs.

## 2.8 Nuclear enrichment of the CSD1 protein

The transgenic Col-0 plants carrying a *35S:CSD1-GFP* construct were grown in liquid  $\frac{1}{2}$  MS medium (0.05% MES, 0.5% Sucrose) for 2 weeks. After 14 days the plants were stressed with 150 mM NaCl for 5, 10 and 15 minutes and frozen in liquid nitrogen. The nuclei of these plants were isolated following the protocol of Kaufmann *et al.*, 2010. Afterwards, the nuclei pellet was diluted in SDS-PAGE buffer and cooked for 10 minutes at 95 degrees to disintegrate the nuclei. Subsequently, the nuclei extract was chilled on ice for 5 minutes and subjected to an SDS-PAGE with 5% stacking and 12% resolving gels. After separation of the proteins, the proteins were transferred to a nitrocellulose membrane by semi-dry blotting at medium range following the manufacturer instructions (Pierce G2 FastBlotter, ThermoFisher). The membrane was incubated for 1 h at RT with 5% milk powder dissolved in TBST. The primary antibodies (anti-GFP 1:5000, anti-H3 1:5000) were incubated overnight at 4 degrees in 5% milk dissolved in TBST. After the incubation, the membrane was washed four times with TBST for 5 minutes followed by a 1.5-hour incubation with the secondary antibody (anti-mouse 1:5000 in 5% milk with TBST) at room temperature. Before imaging, the membrane was washed again with TBST four times for 5 minutes. For detection, 1 ml of the Luminata Crescendo HRP-substrate (Millipore, Burlington, MA, USA) was added onto the membrane and the ChemiDoc (BioRad, Hercules, CA, USA) was used as detection device.

## 2.9 Salt tolerance experiment

Col-0, *csdl-3* knockdown and *35S:CSD1* Arabidopsis plants were sowed on  $\frac{1}{2}$  MS (0.05% MES, 0.5% Sucrose) and stratified at 4 degrees for 48 hours. Three days after germination, the

seedlings were transferred to ½ MS (0.05% MES, 0.5% Sucrose, 125 mM NaCl) and observed for their survival after 5 days growth in the Percival under long-day conditions. The survival rate of the seedlings was determined as dead and alive. The sample-size was 20 seedlings per genotype and condition.

The effect of salt stress on soil-grown *Arabidopsis* plants was explored by sowing Col-0, *csdl-3* and *35S:CSD1* *Arabidopsis* seeds on soil. The seeds were stratified for 48 hours at 4 degree and afterwards transferred into the short-day growth chamber. After four weeks of growth, the plants were watered with a 350 mM salt solution three-times per week. This watering regime was performed for three weeks, and the effects were analysed after three weeks. The phenotype was analysed by leaf scoring where every plant with at least one senescing leaf (transition from green to yellow, chlorophyll breakdown) was scored. Through this analysis, the effects of the salt-stress regime on the different genotypes were discriminated. For each genotype and conditions, the sample size is n= 15.

## 2.10 Transcriptional profiling by RNA-seq

About 20 to 25 seeds of the Col-0, *csdl-3* and *35:CSD1* *Arabidopsis* genotypes were sowed in 20 ml of liquid ½ MS medium (0.05% MES, 0.5% Sucrose). The flasks were directly transferred to the long-day Percival and the seedlings grew for 14 days. After 14 days, the plants were stressed with 150 mM NaCl for 30 minutes and frozen in liquid nitrogen. The plants were grinded in a pebble mill with five metal beads and subsequently the total RNA was isolated following the manufacturer instructions (NucleoSpin® RNA kit, Macherey-Nagel, Düren, Germany). The total RNA was shipped on dry-ice to Novogene (UK) Company Limited (Cambridge, United Kingdom) and the mRNA-sequencing was performed as paired-end (150 bp per read) Illumina sequencing. The raw data was processed according to Pertea *et al.* (Pertea *et al.*, 2016). The *Arabidopsis thaliana* ENSEMBLE46 reference genome from January 2020 was used as reference for the Stringtie and DeSEQ2 analysis. The DeSEQ2 tool was used to generate the final output of the differential expressed genes which is using the WALD statistics and the Benjamini-Hochberg correction for the adjusted p-value. For all analysis, the internal galaxy platform was used (<https://usegalaxy.org>).



## 2.11 Transcriptional profiling by RT-qPCR

Corresponding to the RNA-seq experiment, 20 to 25 seeds of the Col-0, *csd1-3* and *35S:CSD1* Arabidopsis genotypes were grown in 20 ml liquid ½ MS medium (0.05% MES, 0.5% Sucrose) for 14 days and afterwards stressed with 150 mM NaCl for 30 minutes. Subsequently, the total RNA was isolated following the manufacturer's instructions (NucleoSpin® RNA, Macherey-Nagel, Düren, Germany). A genomic DNA digestion is part of the kit and was performed as on-column digestion. The cDNA synthesis was performed with 2.75 µg of total RNA and oligo(dT<sub>18</sub>) primer following the manufacturer's instructions (RevertAid First Strand cDNA synthesis kit, Thermo Fischer). After the synthesis, the cDNA was diluted with 60 µl of ddH<sub>2</sub>O and stored at -80 degrees until further use.

Quantitative RT-PCR was performed in 5 µl reactions with the PowerUP™ SYBR™ Green Master Mix (Thermo Fischer) and measured with the QuantStudio™ 5 Real-Time-PCR system (Applied Biosystems™, Thermo Fischer) according to the manufacturer instructions. The software settings were used to determine the relative quantification of gene expression. All reactions were performed with at least three technical replicates. Expression levels were normalised using Ct values obtained for the housekeeping gene *UBI10* (AT4G05320).

A list of the gene-specific qPCR primers that were used in this study can be found in **Table 2**. These primer pairs were designed with the QuantPrime software tool (Arvidsson et al., 2008).

**Table 2:** List of primers used for the gene expression analysis. Displayed are the forward and reverse primer sequences used in this study. The primers were designed using the QuantPrimer software tool (Arvidsson et al., 2008).

Primer name	Sequence (5' - 3')
AT1G25560_qF_TEM1	GGATGAATCCGTCTCCGACGAAAG
AT1G25560_qR_TEM1	AACCGCCACACTTTCCTGTTC
AT1G68840_qF_TEM2	TGGGAAGCTAAACCGTCTCGTG
AT1G68840_qR_TEM2	ACGGTGACGGTAACGGAAAGTG
AT1G19180.1_qF_JAZ1	TGTTCTGAGTTCGTCCGGTAGCC
AT1G19180.1_qR_JAZ1	AGTTCCATTGACATCAGGCTTGC
AT2G02990.1_qF_RNS1	AATCTTGCCTTCTGTCTTCTCTGC

---

AT2G02990.1_qR_RNS1	GTCACAGTATGATCCTGGCCATTG
AT2G24850.1_qF_TAT3	CCATTCCAACCTTCAGGACTTGCC
AT2G24850.1_qR_TAT3	AAATATTCAGCCACCGCCCTTC
AT3G14440.1_qF_NCED3	TCGAAGCAGGGATGGTCAACAG
AT3G14440.1_qR_NCED3	GCTCGGCTAAAGCCAAGTAAGC
AT3G22830_qF_HSFA6B	TCAGCAGCTAGTAGAGCAGAAGG
AT3G22830_qR_HSFA6B	TCTTCTTGCTGATCGCCTCTTCG
AT1G55330_qF_AGP21	TGGTTGTTGCGGTGGCTTTCTC
AT1G55330_qR_AGP21	GCAGCATCAGAAGTTGGGCTTG
AT2G27690_qF_CYP94C1	AAGAACTGGACCGGGTTATGGG
AT2G27690_qR_CYP94C1	TTTCATCGCAACGAGCAGTGAC
AT3G62100.1_qF_IAA30	CGTGCTAACGTACGCAGACAAAG
AT3G62100.1_qR_IAA30	CTCACGCTAGACAAGAACATCTCC
AT1G02310.1_qF_MAN1	TCCATATCTACCCGGATTCTTGGC
AT1G02310.1_qR_MAN1	ATGTGCTCCGATCCATCTGTCC
AT1G08830.1_qF_CSD1	AACGGTTGCATGTCTACTGGTC
AT1G08830.1_qR_CSD1	GTGATTGTGAAGGTGGCAGTTCC

---

## 2.12 SELEX

The protein coding sequences of *CSD1* and *KUA2* were cloned into the *Flexi*® vector (Promega) by using the *SgfI/PmeI* restriction enzymes. A FLAG-tag was introduced while the coding sequences were amplified from the original *pENTR*® entry clone. The protein expression was performed in the *Wheat Germ Extract* (Promega) following the manufacturer's instructions. After the expression, the FLAG-tagged fusion proteins were cleaned up with 25 ul of Anti-FLAG® M2 magnetic beads (Sigma-Aldrich) following manufacturer instructions. The proteins were bound to the beads by incubation at 4 degrees for 1 hour on a vertical rotor. The

bead-protein mixture was now used for the SELEX approach and incubated with the synthetic DNA library for 1 hour at 4 degrees on an orbital shaker. The synthetic library was amplified with a standard Taq-polymerase PCR and purified by the PureLink® Quick Gel Extraction Kit (Invitrogen). By using the MagneSphere® Technology (Promega) the supernatant was discarded and the bead-protein-DNA complex was washed with a Tris-HCl buffer for three times. The elution was performed with 50 µl of 0.1 M Glycine-HCl (pH 3.0) with subsequent neutralisation with 150 µl 1 M Tris (pH 8.0). 10 µl of this supernatant was used for the next PCR amplification cycle which was performed as indicated above. The described cycle was performed six times. After the last cycle, the small DNA molecules were cloned into the *pJET 1.2/blunt* vector (Thermo Scientific) and sequenced.

### 2.13 DAP-seq

For the DAP-seq experiment, which was performed by Anna Bartlett, analysed by Carol Huang and supervised by Joe Ecker at the Salk Institute in La Jolla, CA, USA, the expression vector of CSD1 fused to a HALO-tag or fused to a FLAG-tag was prepared. The experiment at the Salk Institute was performed and analysed as described before (O'Malley et al., 2016; Bartlett et al., 2017).

### 2.14 ChIP-seq

About 25 Arabidopsis Col-0 seeds were sowed in 25 ml of liquid ½ MS medium (0.05% MES, 0.5% Sucrose) and grown for 16 days under long-day conditions. On the 16<sup>th</sup> day of growth, the plants were treated with 150 mM NaCl for 30 minutes. The ChIP-seq experiment was performed according to the protocol from Kaufmann *et al.* with minor modifications (Kaufmann et al., 2010; Neuser et al., 2019). For each replicate, all grown seedlings were harvested and directly cross-lined in 1% formaldehyde solution. Obtained chromatin pellets were sonicated at 4° C with a standard stab sonicator. From the sonicated chromatin a sample was set aside to serve as input DNA, while the remaining was equally divided into an IP-sample and negative control sample. For the IP sample, the specific CSD1-antibody (25 µl), which was designed and extracted at the IPK, was used together with Pierce™ Protein A magnetic beads

(Thermo Fischer). As negative control only, magnetic beads were used. Obtained DNA from the input, IP and negative control fractions was purified with the MinElute® PCR purification Kit (QIAGEN, Hilden, Germany). The quantitative PCR reactions were performed with PowerUP SYBR Green Master Mix (Applied Biosystems) on a QuantStudio 5 Instrument (Applied Biosystems) using specific primers to various promoter regions of selected putative target genes. Obtained data for the different samples were processed and normalised to their input DNA.

The ChIP sequencing was performed at Novogene (UK) Company Limited (Cambridge, United Kingdom) by sending the samples on dry ice. The analysis of the ChIP-seq raw data was performed by using the internal galaxy platform. After finalising the QC and trimming, the raw data were mapped to the Arabidopsis Araport11 genome version by using Bowtie. In the second step, the MACS2 software was used to call the individual peaks followed by the motif analysis using HOMER. Individual peaks were visualised with the integrated genome browser (IGB).

## 2.15 EMSA

The electrophoretic mobility shift assay (EMSA) was performed by using IRDye680®-conjugated DNA probes of 35-40 nucleotides. The forward and reverse sequences were conjugated with the IRdye680 at the 5' ends. Initial annealing was performed by mixing 5 µl of forward and reverse DNA probe (100 µM stock) in 30 µl of nuclease-free water in amber tubes. The probe mixture was incubated at 95° C for 5 minutes and slowly cooled down to room temperature to allow annealing. The labelled probe was diluted 1:200 in nuclease-free water to be ready for use.

Binding reactions were performed on ice for 60-90 minutes by using the Odyssey® Infrared EMSA kit (LI-COR). A 20 µl binding reaction contained 2 µl 10x binding buffer (100 mM Tris, 500 mM KCl, 10 mM DTT; pH 7.5), 0.5 µl 100 mM MgCl<sub>2</sub>, 0.5 µl 1M KCl, 1.0 µl of Poly(dIxdC) (1 µg/µl in 10 mM Tris, 1 mM EDTA, pH 7.5), 2 µl of labelled probe (1:200), 5 µl of purified CSD1 protein (400 ng/µl, expressed in *E. coli*, His-Tag). For competition, 2 µl of the undiluted unlabelled EMSA probe was added to the binding reaction.

After the incubation of the binding reaction, 2 µl of Orange loading dye was added to the binding reaction. Subsequently, the protein-DNA mixture was loaded onto a pre-run 5% TBE

PAGE gel containing 0.25% glycerol and run at 70 V in the dark at 4° C for 60 minutes. The IRdye680 was imaged using an Odyssey® imaging system (LI-COR).

The EMSA probes used in this study are displayed in **Table 3**.

**Table 3:** EMSA probes used in this study. The individually designed EMSA probes of this study are displayed and the putative CSD1 binding site is highlighted.

Probe name	Sequence (5' - 3')
SPL2_motif1_F	aaacaactcttatac <u>TGCTTT</u> ttaaagtattgaagaat
SPL2_motif1_R	attcttcaatacttaa <u>AAAGCA</u> gtataagaagtgtt
SPL2_motif2_F	aaactaaaacatac <u>TAAAGCA</u> tggtgtcttgattt
SPL2_motif2_R	aaaatcaagacaacca <u>TGCTTTA</u> gtatatgttttagtt
NCED3_motif1_F	tgccaagaattgg <u>AAGCTTTT</u> gttaccaaaact
NCED3_motif1_R	agtttgtaac <u>AAAAGCTT</u> ccaattctttggca
ZAT7_motif1_F	ttgtatttgggag <u>AAAGCA</u> ccaagaacattcctt
ZAT7_motif1_R	aaaggaatgttctgg <u>TGCTTT</u> ccaccacaaaataca
ZAT7_motif2_F	tattcttacttt <u>AGCTTA</u> cttacgcagaagcac
ZAT7_motif2_R	gtgcttgctgcgtaag <u>TAAGCT</u> aaagtgaaggaaata
HSFA6B_motif1_F	gatgccaacaacacaag <u>TGCAA</u> ttctttaatatgaaa
HSFA6B_motif1_R	tttcatataaaagaa <u>TTTGCA</u> ctttgtgttggtgcatc
HSFA6B_motif2_F	aacactctttattata <u>AGCTAT</u> taacaaaactctgcct
HSFA6B_motif2_R	aggcaagattttgtta <u>ATAGCT</u> tataataaagaagtgt
TAT3_motif1_F	gtagtgttcacgag <u>ATCGAAT</u> atttctgtttttg
TAT3_motif1_R	caaaaaacaagaaat <u>ATTCGAT</u> ctcgtgaaactacc
TAT3_motif2_F	gttataactaacatta <u>AGCTAT</u> agttaaatgttagtt
TAT3_motif2_R	Aactaaacatttaact <u>ATAGCT</u> taatgtaagtataac
CIF1_motif1_F	aagagcataatacgacattaatt <u>TGCATT</u> aatcgtaagtgcaattatgt
CIF1_motif1_R	acataattgcaactgacgatt <u>AATGCA</u> aattaatgctgattatgctctt
MDAR4_pemo1_F	agaaacatgggaagagc <u>TTTCGT</u> gtatgtaattctcgagg
MDAR4_pemo1_R	cctccgagaattacatac <u>ACGAAA</u> gctcttcccattggttct
MDAR4_pemo2_F	tcgtgcaagcaaagagt <u>TAAGCTA</u> ggcccactctcataat
MDAR4_pemo2_R	attatgagagtgaggacc <u>TAGCTTA</u> actctttgcttgcacga

## 2.16 Hydrogen peroxide treatment of CSD1

The pre-treatment of CSD1 with hydrogen peroxide was performed on ice by the addition of equal volumes of different H<sub>2</sub>O<sub>2</sub> stocks to ensure equal CSD1 concentrations in the stocks. CSD1 was incubated with different H<sub>2</sub>O<sub>2</sub> concentrations for 4 hours on ice and used for the EMSA or activity assay experiment subsequently.

## 2.17 SOD activity assay

The SOD activity assay was performed by using the *E. coli* expressed CSD1 protein and the SOD assay kit (Sigma Aldrich). This kit is using the WST/WST-formazan formation upon superoxide production by the xanthine oxidase. The assay was performed following the manufacturer's instructions and measured at 30 and 60 minutes after incubation in a standard 96-well plate reader.

## 2.18 Transactivation assay

*Arabidopsis mesophyll* protoplasts were isolated and transfected as previously described (Wu et al., 2009). The coding sequences of the effector proteins like CSD1 and FLAGCSD1 were recombined with the *p2GW7,0* vector (Karimi et al., 2007) containing the CaMV 35S promoter. Upstream promoter regions of putative target genes were cloned with a targeted size of 1 kb and recombined with the *p2GWL7,0* vector to place them upstream of the firefly *LUC* gene (Table 4). Protoplasts were co-transfected with both indicated vectors (5 µg per transfection) and a normalisation vector *UBI10:RnLUC* (1.5 µg per transfection) (Licausi et al., 2011). Dual-Luciferase® Reporter assays (Promega) were performed as previously described (Licausi et al., 2011). Luminescence was measured using a GloMax® Discover device (Promega).

**Table 4:** Primers used in this study to amplify promoter sequences for the transactivation assays. The displayed primers were designed to amplify and clone a promoter sequence of approximately 1kb.

Primer name	Sequence (5' - 3')
AT2G24850_pTAT3_for	CACCCACAATTAGATGCATTTTTTTCATCTG
AT2G24850_pTAT3_rev	GATCTTTCTGTCTTGCCTTTG
AT3G14440_pNCED3_for	CACCGTGTTC AATTAAGGATTTTTGTTCAC
AT3G14440_pNCED3_rev	CAAGTGTGTTC AATCAGTATTTGG
AT3G22830_pHSFA6B_for	CACCGGAAGCTACCCTGCCCATG
AT3G22830_pHSFA6B_rev	CAAAGATTTTTTTATGTGGGTTTGAA

## 2.19 Gal4-based transactivation assay

In Gal4-based transactivation assays, the principle that the Gal4-DNA binding domain (DBD) binds the *upstream-activating-sequence* (*UAS*) was used. Therefore, Arabidopsis mesophyll protoplasts were transfected as described before with the vectors *pDBD-GW7* (*35S:Gal4DBD-GW*) and *pUAS:flUC* (*UAS:flUC*) (Licausi et al., 2011). The effector proteins to study were recombined with the *pDBD-GW7* by an LR reaction following manufacturer instructions (ThermoFisher). For example, Arabidopsis mesophyll protoplasts were transfected with *pDBD-CSD1* (5 µg), *pUAS:flUC* (5 µg) and *35S:RnLUC* (5 µg, reference plasmid) to study the effector protein CSD1.

## 2.20 Bimolecular fluorescence complementation (BiFC)

The expression vectors *pUC:SPYNE* (N-terminal YFP half) and *pUC-SPYCE* (C-terminal YFP half) were used as vector system to study interactions in Arabidopsis mesophyll protoplasts (Schütze et al., 2009). For example, the coding sequence of CSD1 and HIP20 was introduced by recombining the *pENTR-CSD1/HIP20* donor vectors with the *pUC:SPYNE* or *pUC:SPYCE* destination vectors by an LR reaction (ThermoFisher) following manufacturer instructions.

Arabidopsis mesophyll protoplasts were transfected with 10 µg of the *pUC:SPYNE-CSD1* and *pUC:SPYCE-HIPP20* constructs and analysed with a confocal laser scanning microscope the following day. A DAPI staining was used to confirm the nuclear localisation. Other BiFC experiments were performed as described.

## 2.21 Yeast Two-hybrid (Y2H)

The *PJ69-4a* yeast strain was used and transformed via a Y2H transformation protocol (Gietz & Woods, 2002). 10 µg of plasmids were used and 0.1 mg of carrier DNA (salmon sperm). Yeast cells were transformed with the *pDEST22* and *pDEST32* (Invitrogen) destination vectors. Here, the *pDEST32-CSD1* (*pUC:Gal4DBD-CSD1*) and *pDEST22-HIPP20/21/22* (*pUC:Gal4AD-HIPP20/21/22*) vector combinations were used. Transformed yeast cultures were incubated for 3h at 28° C with 250 rpm. Afterwards the cells were centrifuged and diluted in 500 µl ddH<sub>2</sub>O. Each dilution was further diluted 1:10 and 1:100 and subsequently spotted onto SD medium plates lacking tryptophan and leucine (-LW) or lacking tryptophan, leucine and histidine (-LWH) in duplicates. Furthermore, 3-amino-triazole (3-AT) was added to the selection plates in 1 mM and 5 mM concentration to increase the selection pressure towards strong interactions.

## 2.22 Extraction of total soluble protein extracts

To study the abundance and presence of CSD1 proteins in different Arabidopsis plants, the total protein from Arabidopsis seedlings was extracted using the following method. Approximately, 100 to 200 mg of plant material was harvested in a 2.0 ml Eppendorf tube with 3-4 small magnetic beads and quick-frozen in liquid nitrogen. By using a Retsch® mill the plant material was ground and afterwards homogenised with 2 volumes (volume of ground powder) of extraction buffer (50 mM Tris-HCl pH 7.5, 150 mM NaCl, 1% Triton-X-100, protease inhibitor cocktail mix (Roche)). The homogenous mixture was then kept on ice for 30 minutes for solubilisation. Subsequently, the extract was centrifuged at max speed at 4° C for 15 minutes to separate the soluble protein extract from the remaining debris. The soluble protein extract was afterwards used for the western blot analysis.



### 2.23 SDS-PAGE and Western blot

The concentration of protein extracts was determined by using the Pierce Coomassie Protein-Assay-Kit (Lot. No. 23200, ThermoFisher). Afterwards, 30 µg of total protein was denatured with the Protein Sample Loading Buffer (Lot. No. 928-40004, LI-COR) at 95° C for 5-7 minutes and loaded and separated onto a 4/12% SDS-PAGE gel. The SDS-PAGE was performed using and following the *Mini-PROTEAN Tetra Cell* system (Bio-Rad) and instructions. Transfer of the proteins from the SDS-PAGE gel to a nitrocellulose membrane was performed using the Pierce G2 Fast Blotter (ThermoFisher) using the mid-range settings (25 V, 8 minutes) and following the manufacturer's instructions. The nitrocellulose membrane was blocked overnight at 4° C or for 1 h at RT with shaking with 5% non-fat milk powder dissolved in TBST (0.1% Tween). The primary antibody (rabbit anti-CSD1; 1:1000) was incubated at RT for 1.5 h with shaking in 5% non-fat milk powder dissolved in TBST. Before incubation with the secondary antibody (anti-rabbit IRdye680 (LI-COR); 1:5000), the nitrocellulose membrane was washed 4-times with TBST. The incubation with the secondary antibody was performed at RT with shaking for 1.5 h. After incubation with the secondary antibody, the membrane was washed 4-times with TBST. Finally, the membrane was imaged using the LI-COR Odyssey device at 700 nm wavelength. The ponceau staining (0.01 % Ponceau S in 1% acetic acid) was performed after the imaging to control for equal loading.

### 2.24 Immunoprecipitation

To study and explore the complex formation of CSD1 and CSD2 in Arabidopsis, an immunoprecipitation experiment with Arabidopsis Col-0 seedlings using the MagnaChIP™ Protein A magnetic beads (Sigma-Aldrich, Lot. No. 16-661) and the anti-CSD1 antibody was performed. Arabidopsis Col-0 seedlings were grown in liquid ½ MS medium (with 0.5% sucrose) for 13 days and stressed with 150 mM NaCl (5, 10, 30 minutes), 10 mM H<sub>2</sub>O<sub>2</sub> (5 and 30 minutes) and 5 µM paraquat/methyl viologen (5 and 30 minutes). Afterwards, seedlings were immediately frozen in liquid nitrogen. Seedlings were ground with metal beads and a Retsch® mill (approx. 1 g of plant material) and mixed with 2 volumes of extraction buffer (50 mM Tris-HCl pH 7.5, 150 mM NaCl, 1% Triton-X-100, protease inhibitor cocktail and

PhosSTOP mix (Roche)). Samples were kept on ice for 30 minutes for solubilisation and homogenisation. To separate the soluble proteins from the remaining debris, the mixture was centrifuged at max speed at 4° C for 15 minutes and the supernatant was transferred to a new tube. This step was repeated to ensure that no debris remained. The supernatant was diluted with the pulldown buffer (extraction buffer without the Triton-X-100) to adjust the Triton-X-100 concentration to 0.2% in a 15-ml falcon tube. Here, 20 µl of the CSD1-specific antibody (produced in rabbit) and, for four negative control replicates, 20 µl of the mCherry-specific antibody (produced in rabbit) was added to the soluble protein extract. This mixture was incubated overnight at 4° C with end-over-mixing. On the following day, 20 µl of the MagnaCHIP Protein A magnetic beads were prepared by washing them three times with 500 µl of the pulldown buffer to remove the storage solution. A magnetic stand was used to separate the magnetic beads and the supernatant. Subsequently, 20 µl of magnetic beads was added to the total protein-antibody mixture and incubated at 4° C for 3 hours with end-over-mixing. Afterwards, the magnetic beads were precipitated with the magnetic stand to remove the supernatant. The magnetic beads were washed three times with 400 µl of the pulldown buffer. For the mass spectrometry analysis, the beads were again washed four times with 500 µl of 50 mM Tris-HCl pH7.5, 150 mM NaCl to remove the protease inhibitor cocktail. Finally, the beads were resuspended in 100 µl of 50 mM Tris-HCl pH7.5 and prepared for transport to the collaboration partner on dry ice.

## 2.25 Mass spectrometry analysis

The pulldown samples with the protein complexes bound to the magnetic beads were shipped on dry ice to Prof. Dr. Iris Finkemeiner in Münster (Germany). At the lab of Prof. Dr. Iris Finkemeier, the peptides were digested in an on-bead digestion procedure with either GluC (N-terminal acetylation experiment) or Trypsine (Interactome analysis) depending on the application. The mass spectrometry analysis was performed by Dr. Jürgen Eirich and was based on the enrichment of peptides in comparison to the negative control enrichment (magnetic beads + mCherry-specific antibody produced in rabbit). Hereby, an enrichment of the peptides was determined and analysed for significance. Further information about the mass spectrometry analysis is described in Balparda et al., 2022.

## 2.26 Statistical analysis

Significant variations between genotypes or treatments were evaluated by either a Student's t-test, one-way or two-way ANOVA where appropriate. Mean values that were significantly different ( $p < 0.05$ ) from the control or wild type treatment are marked with an asterisk or small alphabetic character. The use of different statistical methods, for example for the RNA-seq and ChIP-seq analysis, is indicated in the corresponding chapters.

## 3 RESULTS

### 3.1 Chapter 1: CSD1 translocates to the nucleus upon salt stress and regulates the expression of salt-responsive genes

Based on previous studies in yeast and human cells, SOD1 does not only act as a scavenging enzyme but also as transcriptional regulator (Tsang et al., 2014; Li et al., 2019). The scope of this chapter is to explore the moonlighting function of CSD1 in Arabidopsis by using a combination of molecular, biochemical and physiological experiments.

#### 3.1.1 CSD1 translocates to the nucleus upon salt stress

CSD1 encodes the cytosolic SOD1 isoform in plants, and its counterparts in yeast and human cells were shown to be present in the nucleus (Tsang et al., 2014; Li et al., 2019). To determine the localisation of the Arabidopsis CSD1 protein, the coding sequence of *CSD1* was cloned, fused to YFP, and transformed into Arabidopsis protoplasts (**Figure 1 A**). Microscopical analysis revealed that the CSD1 protein has a cytosolic and nuclear localisation.

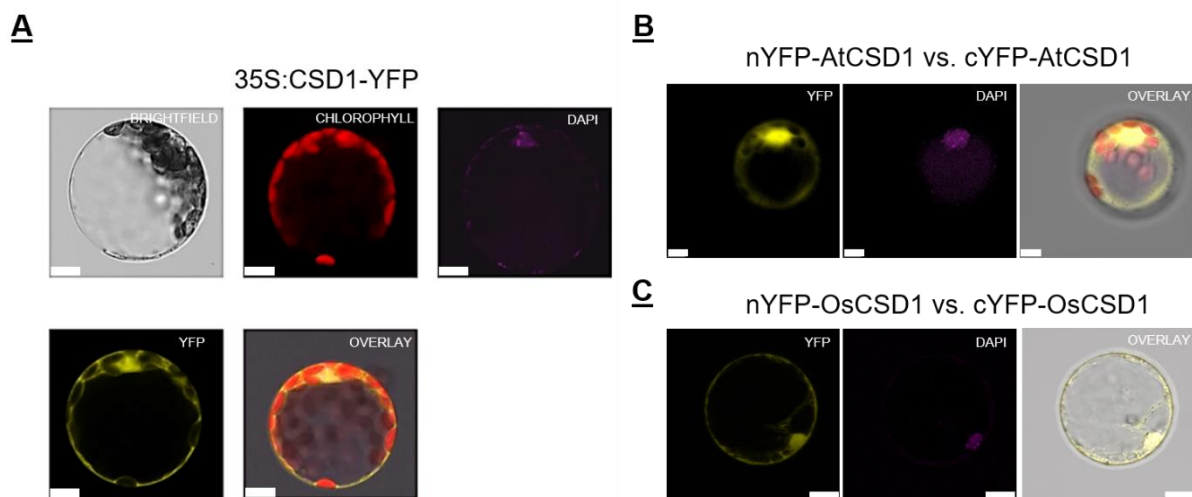


**Figure 1:** Localisation of CSD1 in Arabidopsis and *Oryza sativa* protoplasts. (A) C-terminal fusion of YFP to CSD1 was used to explore the cytosolic and nuclear localisation of CSD1 in Arabidopsis protoplasts. Red is the chlorophyll autofluorescence, magenta is the DAPI staining and yellow is the YFP fluorescence. Scale bar: 7.5  $\mu$ M. (B) Bimolecular fluorescence complementation (BiFC) in Arabidopsis protoplasts was used to analyse the dimer formation of CSD1 in the cytosol and nucleus. Scale bar: 5  $\mu$ M. (C) In *Oryza sativa*, BiFC was used to analyse the cytosolic and nuclear dimer formation of OsCSD1. Scale bar: 10  $\mu$ M. DAPI staining was used to confirm the nuclear localisation.

SOD1 protein is able to form dimers in the cytosol (Kim et al., 2014; Zhong et al., 2017). By a bimolecular fluorescence complementation (BiFC) assay in Arabidopsis, it was tested whether the CSD1 protein can also form dimers and if these dimers are also present in the nucleus. The BiFC assay revealed that CSD1 dimers are localised to the cytosol and the nucleus in Arabidopsis (**Figure 1 B**). To understand if dimer formation and nuclear localisation is conserved, the BiFC experiment was also performed with the CSD1 protein of *Oryza sativa*. Dimer formation in the cytosol and nucleus for OsCSD1 was observed in rice suggesting that it represents a conserved feature (**Figure 1 C**).

As the enzymatic function of CSD1 involves dismutation of superoxide radicals to hydrogen peroxide, which both harbour a molecular damage potency to DNA and proteins, and no direct formation of both molecules in the nucleus is known, there is no obvious protective reason for a nuclear localisation of CSD1 (Waszczak et al., 2018). Also, studies in yeast and human HeLa cells showed a stress-specific enrichment of SOD1 inside the nucleus (Tsang et al., 2014; Li et al., 2019). This provoked the hypothesis that the nuclear localisation of CSD1 might be dynamic. To explore the translocation of CSD1 to the nucleus upon stress, a fluorescence recovery after photobleaching (FRAP) assay in transgenic plants expressing a *35S:CSD1-GFP* fusion protein was performed (**Figure 2**).

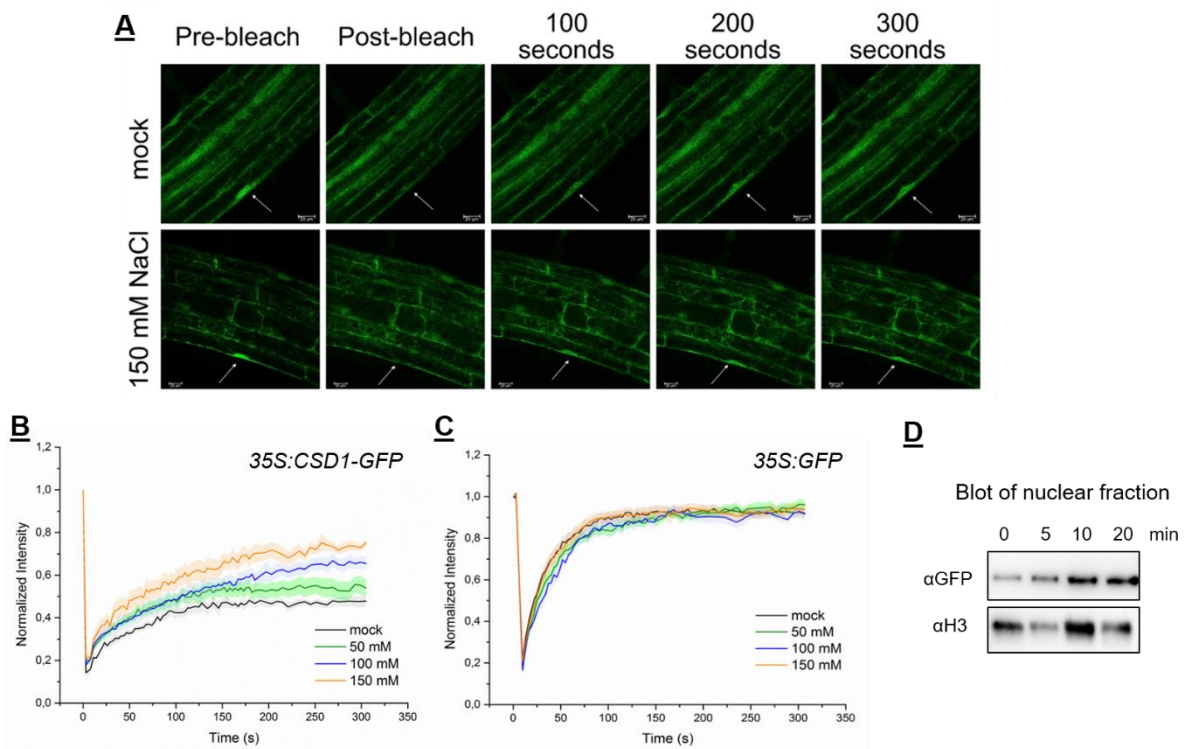


**Figure 2:** CSD1 translocate to the nucleus upon salt stress. **(A)** Stable transgenic *35S:CSD1-GFP* Arabidopsis root cells were used for FRAP analysis. Specific time points of the FRAP analysis are shown. White arrows indicate targeted nucleus. Scale bar: 20  $\mu$ M. **(B)** The quantification of the fluorescence intensity over time is plotted for control and salt stress measurements. The data is represented as the change of the initial pre-bleach signal intensity. Data points represent the average of ten independent measurements. Error bands represent the mean deviation. **(C)** The FRAP quantification for the negative control of stable transgenic *35S:GFP* Arabidopsis plants is shown. Data points represent the average of at least three independent measurements. Error bands represent the mean deviation. **(D)** The isolated nuclear fraction of *35S:CSD1-GFP* Arabidopsis seedlings were analysed for the enrichment of the CSD1-GFP fusion protein by immunoblotting. Nuclei were isolated from untreated and treated (150 mM NaCl) Arabidopsis seedlings. An anti-HISTONE3 antibody was used as loading control.

Under control conditions, 45 % of the pre-bleach signal intensity was restored after 5 minutes of recovery (**Figure 2 B**). To understand if this is due to passive diffusion or an actively triggered process it was hypothesised that stress might promote nuclear localisation and thereby accelerate the signal recovery. Interestingly, nuclear CSD1 levels recovered more rapidly after NaCl stress in a concentration-dependent manner (**Figure 2 B**). As a control, plants expressing only GFP were used to validate the stress-dependent translocation of CSD1 (**Figure 2 C**). Independent of the conditions, the fluorescence signal of GFP recovers in a steady fashion indicating a diffusion-based signal recovery in the nucleus. As GFP translocation alone was not influenced by NaCl, it suggests that the CSD1 protein is actively transported to the nucleus upon stress.

With increasing salt concentration, fluorescence recovery is faster, corresponding with a more rapid translocation of CSD1 to the nucleus. This observation indicates that the translocation of CSD1 to the nucleus occurs in a stress-specific and concentration-dependent manner, most likely by an active transport mechanism.

To validate these observations, the nuclei from transgenic *35:CSD1-GFP* plants under control and salt stress conditions were isolated (**Figure 2 D**). By using a GFP-specific antibody and a HISTONE3-specific antibody as loading control, the salt-induced enrichment of CSD1 in the nucleus within 5 minutes of stress was confirmed.

By using a set of different experimental approaches, the nuclear localisation of CSD1 and also the stress-specific nuclear enrichment of CSD1 was explored. The translocation is most likely facilitated by an active import mechanism; however, the precise mechanism remains elusive. The findings raise a set of subsequent questions: What is the role of CSD1 in the nucleus and why does CSD1 specifically translocate upon salt stress? These questions raised the hypothesis that CSD1 might be an important salt stress regulator in the nucleus.

### 3.1.2 CSD1 is required for the salt stress response in Arabidopsis

The salt stress induced translocation of CSD1 to the nucleus raised the question if CSD1 is a regulator of salt stress responses in Arabidopsis. A T-DNA insertion line of CSD1, *csd1-3* (SALK\_024857) (**Figure 30**), was identified as *CSD1* knockdown line and a stable *35S:CSD1* transgenic line was generated as overexpression line to test the role of CSD1 in salt stress tolerance in Arabidopsis (**Figure 4 C**). Of note, as CSD1 has a dual function, one as a ROS scavenging enzyme and the second a here to be explored nuclear function, it will be challenging to entangle the contribution of each to salt stress tolerance. Seeds of *csd1-3*, WT and *35S:CSD1* plants were germinated and grown for 3 days on ½ MS plates and subsequently transferred to ½ MS plates containing 125 mM NaCl (**Figure 3 A**).

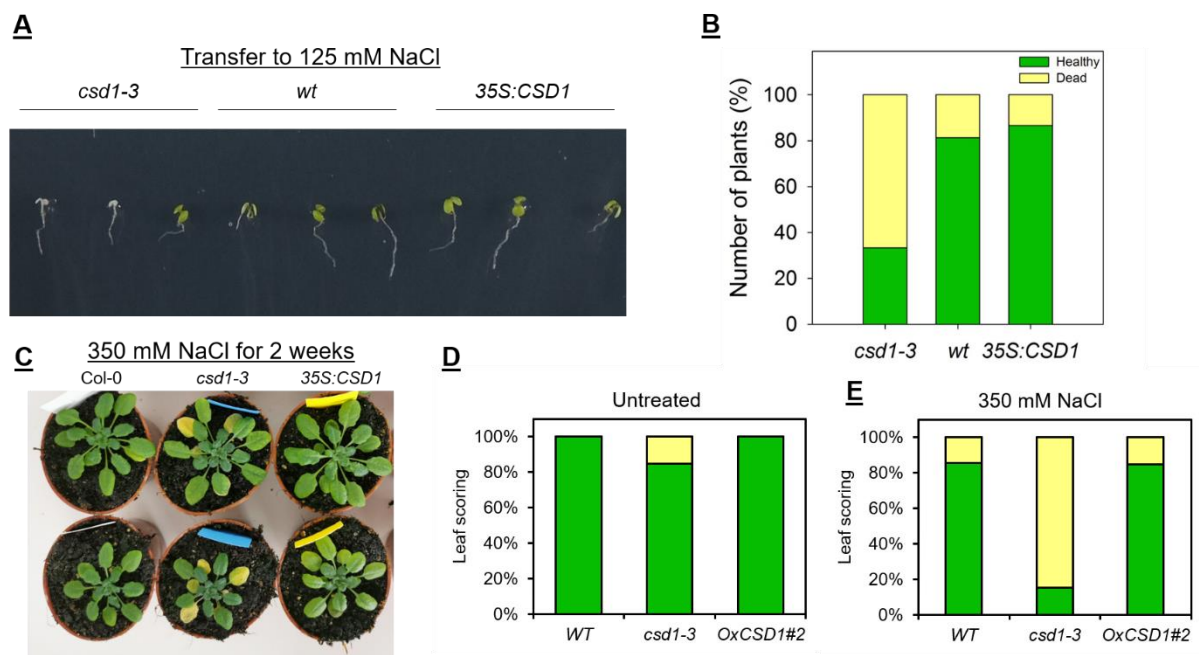


**Figure 3:** CSD1 is required for salt stress tolerance in Arabidopsis. (A) Salt tolerance assay with the transfer of 3 days old seedlings to  $\frac{1}{2}$  MS medium containing 125 mM NaCl. Survival scoring was done after 4 days of growth on salt-containing medium. (B) Quantification of the salt tolerance assay in Panel A. Plants with bleached cotyledons were considered as dead. In total, 20 seedlings per genotype were analysed. The experiment was independently repeated with similar results. (C) Col-0, *csd1-3* and *35S:CSD1* Arabidopsis plants were grown for 6 weeks under short-day regime and then watered for 2 weeks with 350 mM NaCl solution. Afterwards, the senescing leaves were scored. (D and E) Quantification of the salt-stress tolerance assay in Panel C was performed by using a leaf scoring determining percentage of plants with yellow leaves (Yellow leaf in percent). In total, 15 plants were analysed for each condition and genotype. The experiment was repeated independently with similar results.

The *csd1-3* plants showed an impaired growth upon salt stress while the *35S:CSD1* plants showed a wild type-like phenotype. The determination of the survival rate revealed that knock-down of *CSD1* negatively impacts the survival rate of Arabidopsis seedlings during salt stress (Figure 3 B). The *35S:CSD1* plants did not show a significantly increased survival rate compared to the *Col-0* wild type plants. In a follow-up experiment, the response to salt stress in the adult plant phase was analysed by growing the WT, *csd1-3*, *35S:CSD1* plants on soil under short day conditions for 6 weeks followed by a watering-phase with 350 mM NaCl solution. After two weeks of watering with the salt solution the phenotype was analysed (Figure 3 C). A picture of the corresponding control plants can be found in the supplement (Figure 29). The visible inspection of the phenotype showed that salt stress leads to an accelerated senescence phenotype in the *csd1-3* background. The phenotype of the Col-0 and *35S:CSD1* plants was mildly affected by the salt stress and no difference between these phenotypes were



observed. To quantify the salt stress experiment, a leaf scoring for all plants, control and salt stress condition, was performed that scores the appearance of yellow leaves (**Figure 3 D**). The leaf scoring showed that already under control conditions, several *csd1-3* plants display early senescence which is dramatically increased under salt stress where more than 80 % of all *csd1-3* plants contain one or more yellow leaves. In contrast, wild type and *35S:CSD1* plants did not show a difference in their phenotype with about 20 % of plants displaying yellow leaves. However, it is important to note that under control conditions, wild type and *35S:CSD1* plants did not show any yellow leaves, only upon salt stress.

Summarised, lower levels of CSD1 result in an impaired response to salt stress with a decreased survival rate during the early seedling stage and an accelerated senescence response during the adult plant phase in Arabidopsis.

### 3.1.3 Transgenic *35S:FLAG-CSD1* plants indicate role of CSD1 in developmental processes

Initially, prior to obtaining a CSD1 antibody, transgenic lines expressing a FLAG-tagged CSD1 protein were established for performing a ChIP-seq experiment. However, instead of obtaining an overexpression line, the overexpression of the FLAG-tagged CSD1 protein resulted in a complete knock-down of the transgene and the endogenous gene. A *pK7GW2:FLAG-CSD1* construct was transformed into Col-0 wild type plants to generate the *35S:FLAG-CSD1* transgenic line. Several independent transformations events were screened into the T<sub>2</sub> generation. The transgenic lines showed an astonishing phenotype that does not overlap with the phenotype of *35S:CSD1* plants, but rather mimicked the *csd1-3* lines (**Figure 4**).

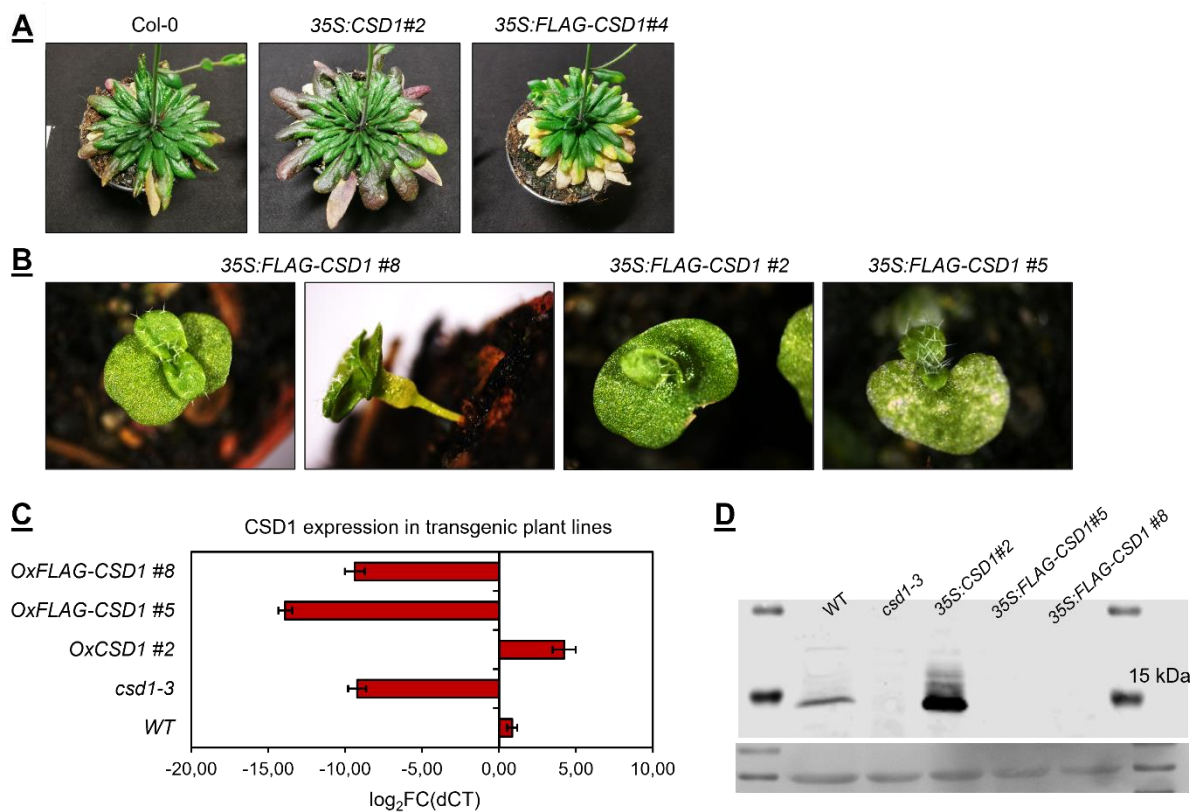


**Figure 4:** Overexpression of FLAG-CSD1 in Arabidopsis results in severe knock-down phenotype. **(A)** The phenotype of Col-0, 35S:CSD1#2 and 35S:FLAG-CSD1#4 Arabidopsis plants at bolting, grown under short-day conditions is shown. 35S:CSD1 plants showed red leaf pigmentation while 35S:FLAG-CSD1 plants showed an early senescence phenotype and a growth reduction. **(B)** The cotyledon phenotype of independent 35S:FLAG-CSD1 lines is shown. Plants were grown under short-day conditions. **(C)** The results of the expression analysis of the CSD1 gene in different transgenic lines is shown. The RNA was isolated from leaves of 6-week old plants grown under short-day conditions. Each data point represents at least three biological replicates. Error bars represent the mean deviation. **(D)** Western blot of total protein extracts from different plant lines is shown. Plants were grown under short-day conditions for 6 weeks and total protein extracts were isolated from leaves. The CSD1-specific antibody was used as the primary antibody. Approx. 30  $\mu$ g of total protein was used. A Ponceau staining was used as loading control (lower panel).

During the seedling growth stage, approximately 7% of seedlings showed a cup-shaped cotyledon phenotype that is either characterised by fused cotyledons, abnormal size of cotyledons or even the lack of one cotyledon (**Figure 4 B**). In contrast to other cup-shaped related phenotypes (Aida et al., 1997; Vroemen et al., 2003; Hasson et al., 2011), the fusion of the cotyledons is independent of the meristem growth and did not result in arrest of the shoot apical meristem. At the time of bolting, the 35S:FLAG-CSD1 plants showed an early senescence phenotype with smaller rosette diameter as compared to Col-0 plants and 35S:CSD1 plants. Moreover, the 35S:FLAG-CSD1 plants did not show the characteristic anthocyanin accumulation as observed for the 35S:CSD1 plants. In general, the 35S:FLAG-CSD1 plants

showed a phenotype that resembles the phenotype of *csd1-3* knockdown plants, which is also characterised by smaller rosette size and early senescence. Interestingly, transgenic plants expressing a *pK7WG2:CSD1-GFP* construct which have been used for the FRAP experiment (**Figure 2**) did not show the characteristics of the *35S:FLAG-CSD1* plants (data not shown).

To further understand the phenotype of the transgenic *35S:FLAG-CSD1* plants, the expression level of *CSD1* was analysed by RT-qPCR (**Figure 4 C**). Strikingly, the expression level of *CSD1* in the *35S:FLAG-CSD1* lines was strongly downregulated (nearly 1000-times compared to the wild type level). This downregulation resembled the level of the *csd1-3* knockdown line. In comparison, the *35S:CSD1* plants show a 32-times increased expression compared to the Col-0 background.

As the expression level does not necessarily represent the proportional protein level, the *CSD1* protein abundance was analysed in total protein extract from leaves by western blot analysis with the *CSD1*-specific antibody (**Figure 4 D**). Here, the *CSD1* protein levels correlated with the gene expression levels in the different transgenic lines. An abundant *CSD1* protein band was visible in the *35S:CSD1* plants and Col-0 plants showed a less abundant *CSD1* protein band compared to the *35S:CSD1* plants. Interestingly, in neither the *csd1-3* knockdown plants nor the *35S:FLAG-CSD1* plants the *CSD1* protein was detected. This is especially striking as the *35S:FLAG-CSD1* plants carry the Col-0 wild type background and therefore the wild type *CSD1* protein should theoretically be detected.

Summarised, the expression of *CSD1* with an N-terminal FLAG-tag results in a phenotype and genotype that resembles the *csd1-3* T-DNA insertion knock-down plants. It remains elusive how the endogenous *CSD1* expression and protein level is so dramatically affected by overexpression of *FLAG-CSD1* in the Col-0 background. One explanation for the phenotype and genotype might be co-suppression (Stam et al., 1997). In co-suppression, the introduction of a transgene results in the silencing of the introduced gene and the endogenous plant gene. Unexpectedly, the transgenic *35S:FLAG-CSD1* plants revealed that *CSD1* is also an important development regulator during both embryogenesis and vegetative growth.

### 3.1.4 *CSD1* affects the early transcriptional salt stress response in *Arabidopsis*

The translocation of *CSD1* to the nucleus indicates a role in the early transcriptional response towards salt stress. Although SOD proteins are known for their superoxide scavenging function,

it was tested if the transcriptional response during early salt stress is affected by CSD1. As CSD1 rapidly translocates to the nucleus within 5 minutes of salt stress (**Figure 2**), Arabidopsis plants (knock-down, overexpression and wild type) were grown for 14 days and exposed for 30 minutes to 150 mM NaCl after which the transcriptional response was tested by RNA-seq (**Figure 5**). The analysis of the RNA-seq data was performed according to the method described in Pertea *et al.* (Pertea *et al.*, 2016).

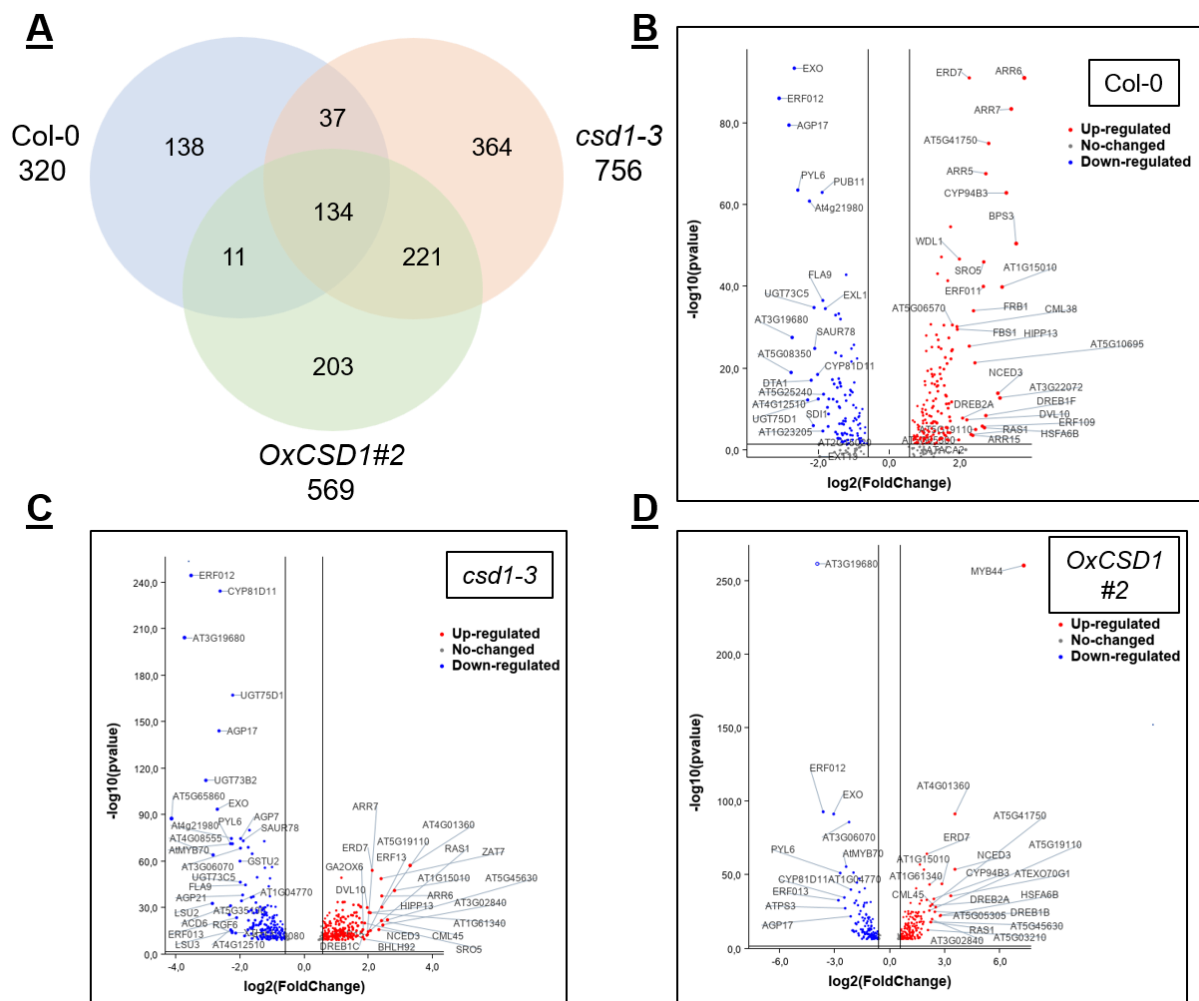


**Figure 5:** Differential expressed genes (DEGs) in Col-0, *csd1-3* and Ox*CSD1* Arabidopsis seedlings after 30 minutes of 150 mM NaCl treatment determined by RNA-seq analysis. (**A**) The overlap of DEGs between the three different genotypes is shown in a Venn-diagram. The threshold ( $\log_2(\text{FC}) > 1.5$ ,  $p\text{-value} < 0.05$ ) was used. (**B-D**) The  $\log_2(\text{FC})$  of the TOP300 DEGs is plotted in relation to the  $-\log_{10}(p\text{-value})$ . Up-regulated genes are highlighted in red and down-regulated genes in blue.

By using a threshold of 1.5 for the  $\log_2(\text{FC})$  and an adjusted  $p$ -value of 0.05, 320 differentially expressed genes (DEGs) in the Col-0, 756 in the *csd1-3* and 569 in the 35:*CSD1* lines (**Figure 5 A**) were identified, respectively. As the three different lines share only 134 DEGs, the altered CSD1 level appears to strongly affect the transcriptional response upon salt stress. A more

detailed impression of the DEGs in each different genetic background is presented by plotting the  $\log_2(\text{FC})$  and the adjusted p-value of the TOP300 DEGs of the RNA-seq experiment (**Figure 5 B-D**). For example, several *TYPE-A RESPONSE REGULATOR (ARR)* genes (Tran et al., 2007) are differentially expressed in the Col-0 background. Furthermore, typical salt-stress genes as *9-CIS-EPOXYCAROTENOID DIOXYGENASE 3 (NCED3)* (Barrero et al., 2006), *SIMILAR TO RCD ONE 5 (SRO5)* (Borsani et al., 2005), *EARLY-RESPONSIVE TO DEHYDRATION 7 (ERD7)* (Krebs et al., 2002) or *DEHYDRATION-RESPONSIVE ELEMENT BINDING2A (DREB2A)* (Mallikarjuna et al., 2011) are differentially expressed in the Col-0 plants upon 30 min of 150 mM NaCl treatment. Several of these genes are shared as differentially expressed genes between the three genetic backgrounds, however the  $\log_2(\text{FC})$  for the individual genes can differ significantly. An overview of these expression changes is highlighted in a heatmap for salt-stress related genes (**Figure 6 A**).

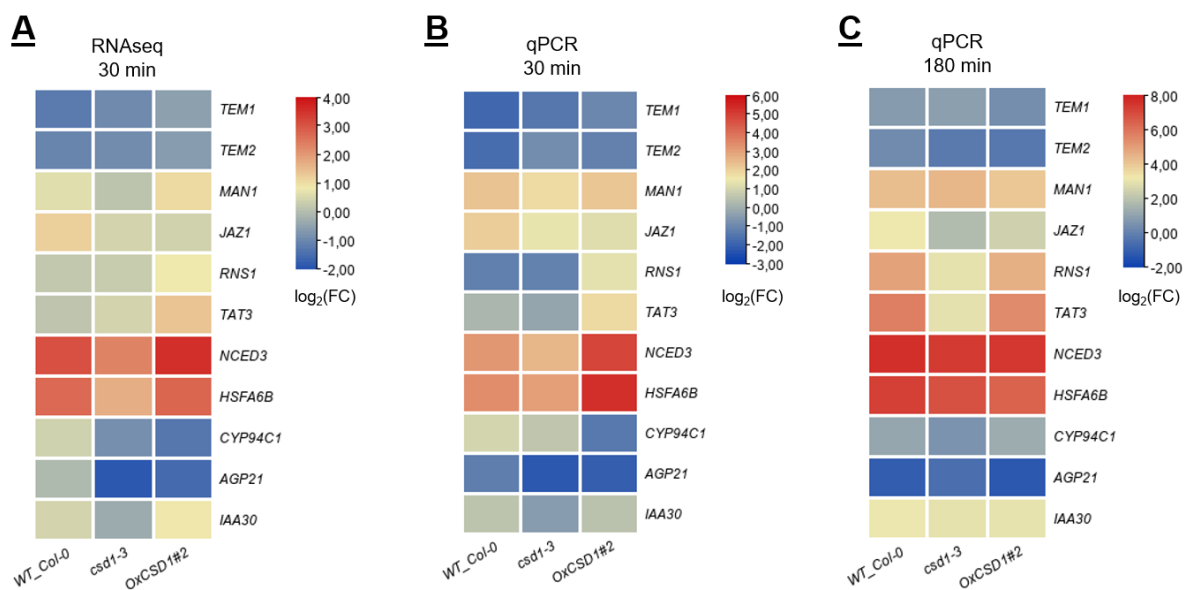


**Figure 6:** Expression of ten salt-stress related genes after 30 minutes of 150 mM NaCl treatment in Arabidopsis seedlings. **(A)** Expression changes after 30 min NaCl treatment compared to untreated seedlings are shown as  $\log_2(\text{FC})$ . The data shown are based on the RNA-seq analysis. **(B)** The expression of the 10 selected genes shown is based on an independent qPCR experiment where the relative expression difference between treated (30 minutes, 150 mM NaCl) and untreated samples was calculated. **(C)** A second qPCR experiment was performed after 180 minutes of salt stress. The relative expression shown is based on the difference between treated and untreated samples. Each data point represents at least three biological replicates. The scale bar represents the expression as  $\log_2(\text{FC})$ .

For example, *HEAT SHOCK TRANSCRIPTION FACTOR A6B (HSFA6B)* (Huang et al., 2016) and *NCED3* showed a distinct expression pattern between the wild type, *csd1-3* and *35S:CSD1* plants. Both genes are upregulated upon salt stress in the wild type, but this induction was

affected by altered levels of the CSD1 protein. In the *csd1-3* background, the expression for both is weaker compared to the wild type whereas the expression is stronger in the *35S:CSD1* plants compared to the wild type, suggesting that they might be direct targets for CSD1. Also, the expression of the *TYROSINE AMINO TRANSFERASE 3 (TAT3)* and *RIBONUCLEASE 1 (RNS1)* gene is elevated in the *35S:CSD1* plants and not induced in the wild type and *csd1-3* background. The *TEMPRANILLO 1 (TEM1)* and *TEMPRANNILO 2 (TEM2)* genes are downregulated in the wild type background upon salt stress. This downregulation is weaker in the *csd1-3* and *35S:CSD1* plants. Another pattern was explored for the *CYTOCHROME P450 FAMILY94 SUBFAMILY C POLYPEPTIDE 1 (CYP94C1)* and *ARABINOGALACTAN PROTEIN 21 (AGP21)* genes that do not show an expression change in the wild type plants but a downregulation in the *csd1-3* and *35S:CSD1* plants. Overall, CSD1 strongly affects the early transcriptional response upon salt stress.

To validate the RNA-seq dataset, a qPCR analysis on an independent experiment was performed under the exact same conditions (**Figure 6 B**). The expressional response of most genes, including *TEM1*, *TEM2*, *TAT3*, *NCED3*, *HSFA6b* and *INDOLE-3-ACETIC ACID INDUCIBLE 30 (IAA30)*, was confirmed. The qPCR experiment shows overall a higher expression change as compared to the RNA-seq data, however the pattern is consistent. For two of the highlighted genes, *RNS1* and *CYP94C1*, a change in the expression pattern between RNA-seq and qPCR was detected. The *RNS1* gene expression is not changed in the RNA-seq experiment in the wild type and *csd1-3* plants, but is downregulated in the qPCR experiment. The enhanced expression in the *35S:CSD1* plant is consistent between the RNA-seq and qPCR experiment. Also, the *CYP94C1* gene shows an altered expression with an induced expression upon salt stress in the *csd1-3* plants in the qPCR experiment, whereas it was downregulated in the RNA-seq experiment. The strong downregulation in the *35S:CSD1* plants is consistent and reproducible for the *CYP94C1* gene. Overall, the differential expression of salt-stress responsive genes is reproducible and appears to be due to different CSD1 levels.

To extend the gene expression dataset, an additional salt stress time point of 180 minutes after treatment was included (**Figure 6 C**). Here, the effect of CSD1 on an extended salt stress response was analysed. Several genes like *JASMONATE-ZIM-DOMAIN PROTEIN 1 (JAZ1)*, *RNS1* and *TAT3* showed a strong expressional induction at the 180 minutes time point in the wild type and *35S:CSD1* plants. Interestingly, the induction is significantly reduced in the *csd1-3* plants.

It is important to note that several genes did not show or showed only a weak expression change after 180 minutes of salt stress like *TEM1*, *TEM2* and *CYP94C1*. Other genes like *NCED3*, *IAA30* and *HSFA6B* showed a prolonged and strong expressional induction at 180 minutes, however no differences were observed between the three different genetic backgrounds.

Summarised, CSD1 affects the expression of several genes during the early salt stress response. The genes, *NCED3* and *HSFA6B*, show an impairment in the early salt stress response while this difference is equalled at the 180 minutes time point. Other genes like *TAT3* and *RNS1* are significantly stronger induced in the early response in the *35S:CSD1* plants compared to the wild type plants. This enhanced induction is not present in the 180 minutes time point where the genes showed the same induction in both genetic backgrounds. However, both of the genes show a significantly reduced induction at the 180 minutes time point in *csd1-3* plants. By using two independent transcriptome approaches and two different salt stress time points, it is evident that CSD1 has a major impact on the initial transcriptional response during salt stress.

### 3.1.5 CSD1 binds DNA in a sequence-specific manner

As CSD1 enters the nucleus and affects the expression of hundreds of genes during the early salt stress response, it suggests that CSD1 might directly interact with DNA to regulate transcription. To understand if CSD1 binds a specific DNA sequence, a SELEX (Systematic evolution of ligands by exponential enrichment) experiment was performed (**Figure 31 A**). In this approach, the iteration of the displayed experimental procedure to select and reamplify bound synthetic DNA sequences leads to the enrichment of the DNA-binding sequence of the protein of interest. Here, six repetitions of the SELEX approach were performed for CSD1. The SELEX experiment revealed the binding of CSD1 to an A/T-rich motif TGCTTT (**Figure 31 B**). This confirmed the hypothesis that CSD1 is able to bind to DNA and that this occurs in a sequence-specific manner.

By SELEX, the ability of CSD1 to bind to DNA and a specific sequence motif it binds was discovered. However, this approach is limited as it is using a synthetic DNA library and does not allow for interfering in which genomic context CSD1 binds DNA. The DAP-seq (DNA affinity purification sequencing) approach circumvents this limitation (Bartlett et al., 2017), as a fragmented library of genomic DNA from the organism is used (**Figure 32 A**). Combined with the subsequent sequencing of all bound gDNA sequences, the DAP-seq approach allows to map the sequenced DNA to specific genomic sequences of the target organism. In

collaboration with the group of Prof. Dr. Joseph Ecker (Salk Institute, San Diego, USA), a DAP-seq experiment was performed with a FLAG-tagged CSD1 protein. In this approach, the FLAG-tagged CSD1 protein was expressed *in vitro* and a binding reaction with sheared genomic DNA was performed. Afterwards, the bound genomic DNA sequences were sequenced and mapped to the Arabidopsis genome. This approach resulted in 145 logical hits that can be located to specific genes within the Arabidopsis genome (**Figure 32 B-C**). Logical hits are defined as genomic sequences that are up- or downstream of annotated coding areas, whereas hits with genomic sequences related to not annotated sequences were neglected. In this experiment, four different replicates were used and a FLAG empty vector as control. The logical hits between the individual replicates varied. Nevertheless, the 145 logical hits that were identified between all four replicates were screened to use them in a ChIP-qPCR experiment for validation. Here, the binding of CSD1 to specific sequences in the promoter region of *Cys2/His2-type ZINC FINGER PROTEIN 7 (ZAT7)* and *TRANSPARENT TESTA GLABRA 1 (TTG1)* *in-vivo* was confirmed by ChIP-qPCR (**Figure 32 D**).

The synthesis of a CSD1-specific antibody in rabbits in collaboration with the Phytoantibody group of Prof. Dr. Udo Conrad was performed at the IPK. To this end, CSD1 was His-tagged, expressed in *Escherichia coli* and purified. Two rabbits were immunised twice with 800 µg of CSD1 protein subcutaneously and subsequently, the CSD1-specific antibody was extracted and purified. This opened the possibility to perform a ChIP-seq experiment in the wild type background under control and salt stress conditions (**Figure 33**). For control and salt stress, three individual replicates were taken and named as IP1 to IP3 for the control replicates, IP4 to IP6 for the salt stress replicates. The individual samples were sequenced and mapped to the genome of Arabidopsis. Combined, 1219 hits were found for the control replicates and 1867 hits for the salt stress replicates (**Figure 7 B and C**).



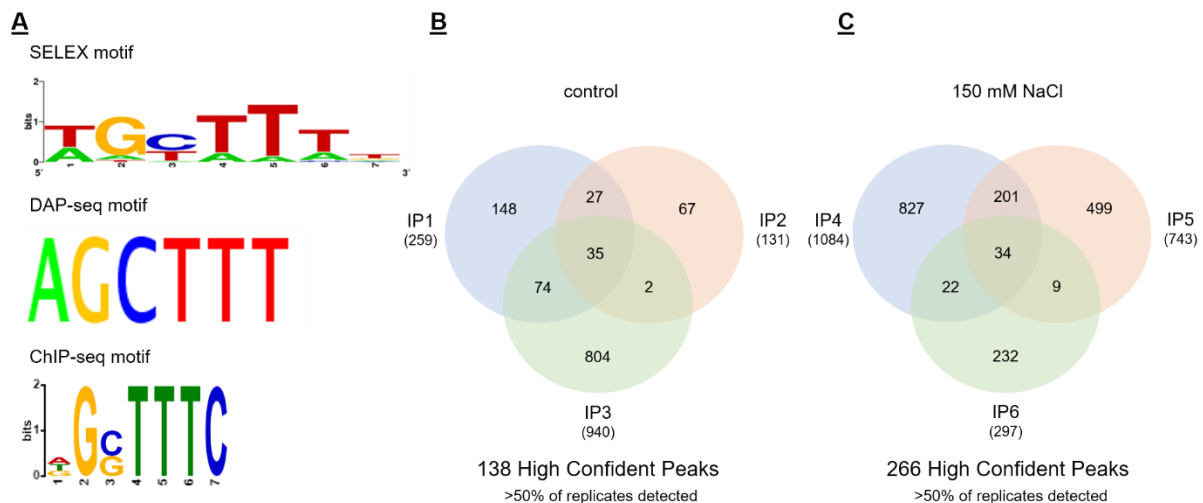


**Figure 7:** CSD1 associates with specific genomic regions in *Arabidopsis in-vivo*. ChIP-seq analysis of untreated and 30 minutes 150 mM NaCl treated seedlings explored the DNA-association of CSD1 *in-vivo*. (A) The DNA-binding sequence of CSD1 identified in three independent experiment is shown. (B) The identified ChIP-seq hits in the three control replicates are shown in a Venn-Diagram. In total, 1219 hits were identified and 138 hits are considered to be high confident peaks (>50% of replicates detected). (C) The identified ChIP-seq hits in the three 30 minutes 150 mM NaCl treated samples are shown in a Venn-Diagram. In total, 1867 hits were identified and 266 were considered to be high confident peaks.

The amount of enriched hits highly varies between the individual replicates (1084 in IP4 versus 131 in IP2) under control and salt stress conditions. Here, peaks were considered as high confident if they appear in at least two out of the three biological replicates. As an example, the peak for the *SQUAMOSA PROMOTER BINDING PROTEIN-LIKE 2 (SPL2)* gene is highlighted in the supplement (Figure 33 C). Genes with enriched peaks were defined as CSD1 target genes if an enriched peak was detected within the first 3kb upstream of their ATG or transcriptional start site (TSS). It is important to note that some genes contained more than one high confident peak. In total, 106 target genes under control conditions and 188 target genes under salt stress conditions were identified. This indicates that CSD1 associates with the promoter sequence of the identified genes. Furthermore, the number of targets increased during salt stress indicating that the DNA-binding of CSD1 is enhanced under stress. This is further supported by the fact that 126 of 188 target genes identified under salt stress were unique hits. Only 46 hits were shared between control and salt stress conditions. A motif enrichment analysis for sequences covered by the peak areas revealed a highly enriched sequence motif that was previously already identified as the *cis*-element that is recognised by CSD1 (Figure 7 A).

By using four different experimental approaches (*in vitro* and *in vivo*), the binding of CSD1 to specific DNA sequences was elucidated. In addition, direct target genes for CSD1 under control and salt stress conditions were uncovered, allowing for understanding the gene regulatory network that CSD1 controls.

### 3.1.6 CSD1 binds to the promoter of salt-stress responsive genes

Above, it was shown that CSD1 can bind to specific DNA-sequences *in vitro* and *in vivo* by four different experimental approaches. To further validate the binding to the identified sequence motif, electrophoretic mobility shift assays (EMSA) were performed with selected promoter sequences and heterologously expressed CSD1. First, the sequence of the ChIP-seq peak in the promoter of the *SPL2* gene was used as an EMSA probe (**Figure 8 A**).

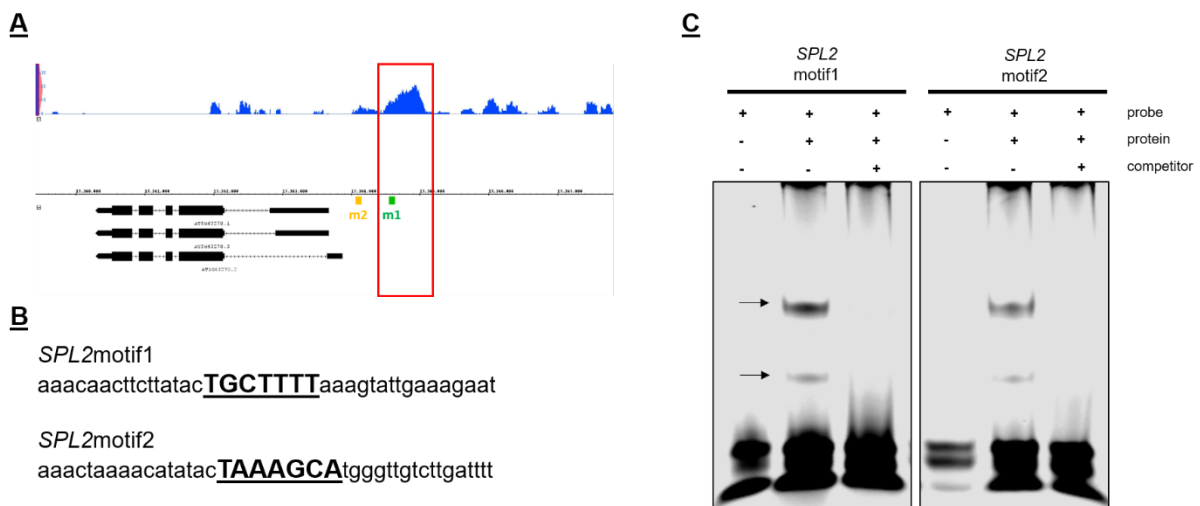


**Figure 8:** CSD1 associates with the promoter of *SPL2*. (A) The identified ChIP-seq peak in the *SPL2* promoter is shown and highlighted in red. The position of the CSD1 binding motif is highlighted in orange (m2) and green (m1). (B) Motif m1 and m2 from the *SPL2* promoter were selected for designing probes for an EMSA assay. The CSD1-binding sequence is shown in bold and underlined. (C) The EMSA was performed with a recombinant CSD1 protein (2000 ng) and IR-labelled oligos that contain one of the two different *SPL2* promoter motifs. Band shifts indicate binding of CSD1 to both motifs as monomer and dimer (black arrows). Addition of unlabeled competitor probes in 200-fold excess removed the band shift. The three lower bands represent unbound labelled probes.

The *SPL2* gene is known to be an important regulator in the vegetative-to-reproductive transition and during embryogenesis by regulating *BONOBO* (Wang et al., 2016c; Xu et al., 2016; Chao et al., 2017; Tsuzuki et al., 2019). The direct regulation of *SPL2* by CSD1 is of particular interest when considering the developmental defects observed in the *35S:FLAG-CSD1* plants, including the partially impaired embryogenesis (**Figure 4**). Two individual sequences within the peak sequences that both contain the A/T-rich CSD1 binding motif were

used (**Figure 8 B**). By performing the EMSA experiment, the binding of CSD1 to both sequences was observed by a shift of the labelled probe indicated by the black arrow (**Figure 8 C**). Interestingly, two shifts are presented which in this case results from both the dimer as well as the monomer of CSD1 binding to the motif. The shift intensity differences between the CSD1 dimer and monomer do not reflect affinities towards the motifs as the distribution of dimer and monomer in the CSD1 protein samples is unknown. The addition of the same probe as unlabelled competitor in 200-fold excess confirmed specific binding of CSD1 to the motifs. Therefore, the binding of CSD1 to the upstream promoter region of *SPL2* that was previously identified within the ChIP-seq experiment was validated.

Two additional promoter sequences based upon the ChIP-seq peaks were chosen for the *CASPARIAN STRIP INTEGRITY FACTOR 1 (CIF1)* and the *MONODEHYDROASCORBATE REDUCTASE 4 (MDAR4)* as EMSA probes (**Figure 34 A**). *CIF1* is of interest as it is an important factor in the development of the casparian strip (Nakayama et al., 2017), which also requires the activity of a thus far unknown SOD isoform (Fujita et al., 2020; Castro et al., 2021). *MDAR4* is an important enzymatic regulator of ROS homeostasis in Arabidopsis (Eastmond, 2007). Both EMSA probes were specifically bound by CSD1 as dimer as well as monomer (**Figure 34 B**). However, the affinity to the promoter sequences of *CIF1* and *MDAR4* seems to be lower as the shift intensity is reduced compared to the *SPL2* EMSA probe. Potentially this is due to single base differences in the recognition motifs of these two genes as compared to the motif present in the *SPL2* promoter. Nevertheless, CSD1 binds a specific sequence in the upstream promoter of *SPL2*, *CIF1* and *MDAR4 in-vitro*.

As the expression of several genes like *NCED3*, *ZAT7*, *TAT3* or *HSFA6B* in the early response to salt stress depends on the CSD1 protein level, the upstream promoter sequence was screened for the CSD1 binding sequence. In all promoters, the A/T-rich CSD1 binding motif was found, therefore several EMSA probes for the individual upstream promoter sequences were designed.

First, the ability of CSD1 to bind to specific sequences in the upstream promoter of *NCED3* and *ZAT7* was analysed by an EMSA (**Figure 9 A**).

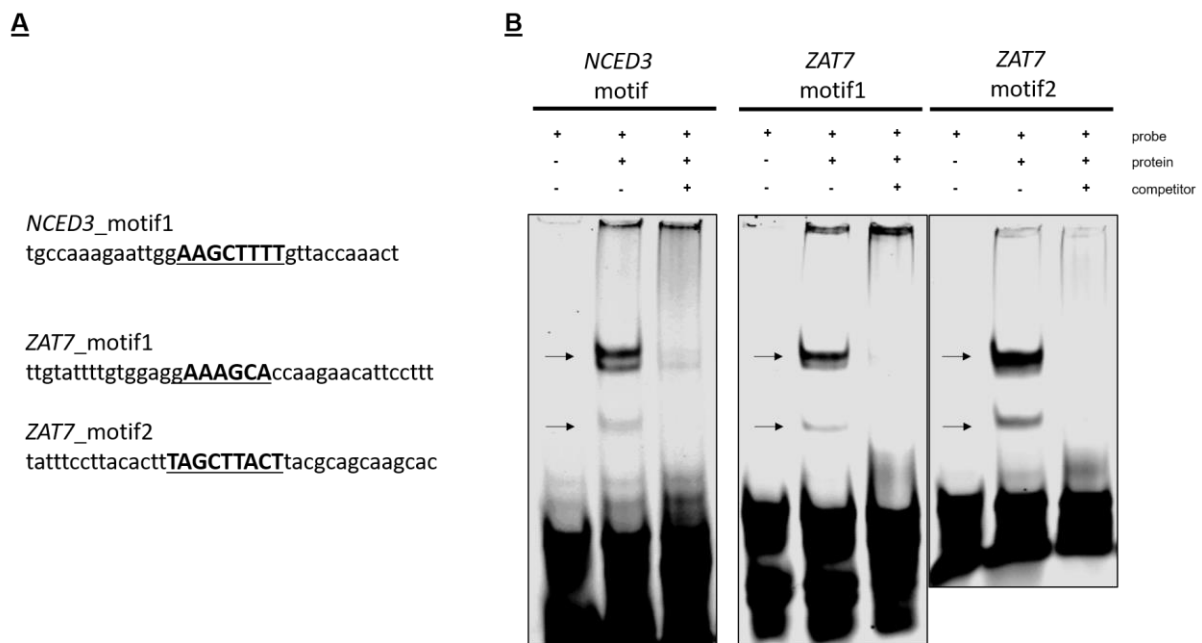


**Figure 9:** CSD1 binds specific sequences from the *NCED3* and *ZAT7* promoter. **(A)** Depicted sequences are used as probes in the EMSA, Panel B. The bold and underlined sequence is the putative CSD1-binding sequence. **(B)** The EMSA showed the retention of the labelled probe indicating the binding of CSD1 (2000 ng). The addition of the competitor sequence in 200-fold excess indicates specific binding. EMSA gels were imaged with a LI-COR Odyssey device.

The shift of the labelled probe confirmed that the CSD1 protein binds to the specific sequence in the upstream promoter of *NCED3* and two specific sequences in the upstream promoter of *ZAT7* (**Figure 9 B**).

To understand the impact of the amount of CSD1 protein used, an EMSA experiment with a probe containing motif 2 from the *ZAT7* promoter and different amounts of CSD1 protein was performed (**Figure 10 A**).

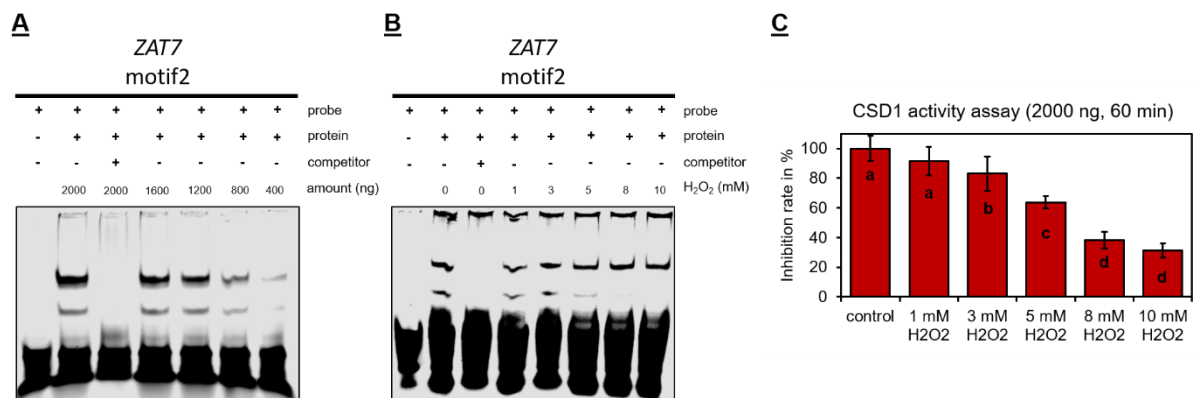


**Figure 10:** Dilution series and H<sub>2</sub>O<sub>2</sub> treatment of CSD1 affects the binding to the ZAT7 promoter. The loading of the lanes in Panel A and B is indicated above the gel. (A) An EMSA was performed with a dilution series of the CSD1 protein ranging from 2000 ng to 400 ng. (B) CSD1 protein that was treated with different H<sub>2</sub>O<sub>2</sub> concentrations was used in the EMSA. (C) The enzymatic activity of CSD1 in the presence of different H<sub>2</sub>O<sub>2</sub> concentrations is shown as inhibition rate in percentage. The inhibition rate indicates if the superoxide radicals in the assay are able to generate formazon dye, the lower the value, the less active SOD1 is. Each data point is based on three technical replicates and the mean deviation is depicted as error bar. This experiment was repeated two times with similar results. One-way ANOVA and post hoc Tukey test were performed ( $p < 0.01$ ) and significant differences are shown with small letters.

It was visible that with decreasing CSD1 protein amounts, the intensity of the probe shift was also decreasing. Nevertheless, a shift for the labelled probe was still visible with a protein amount of 400 ng that results in a protein concentration in the binding reaction of 20 ng/ $\mu$ l. This showed that relative small amounts of CSD1 result in a shift of the probe that covers the upstream promoter sequence of ZAT7, indicating a specificity for this DNA sequence.

To understand if an enzymatically inhibited CSD1 protein is still able to bind to DNA, the CSD1 protein was treated with an inhibitor prior to the EMSA assay. As hydrogen peroxide (H<sub>2</sub>O<sub>2</sub>) is known to inhibit the enzymatic function of CSD1 (Gottfredsen et al., 2013), the CSD1 protein was treated with different concentrations of H<sub>2</sub>O<sub>2</sub>. In parallel, the enzymatic activity of CSD1 was monitored. With the increase of the H<sub>2</sub>O<sub>2</sub> concentration from 1 mM to 10 mM the ability of the CSD1 dimer to bind to the ZAT7 promoter sequence was not impaired, however, the binding of the monomer was impaired upon treatment with 5 mM H<sub>2</sub>O<sub>2</sub> (Figure 10 B). The enzymatic function of CSD1 was significantly impaired upon treatment with 5 mM H<sub>2</sub>O<sub>2</sub> and more strongly impaired with increasing H<sub>2</sub>O<sub>2</sub> concentrations (Figure 10 C). Here, it was found that the ability of the CSD1 dimer to bind to the EMSA probe is not impaired while the ability of the monomer to bind to the DNA sequenced is strongly impaired upon pre-treatment with 5 to 10 mM of H<sub>2</sub>O<sub>2</sub>. Similarly, the enzymatic function of CSD1 was significantly impaired upon pre-treatment with H<sub>2</sub>O<sub>2</sub> concentrations ranging between 5 to 10 mM. These results indicate

that the CSD1 monomer loses its ability to bind to DNA, while the enzymatically inhibited CSD1 dimer still can bind to DNA.

To understand if the binding of CSD1 towards promoter sequences *in vivo* might affect the expression of specific genes during the early salt stress response, DNA-sequences from the promoter of *HSFA6B* and *TAT3* were used to perform an EMSA (**Figure 11**).

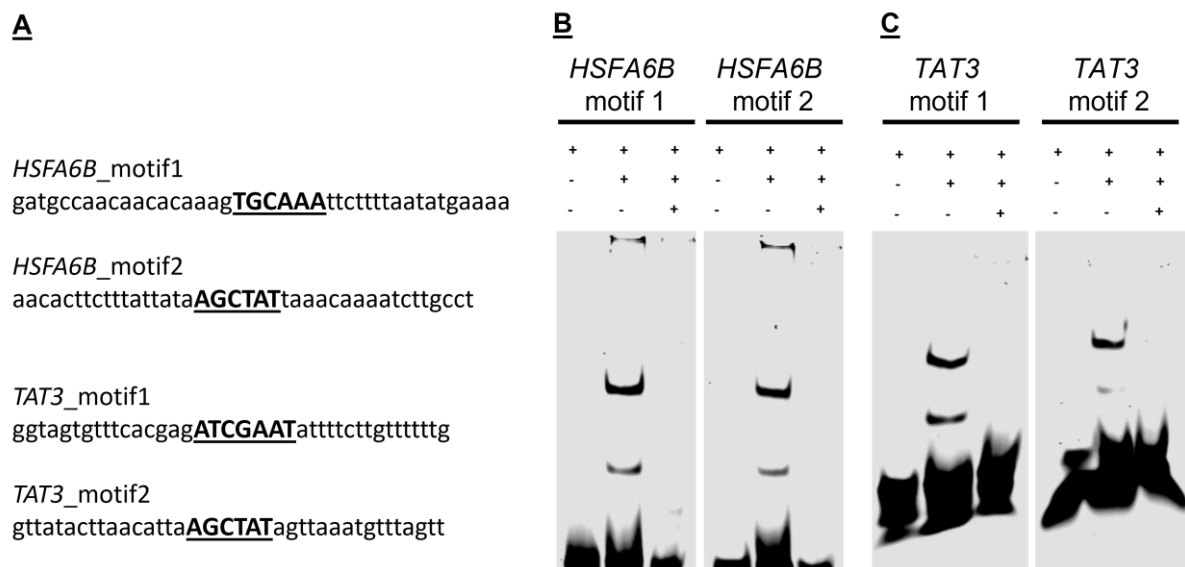


**Figure 11:** EMSA confirms the binding of CSD1 to the promoter of *HSFA6B* and *TAT3*. The EMSA gels were imaged using the LI-COR Odyssey device. (A) Depicted sequences are used as probes in the EMSA, Panel B-C. The bold and underlined sequence is the putative CSD1-binding sequence. (B-C) The binding of the CSD1 monomer and dimer to motifs in the promoter of *HSFA6B* and *TAT3* is shown.

For all performed EMSA assays, two shifts were observed indicating that the CSD1 monomer and dimer bound to the chosen motifs of these two promoters. The lower shift for the motif 2 of the *TAT3* promoter was weaker indicating that the CSD1 monomer did bind less strongly.

Taken together, CSD1 binds to specific upstream promoter sequences of *NCED3*, *ZAT7*, *TAT3* and *HSFA6B*. This indicates that the altered expression of these genes during the initial salt stress response directly depends on CSD1.

### 3.1.7 CSD1 regulates the transcriptional activity of salt-stress responsive genes

As the CSD1 proteins binds to promoter sequences of several salt-stress responsive genes and the transcriptional response upon salt stress was impaired in transgenic plants with altered CSD1 protein levels, it was hypothesised that CSD1 regulates the transcriptional activity of

these genes. This hypothesis was tested by using the *trans-activation* assay (TA assay) in *Arabidopsis* mesophyll protoplasts. To this end the promoter sequences of *NCED3*, *HSFA6B* and *TAT3* were cloned upstream of a firefly luciferase reporter gene in the *pGWL7* vector. *Arabidopsis* mesophyll protoplasts were transformed with three different plasmid constructs: (1) the promoter sequences fused to the *firefly* luciferase gene, (2) a transfection control construct using the *Renilla* luciferase gene and (3) a construct expressing the effector proteins with the *35S* promoter.

By co-transfection of the *NCED3* promoter with *CSD1* or *FLAG-CSD1* in *Arabidopsis* mesophyll protoplasts, it was found that the *35S:FLAG-CSD1* co-transfection results in a two-fold increase of the firefly luciferase activity indicating that the *FLAG-CSD1* protein fusion was able to activate the transcription of the *NCED3* promoter (**Figure 12 A**). The co-transfection with the *35S:CSD1* construct resulted in a weaker increase of the firefly activity, but this change was not significant.

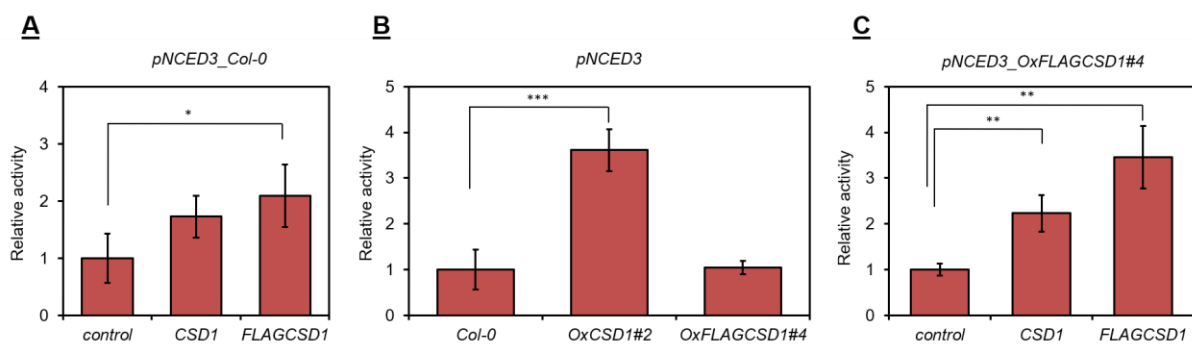


**Figure 12:** *CSD1* activates the transcription of the *NCED3* promoter. The results of the transactivation (TA) assays with the promoter of *NCED3* and the effector constructs *35S:CSD1* or *35S:FLAG-CSD1* are shown. (A) The TA assays were performed with protoplasts from *Col-0* plants. (B) The *NCED3* luciferase reporter was tested in protoplast derived from different genetic backgrounds to compare the basal activity of the promoter. (C) The TA assay was performed with protoplasts from the stable transgenic *35S:FLAG-CSD1#4* line, which is essentially devoid of *CSD1*. Each data point is based on four technical replicates. Error bars represent the mean deviation. Statistical significance was determined by a Student's t-test: \* p-value < 0.05, \*\* p-value < 0.005, \*\*\* p-value < 0.0005.

By using the wild type, the *35S:CSD1* and the *35S:FLAG-CSD1* genetic backgrounds as origins for the mesophyll protoplasts, it was analysed if the basal activity of the reporter gene is affected in lines that contain higher or lower *CSD1* protein levels as compared to wild type (**Figure 12 B**). Indeed, in *35S:CSD1* protoplasts, the *NCED3* reporter constructs showed a significant higher activity as in wild type, while in *35S:FLAG-CSD1* protoplasts no altered activity was observed. Furthermore, an experiment with the *35S:CSD1* and *35S:FLAG-CSD1*

construct in a transgenic *35S:FLAG-CSD1* genetic background, which is virtually devoid of CSD1, was performed. Here, both CSD1 and FLAG-CSD1 significantly activated the transcription of the *NCED3* promoter (**Figure 12 C**).

Similar effects of CSD1 on the transcriptional activity of the promoter of *HSFA6B* and *TAT3* were found (**Figure 13**). CSD1 and FLAG-CSD1 activated the transcription of the *HSFA6B* promoter in wild type protoplast (**Figure 13 A**). Similar to *NCED3*, the co-expression of the FLAG-CSD1 protein had a stronger effect on the transcriptional activity as compared to the untagged CSD1 protein.

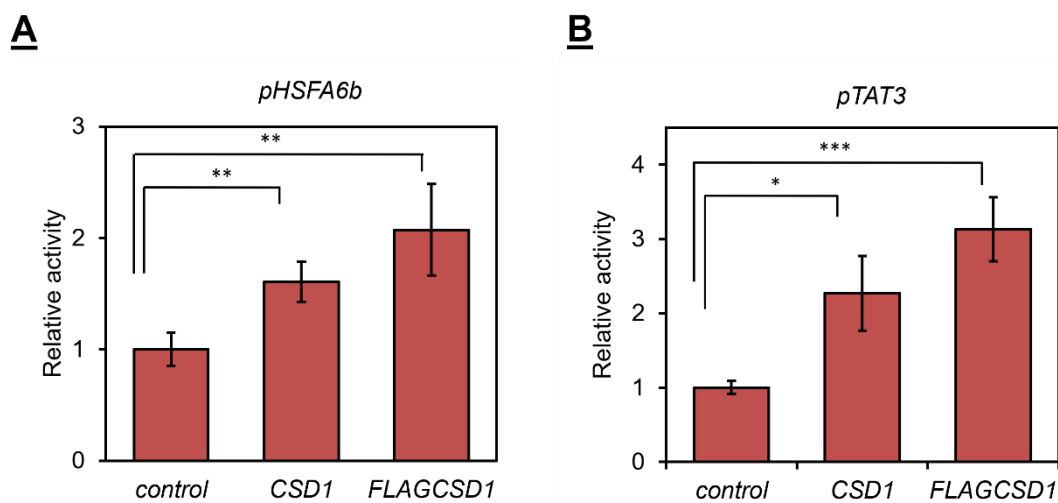


**Figure 13:** CSD1 activates the transcription of the *HSFA6B* and *TAT3* promoter. **(A)** The results of the TA assays of the promoter of *HSFA6B* and the effector constructs *35S:CSD1* and *35S:FLAG-CSD1* are shown. The transactivation assay was performed with Col-0 protoplasts. **(B)** The results of the TA assays with the promoter of *TAT3* and the effector constructs *35S:CSD1* and *35S:FLAG-CSD1* are shown. The TA assay was performed with protoplasts from Col-0 plants. Each data point is based on four technical replicates. Error bars represent the mean deviation. Statistical significance was determined by a Student's t-test: \* p-value < 0.05, \*\* p-value < 0.005, \*\*\* p-value < 0.0005.

Also, the expression of the *TAT3* promoter can be induced by CSD1 (**Figure 13 B**). Here, the *TAT3* promoter was co-transfected with the *35S:CSD1* or *35S:FLAG-CSD1* construct which both resulted in a significantly increased transcription of the *TAT3* promoter. Similar to *NCED3* and *HSFA6B*, the FLAG-CSD1 co-transfection leads to a stronger transcriptional activation compared to CSD1.

By using the *trans-activation* assay in *Arabidopsis* mesophyll protoplasts, it was found that CSD1 not only directly bind the promoter regions of the selected genes, but can also activate



the expression of *NCED3*, *HSFA6B* and *TAT3*. Interestingly, for most promoters the transcriptional activation was stronger if co-transfected with the FLAG-CSD1 protein.

### 3.1.8 Summary

In this chapter, it has been discovered that CSD1 is a cytosolic and nuclear localised protein. The nuclear localisation is inducible and the translocation towards the nucleus occurs in a concentration-dependent manner upon salt stress, most likely facilitated by an active transport mechanism. Transgenic lines with decreased CSD1 protein levels showed an impaired salt stress tolerance in the early seedling stage and an accelerated senescence response during the adult plant phase. Furthermore, the transgenic *35S:FLAG-CSD1* plants which are virtually devoid of CSD1 showed that CSD1 is also an important developmental regulator. The transcriptional response of salt-stress responsive genes like *NCED3*, *TAT3* and *HSFA6B* was impaired in transgenic lines with altered CSD1 levels, which underlines the observed salt-sensitivity of the mutant. In a combinatorial approach, it could be shown that CSD1 binds DNA in a sequence-specific manner and hundreds of potential target genes were identified by ChIP-seq. The A/T-rich DNA binding motif AGCTTT was confirmed independently. The binding of CSD1 to the promoter sequence of the salt-stress responsive genes *NCED3*, *HSFA6B* and *TAT3* was validated with EMSA assays. Furthermore, it was found that CSD1 activates the transcription of the salt-stress responsive genes like *NCED3*, *TAT3* and *HSFA6B*. These results indicate that CSD1 features a novel molecular function as a transcriptional regulator in the early salt stress response by binding and regulating the expression of salt-stress responsive genes.

### 3.2 Chapter 2: CSD1-interacting protein HIPP20 is member of a novel class of transcriptional activators

Within the first chapter of this thesis, the conserved moonlighting function of CSD1 was uncovered, indicating that in plants it acts as a transcriptional regulator. Although CSD1 can activate the transcription of several salt-responsive genes, CSD1 has no transcriptional activation domains, suggesting that in the nucleus it might recruit other proteins to exert this function. To understand the transcriptional function of CSD1 in Arabidopsis, databases were screened for putative interaction partners.

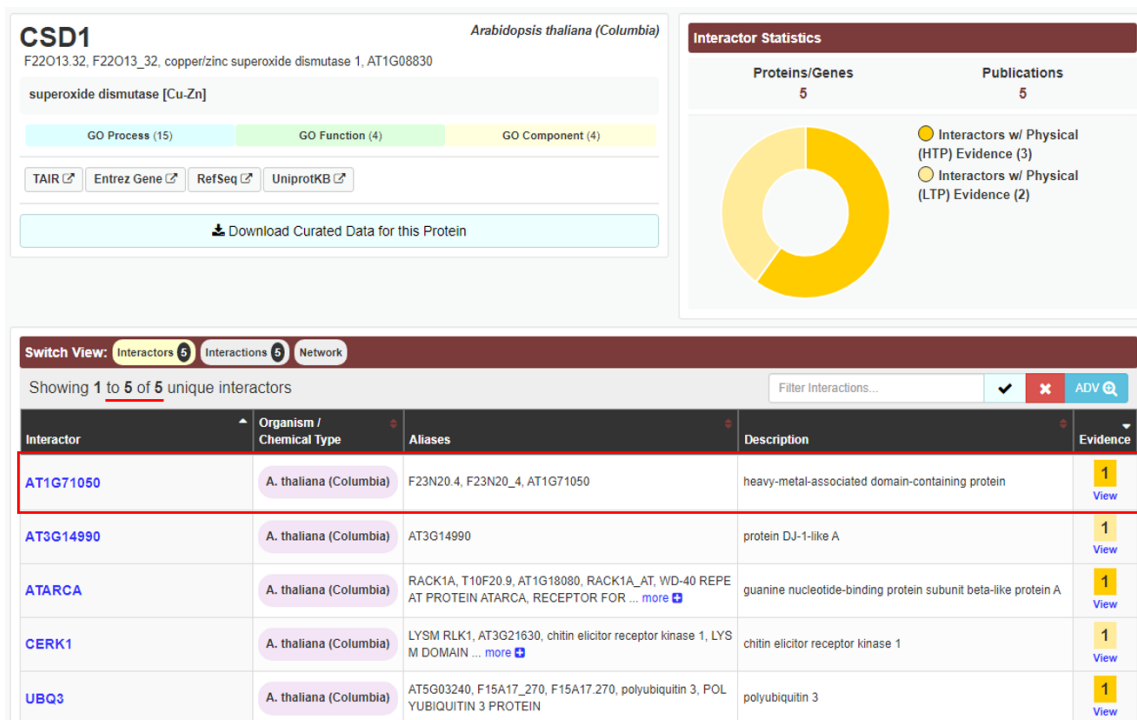


**Figure 14:** Previously reported interaction partners of CSD1. Shown is data from the BioGRID database (<http://thebiogrid.org>, Stark et al., 2006) which indicates five interaction partners for the Arabidopsis CSD1 protein. Highlighted with a red box is the interaction with the HIPP20 protein.

A genome wide interactome study (Braun et al., 2011) by the Arabidopsis Interactome Consortium, reported an interaction of CSD1 with the HIPP20 (AT1G71050) protein (**Figure 14**, red box). Of interest, HIPP20 is containing a heavy-metal associated (HMA) domain that is similar to that of the COPPER CHAPERONE FOR SOD1 (CCS) protein. As HIPP proteins contain an HMA domain, it is speculated that they are mainly involved in regulating metal ion stress. Furthermore, HIPP proteins contain an isoprenylation motif, whose reversible nature

suggests a direct impact on the function of HIPP proteins by linking and releasing them from membranes (Cowan et al., 2018). Despite being linked to abiotic and biotic stress, the precise molecular function of HIPP proteins remains elusive (Barth et al., 2009; Cowan et al., 2018; Guo et al., 2021). The scope of this chapter is to examine the potential interaction of CSD1 and HIPP20 and the molecular function of HIPP proteins in Arabidopsis.

### 3.2.1 HIPP20 and homologs are nuclear localised proteins in Arabidopsis

The HIPP20 protein is predicted to be cytosolic localised, however, it does contain a putative nuclear localisation signal (**Figure 35 A**). To determine the subcellular localisation of the predicted CSD1-interacting HIPP20 protein, the coding sequence of HIPP20 was fused to GFP and transformed into Arabidopsis protoplasts. The HIPP20 protein showed a specific nuclear localisation in Arabidopsis protoplasts (**Figure 15 A**). The dispersion of the fluorescence signal inside the nucleus indicates a subnuclear localisation. A transgenic Arabidopsis plant expressing the *35S:HIPP20-GFP* was generated and confirmed the nuclear localisation in root and leaf cells (**Figure 15 B**). Thus, HIPP20 is a nuclear localised plant protein.

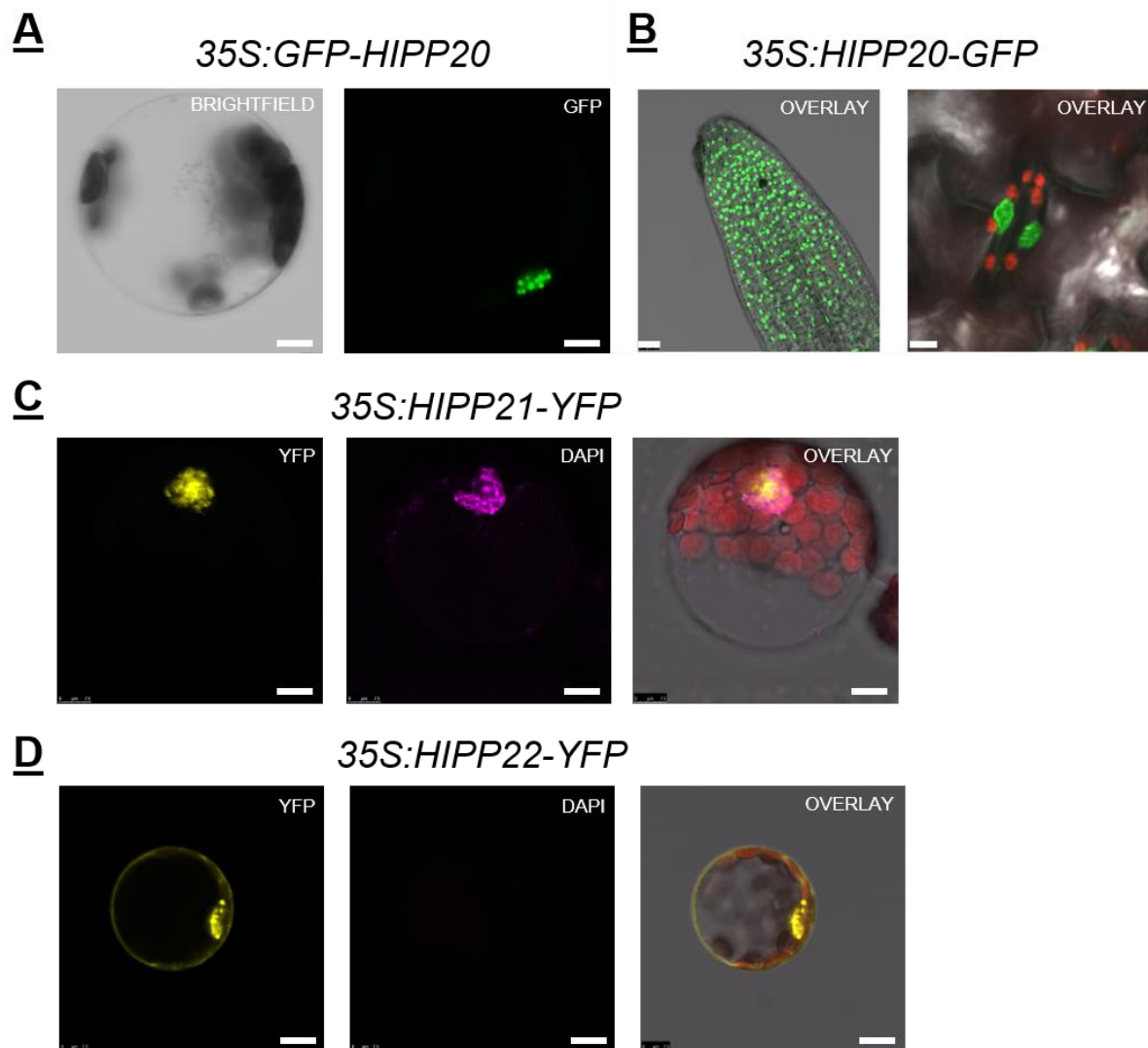


**Figure 15:** Nuclear localisation of HIPP20, HIPP21 and HIPP22 in Arabidopsis. (A) Arabidopsis protoplasts were transfected with a *35S:GFP-HIPP20* construct and imaged with a confocal microscope. Scale bar: 7.5  $\mu\text{M}$ . (B) Stable transgenic Arabidopsis plants expressing *35S:HIPP20-GFP* were analysed using a confocal microscope. The Arabidopsis root tip and a stomata cell are shown. Scale bar: 25  $\mu\text{M}$  and 10  $\mu\text{M}$ . (C-D) Arabidopsis protoplasts were transfected with either *35S:HIPP21-YFP* or *35S:HIPP22-YFP* to analyse their subcellular localisation. Scale bar: 7.5  $\mu\text{M}$ . The DAPI staining was used to confirm the nuclear localisation. In green and yellow the fluorescence of the GFP and YFP is visible while magenta corresponds with the DAPI staining. The autofluorescence of the chloroplasts is represented in red.

HIPP20 belongs to clade II of the HIPP protein family that is comprised of 14 members including HIPP26 (**Figure 36**). The closest homologs of HIPP20 are HIPP21 and HIPP22, which are predicted to be cytosolic localised (**Figure 35 B-C**). Furthermore, HIPP22 does contain a nuclear localisation signal, whereas HIPP21 does not. To determine the subcellular localisation of HIPP21 and HIPP22, the coding sequence of both proteins was fused to the YFP protein and transformed into Arabidopsis mesophyll protoplasts. The HIPP21 protein showed a nuclear localisation like HIPP20, whereas the HIPP22 protein showed a nuclear and cytosolic

localisation (**Figure 15 C-D**). Both homologs showed also a subnuclear localisation to specific structures. Therefore, it was concluded that HIPP20 and its close homologs, HIPP21 and HIPP22, are nuclear localised proteins while HIPP22 is also localised in the cytosol. These results did not match the predicted subcellular localisation by SUBA4 (**Figure 35**) and indicate the necessity of experimental confirmation of predictive data.

### 3.2.2 HIPP20 protein levels do not impact vegetative growth of Arabidopsis

To gain insights into the potential role of the HIPP20 protein in Arabidopsis, a T-DNA insertion line, *hipp20-1* (SALK\_048115), was identified as knock-out and a stable transgenic *35S:HIPP20-GFP* was generated. The plants were grown under long-day conditions and the phenotype was observed during the period of growth. After 8 weeks of growth the phenotype was documented by a photograph (**Figure 16**).

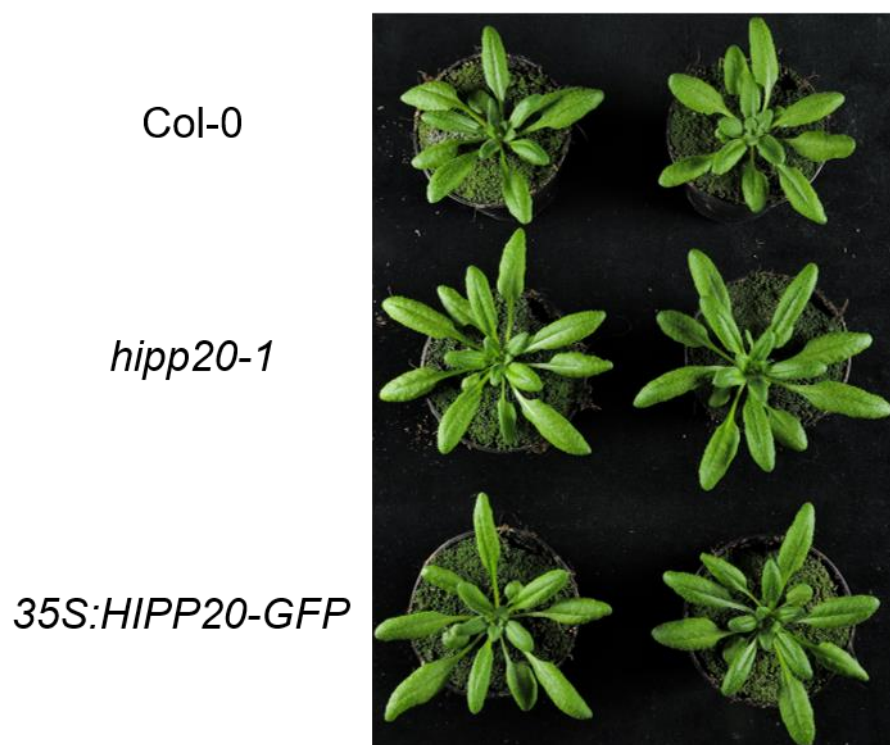


**Figure 16:** Phenotype of Col-0, *hipp20-1* and *35S:HIPP20-GFP* Arabidopsis plants. The Arabidopsis plants were grown under long-day conditions and imaged after 8 weeks of growth.

The phenotypes of the *hipp20-1* and *35S:HIPP20-GFP* plants did not show any obvious differences in growth compared to the Col-0 wild type plants. Similar phenotypes were observed for *hipp21-1* (SALK\_131715.53.60) and *hipp22-1* (SALK\_204024) T-DNA insertion lines (data not shown). This indicates that the individual HIPP proteins do not affect the

vegetative growth of *Arabidopsis* plants under beneficial conditions. Potentially, the HIPP proteins might act redundantly, and higher order mutants are required (Tehseen et al., 2010). In addition, the function of the here analysed HIPP proteins might also be restricted to stress conditions.

### 3.2.3 Nuclear interaction between CSD1 and HIPP20 in *Arabidopsis* and *Oryza sativa*

The HIPP20 protein and its closest homologs are nuclear localised proteins. This directly leads to the hypothesis that the putative interaction of CSD1 and HIPP20 is an exclusive nuclear interaction and might therefore be related to CSD1's moonlighting function as transcriptional regulator. To determine if CSD1 and HIPP20 are able to interact *in planta*, and to determine the localisation of their interaction, the coding sequences of CSD1 and HIPP20 were fused to the C-terminal half (cYFP) or the N-terminal half (nYFP) of YFP and transformed into *Arabidopsis* mesophyll protoplasts. The bimolecular fluorescence complementation (BiFC) showed a nuclear interaction of CSD1 and HIPP20 in *Arabidopsis* protoplasts (**Figure 17 A**).

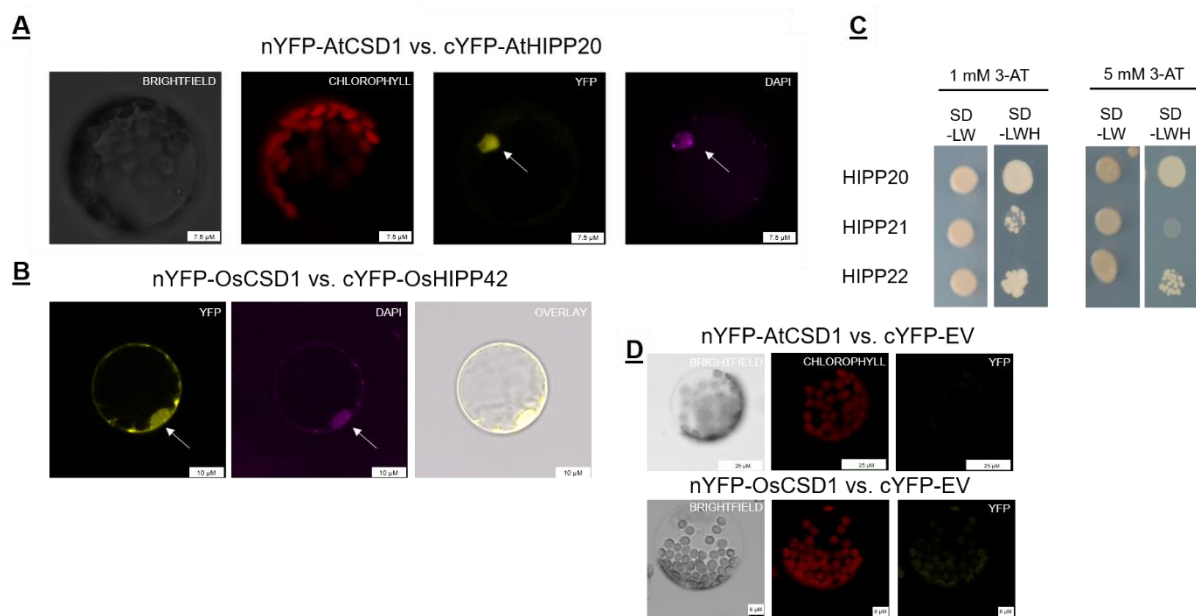


**Figure 17:** CSD1 interacts with HIPP20 in the nucleus. Red represents the autofluorescence of the chlorophyll, yellow corresponds with the YFP fluorescence and magenta indicates the DAPI staining. **(A)** Arabidopsis protoplasts were transfected with the *pUC:SPYNE-CSD1* and *pUC:SPYCE-HIPP20* construct and analysed for the interaction. Scale bar: 7.5  $\mu$ M. **(B)** *Oryza sativa* protoplasts were transfected with the *pUC:SPYNE-OsCSD1* and *pUC:SPYCE-OsHIPP42* construct and analysed for their interaction. Scale bar: 10  $\mu$ M. **(C)** Yeast-two-hybrid (Y2H) results to test the interaction between CSD1 and HIPP20, HIPP21 and HIPP22 are shown. Two concentration of 3-AT were used to select for the strength of the interaction. The *pDEST22* and *pDEST32* vector system was used. **(D)** Arabidopsis (upper panel) and *Oryza sativa* (lower panel) protoplasts were transfected with the *pUC:SPYNE-CSD1/OsCSD1* and the *pUC:SPYCE* empty vector construct and analysed for their interaction. Scale bar: 25  $\mu$ M (upper panel), 8  $\mu$ M (lower panel).

To test if the interaction between HIPP20 and CSD1 is conserved in *Oryza sativa*, the HIPP20 homolog, OsHIPP42, was fused to the cYFP and OsCSD1 was fused to the nYFP. The BiFC assay in *Oryza sativa* stem protoplast cells showed the interaction of OsCSD1 and OsHIPP42 in the nucleus and also the cytosol (**Figure 17 B**). This indicates that the interaction of CSD1 and HIPP20 is conserved *in planta*.

In Arabidopsis, HIPP21 and HIPP22 proteins are very similar to the HIPP20 protein. Therefore, CSD1 might also be able to interact with HIPP21 and HIPP22. To test this hypothesis, the Yeast-Two-Hybrid (Y2H) system was used by fusing the coding sequence of CSD1 to the *Gal4*-DBD in the *pDEST32* vector and the coding sequence of the HIPP proteins to the *Gal4*-AD in the *pDEST22* vector. The interaction of both proteins enables the yeast cells to grow on SD medium without lysine (L), tryptophan (W) and histidine (H). The growth of the yeast cells showed that CSD1 interacts with HIPP20, HIPP21 and HIPP22 (**Figure 17 C**). By using the competitive inhibitor of the *HIS3* gene product, 3-amino-1,2,4-triazol (3-AT), clones are selected with high levels of the *HIS3* gene product which depends on the strength of the

interaction between bait and prey. The use of 1 mM and 5 mM 3-AT showed that the interaction of CSD1 with HIPP20 is the strongest among all three HIPP proteins followed by HIPP22 and HIPP21.

Summarised, a nuclear interaction between the CSD1 protein and HIPP20 was found *in planta*. Furthermore, HIPP21 and HIPP22 can interact with CSD1 in yeast, suggesting that all three HIPP proteins might act redundantly.

### 3.2.4 HIPP proteins are a novel class of transcriptional activators

The nuclear interaction of CSD1 and HIPP20 as well as the limited experimental data about the HIPP protein family raises the question about their molecular function within the nucleus. In light of CSD1's moonlighting function as transcriptional regulator, the hypothesis that HIPP proteins are involved in transcriptional regulation was established. One major research question in this hypothesis is the involvement of CSD1 in transcriptional complexes and in detail the individual ability of CSD1 to activate transcription. By using the *Gal4*-based TA assay in *Arabidopsis* mesophyll protoplasts, it was found that the CSD1 protein fused to the *Gal4*-DBD showed no significant activation of transcription (**Figure 18 A-B**).



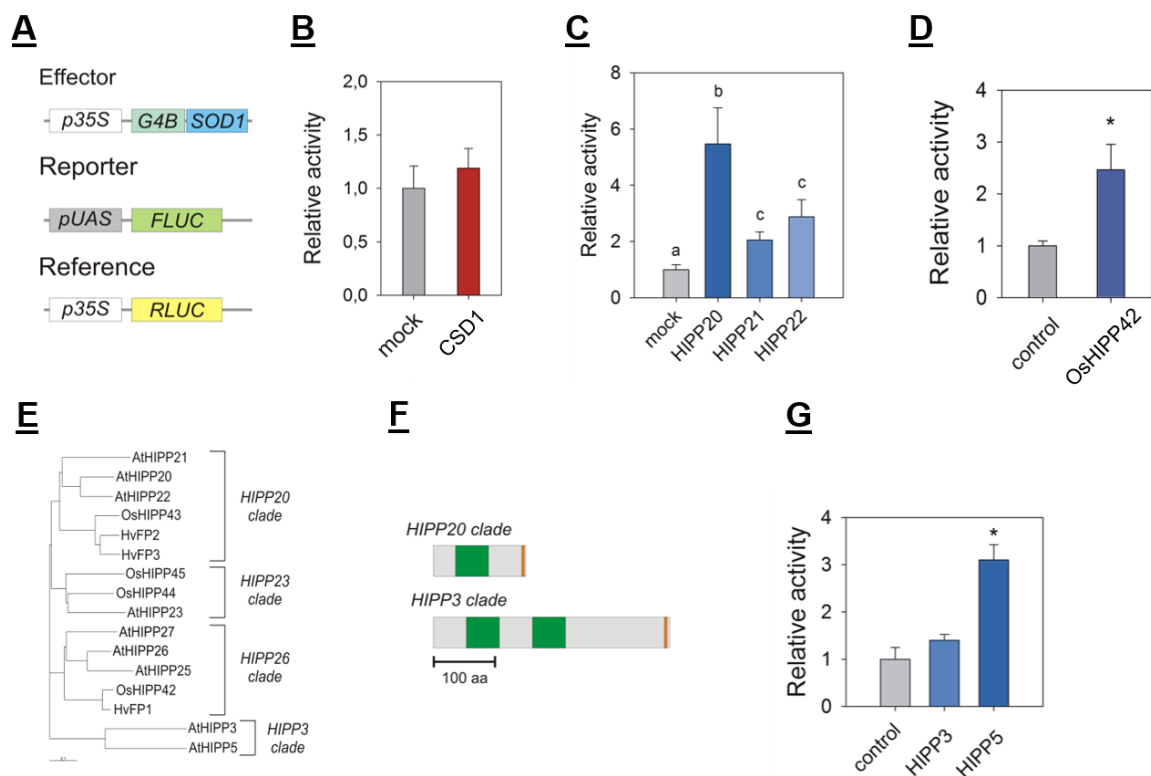


**Figure 18:** HIPP proteins are transcriptional activators. **(A)** Schematic overview of the *Gal4*-based transactivation assay. The *Gal4*-binding domain (*G4B*) binds to the *upstream-activating sequence* (*UAS*). If the fusion proteins, in this case *SOD1/CSD1*, possess transcriptional activity, the firefly luciferase (*FLUC*) reporter gene is expressed. The reference construct expressing the renilla luciferase (*RLUC*) reporter gene is used as transfection control. **(B)** *Gal4*-based TA assay of *CSD1* as effector protein is shown. **(C)** *Gal4*-based TA assay with the three HIPP proteins is shown. Different letters above the bars indicate significant differences according to one-way ANOVA and post-hoc Tukey test. **(D)** The *Gal4*-based TA assay for the HIPP20 homolog in *Oryza sativa*, *OsHIPP42*, is shown. **(E)** A phylogenetic tree displaying chosen HIPP family members from *Arabidopsis* (*At*), *Hordeum vulgare* (*Hv*) and *Oryza sativa* (*Os*) is shown. **(F)** The schematic structure of the HIPP3 and HIPP20 protein is shown as representatives for their clade. The green box indicates the HMA domain and the orange band represents the isoprenylation motif. **(G)** The *Gal4*-based TA assay of HIPP3 and HIPP5 is shown. For each data point at least three technical replicates are represented. Statistical significance was tested by a Student's t-test. Error bars represent the mean deviation. The p-value (\* < 0.05) is indicated by an asterisk.

Contradictory, the *CSD1* protein was able to activate the transcription of *NCED3*, *TAT3* and *HSFA6B* promoters (see 3.1.7). To test if HIPP proteins possess transcriptional activity, the coding sequence of the HIPP proteins was fused to the *Gal4*-DBD and transformed with the reporter and reference construct into *Arabidopsis* mesophyll protoplasts (Figure 18 A). The HIPP proteins activated the transcription of the reporter construct indicating that HIPP20, HIPP21 and HIPP22 can function as transcriptional activators (Figure 18 C). Interestingly, HIPP20 appears to be a more potent transcriptional activator as the other two tested HIPP proteins. Furthermore, the HIPP20 homolog from *Oryza sativa*, *OsHIPP42*, activated the reporter and acted as transcriptional activator indicating a functional conservation *in planta*

(**Figure 18 D**). These results indicate that the small HIPP proteins with one HMA domain (**Figure 36**) function as transcriptional activators which represent a novel function for HIPP proteins.

The HIPP protein family is a structurally diverse protein family where individual HIPP proteins can contain, for example, more than one HMA domain (**Figure 18 E-F**). The HIPP3 and HIPP5 proteins belong to clade I of the HIPP protein family and are phylogenetically distinct to the members of clade II (**Figure 18 E**). They are distinct to the clade II as they are larger in size and contain two HMA domains (**Figure 18 F**). As these HIPP3 and HIPP5 proteins are structurally distinct to the HIPP20 protein, it was tested if the transcriptional activity is a commonality between different HIPP members. To this end, the HIPP3 and HIPP5 coding sequences were fused to the *Gal4*-DBD and a TA assay in *Arabidopsis* protoplasts was performed. This experiment showed that the HIPP5 protein activated transcription, however the HIPP3 protein not (**Figure 18 G**). This indicates that even within the same clade of HIPP protein a functional diversity might exist. Nevertheless, these results indicate that at least two out of five clades in the HIPP protein family can activate transcription.

### 3.2.5 Summary

In this chapter, it was found that CSD1 interacts with HIPP20 in the nucleus and might form a transcriptional complex with HIPP20. In addition, the HIPP20-homologous HIPP21 and HIPP22 can interact with CSD1 in a Y2H assay, suggesting that they act in part redundantly. In line with this, the individual knockout of the *HIPP20*, *HIPP21* and *HIPP22* genes did not lead to a vegetative growth phenotype under beneficial conditions. HIPP20, HIPP21 and HIPP22 are nuclear localised proteins with a specific subnuclear localisation. Here, it was shown through transactivation assays that HIPP20 and its close homologous act as transcriptional activators. Moreover, even HIPP proteins from other clades can act as transcriptional activators, suggesting that the HIPP family represents a novel class of transcriptional regulators in plants.

### 3.3 Chapter 3: Co-IP reveals novel PTM of CSD1 and temporal and stress-dependent interactome of CSD1 and CSD2

The view that the molecular function of CSD1 is exclusively to act as detoxifying enzyme through dismutation of superoxide to hydrogen peroxide has been severely challenged by the discoveries made in yeast and human cells (Tsang et al., 2014; Li et al., 2019).

In yeast and human literature on SOD1 many PTMs for SOD1 have been uncovered including phosphorylation, acetylation, sumoylation and ubiquitination which are directly linked to the molecular function of SOD1 (Banks & Andersen, 2019). For example, the nuclear translocation of SOD1 in yeast depends on the phosphorylation of two conserved serine residues (Tsang et al., 2014). SOD1s function in nutrient sensing and redox regulation involves a reversible phosphorylation at S39 in yeast and T40 in humans (Tsang et al., 2018). In contrast, to date no PTMs for SOD1 in plants have been reported. Although attempts to identify phosphorylation events for CSD1 in Arabidopsis failed (data not shown), here a novel PTM for CSD1 was identified that might be linked to protein stability and therefore might explain the higher transcriptional activity of the FLAG-CSD1 protein (**Figure 12, Figure 13**).

Furthermore, the discrepancies in the predicted and confirmed interaction partners between CSD1 and its counterparts in yeast and human cells were a point of interest to further understand the molecular functions of CSD1 in plants (**Figure 19**).

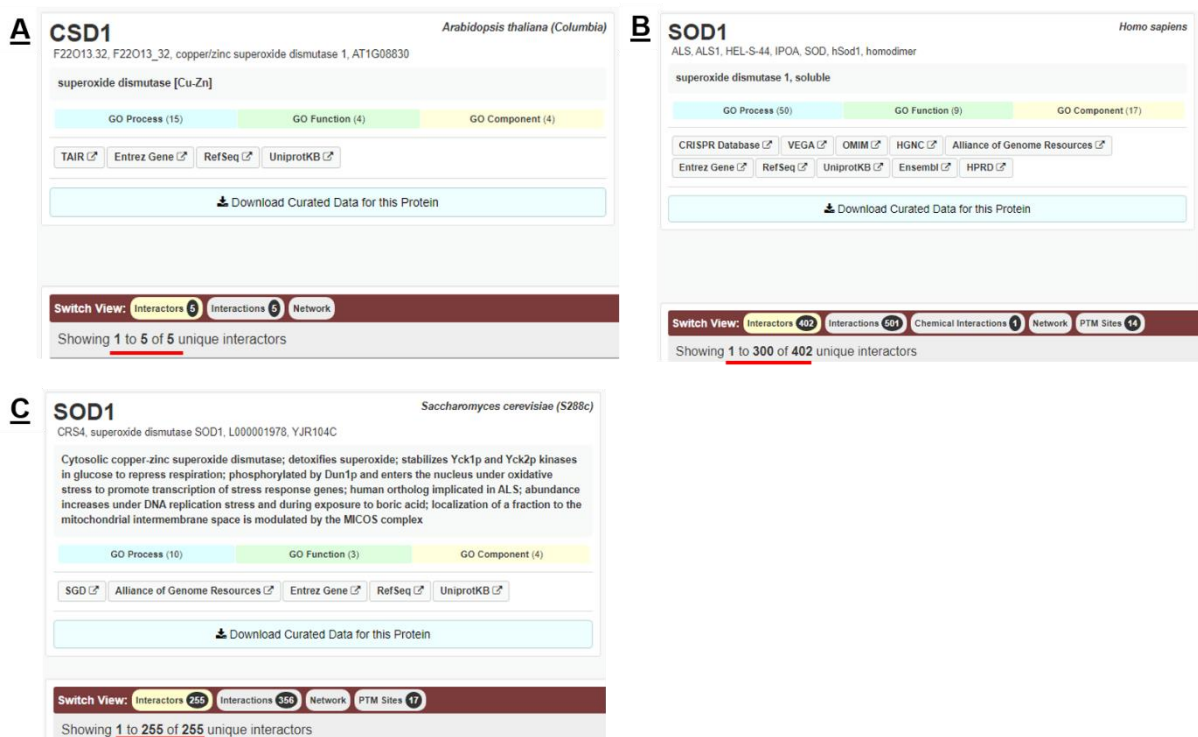


**Figure 19:** Reported interaction partners of CSD1/SOD1 proteins. Based on data of the BioGRID database (<http://thebiogrid.org>, Stark et al., 2006) the number of interaction partners is shown for the different SOD1/CSD1 proteins. The Arabidopsis CSD1 protein is reported to interact with 5 proteins (A), while the SOD1 protein from humans is known to interact with 402 partners (B) and the yeast SOD1 protein with 255 partners (C).

The scope of this chapter is to identify PTMs of CSD1 and explore the CSD1 and CSD2 interactome *in-vivo* using the CSD1-specific antibody for state-of-the-art protein pulldown assays.

### 3.3.1 The CSD1 protein receives an NTA in Arabidopsis

To explore posttranslational modifications of CSD1 in Arabidopsis, the CSD1-specific polyclonal rabbit antibody was used, which was synthesised in collaboration with the Phytoantibody group of Prof. Dr. Udo Conrad at the IPK. This specific antibody allows for immunopurification of CSD1 from a Col-0 total protein extract with magnetic beads coated with Protein A (Figure 20 A). Important to note is that CSD1 is purified from the protein extract but also CSD2, however in a smaller quantities.

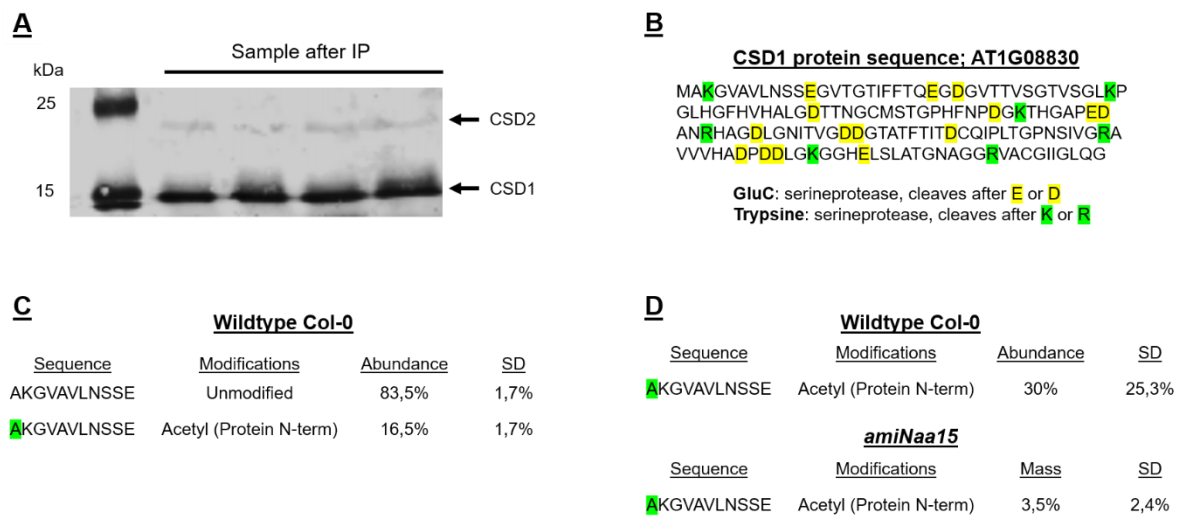


**Figure 20:** CSD1 receives an N-terminal acetylation *in-vivo*. (A) The western blot image of the immunoprecipitation with the CSD1-specific antibody (rabbit) is shown. Both, the CSD1 and CSD2 protein, were identified by using the CSD1-specific antibody for the western blot analysis. The samples are from untreated Arabidopsis seedlings (grown in liquid culture) and denatured to be released from the magnetic beads. (B) Shown is the amino acid sequence of CSD1 with the predicted sites of digestion for the GluC and trypsin protease. (C) The CSD1-corresponding N-terminal peptide sequence and the detected mass is shown. Three technical replicates were used. This experiment was once repeated with similar results. (D) Shown data were taken and adapted from the supplementary data of Linster *et al.*, 2015.

In collaboration with Dr. Jürgen Eirich and Prof. Dr. Iris Finkemeier (Plant Physiology, University of Münster), a mass spectrometry analysis of immunopurified CSD1 was performed. Based on the amino acid sequence of CSD1 both trypsin and the endoproteinase GluC were used to digest the CSD1 protein in separate on-bead digestion reactions (Figure 20 B). The presence of a lysine at position 3 does not allow for a N-terminal peptide detection after trypsin digestion, therefore the GluC enzyme was used to generate a detectable N-terminal peptide. By mass spectrometry analysis, a N-terminal peptide of CSD1 with a different mass was detected which correlates to an acetyl-residue and therefore an N-terminal acetylation (NTA). In total, 16.5% of all detected N-terminal peptides carried the NTA, which represents the acetylation yield (Figure 20 C). This discovery is supported by the mass spectrometry analysis of Linster *et al.* (Linster *et al.*, 2015) who isolated and analysed total protein extracts of Arabidopsis Col-0 and transgenic *amiNaa10* and *amiNaa15* plants (Figure 20 D). This analysis showed that the acetylation yield of CSD1 dropped to 3.5% in the *amiNaa15* transgenic line indicating that the NatA complex facilitates the NTA. This represents a novel posttranslational modification of CSD1 in Arabidopsis and provokes the question what the biological function of the acetylated CSD1 protein pool might be. Although the PTM analysis also focussed on identifying phosphorylation events, the large number of phosphorylatable residues in each CSD1 peptide

after trypsin or GluC digestion prevented identifying specific residues that might have been phosphorylated. In other words, CSD1 is likely to be phosphorylated *in planta*, but it was not possible to pinpoint the specific residue on which it occurred. Of note, CSD1 has 24 putative phosphorylation sites (S/T) which is a lot considering it represents 15% of the 152 amino acids (**Figure 20 B**). In future experiments, the combination of specific tryptic enzymes will be used to pinpoint the phosphorylated residues.

### 3.3.2 *In-silico* analysis suggests N-terminal acetylation of several SOD proteins

As the SOD proteins are evolutionary conserved and found in all eukaryotes, the N-terminal acetylation and the subsequent *in vivo* impact of the modification might be conserved as well. To further support this hypothesis, the protein sequences of different SOD proteins were retrieved and compared in an *in-silico* analysis. Interestingly, the alanine at the second position is conserved between several distinct species (**Figure 21 A**).

**A**

Protein sequence	N-terminal protein sequence
AtCSD1	MAKGVAVLNSSEG
HsSOD1	MATKAVCVLKGDP
ScSOD1	MVQAVAVLKGDA
MpSOD1	MAVTKKAVAVLKG
HvSOD1	MAKGPSSLKGVAL

**B**

Protein sequence	N-terminal protein sequence
CSD1	MAKGVAVLNSSEG
CSD2	MAATNTILAFSSPS
CSD3	MEAPRGNLRAVAL
MSD1	MAIRCVASRKTLAG
FSD1	MAASSAVTANYVLK

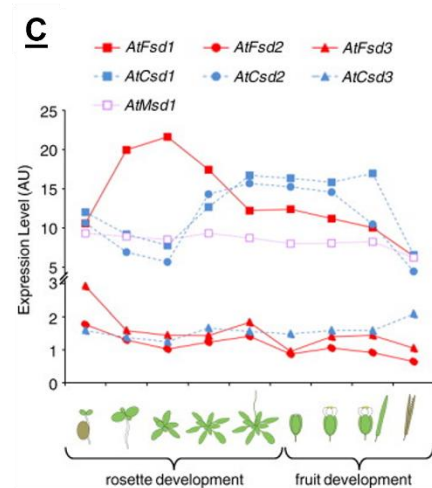


**Figure 21:** *In-silico* analysis suggests that most SOD proteins undergo N-terminal acetylation. (A) The N-terminal amino acid sequence of several SOD isoforms from the species *Arabidopsis thaliana* (At), *Homo sapiens* (Hs), *Saccharomyces cerevisiae* (Sc), *Marchantia polymorpha* (Mp) and *Hordeum vulgare* (Hv) are shown. Amino acids that might receive an NTA are highlighted. (B) The N-terminal amino acid sequences of several SOD isoforms of *Arabidopsis* are shown. Amino acids that might receive an NTA are highlighted. (C) The expression level of several SOD isoforms of *Arabidopsis* are shown at different developmental stages of the plant. The figure was taken and adapted from Pilon *et al.*, 2011. Data used are based on the Genevestigator (<http://www.genevestigator.com>).

For example, the CSD1/SOD1 proteins in human cells, in *Saccharomyces cerevisiae*, in *Marchantia polymorpha* and *Hordeum vulgare* share the alanine at position 2 indicating an evolutionary conservation. Furthermore, several other SOD proteins in *Arabidopsis* contain an alanine at position two (**Figure 21 B**). Both CSD1, CSD2 as well as MSD1 and FSD1 share the alanine. Therefore, all SOD proteins that share the conserved alanine at position two are potential targets for the NTA. By analysing the expression patterns of the *SOD* genes in *Arabidopsis* through the gene investigator portal (<https://genevestigator.com/>), it was found that those SOD proteins that might be N-terminal acetylated were the most strongly expressed genes during all developmental stages of *Arabidopsis* (**Figure 21 C**). This provoked the question if

the NTA represents another mechanism to control the protein abundance of SOD proteins *in vivo* which will be tackled in the future.

### 3.3.3 Co-IP of CSD1 and CSD2 from total protein extracts of Arabidopsis identified a plethora of interactors

The scientific achievement to synthesise a CSD1-specific antibody allowed for exploring the interactome of CSD1 in the wild type background *in vivo*. The experiment was designed to gain further insight into the molecular function of CSD1. Here, protein A bound to magnetic beads was used to pulldown CSD1 protein complexes from soluble protein extracts of Arabidopsis with the CSD1-specific antibody. To confirm the specific pulldown of CSD1, the complexes bound to the magnetic beads were denatured, separated via an SDS-PAGE and analysed by a Western blot. The pulldown of CSD1 and CSD2 was confirmed by using the CSD1-specific antibody in Arabidopsis Col-0 plants (**Figure 22 A**).

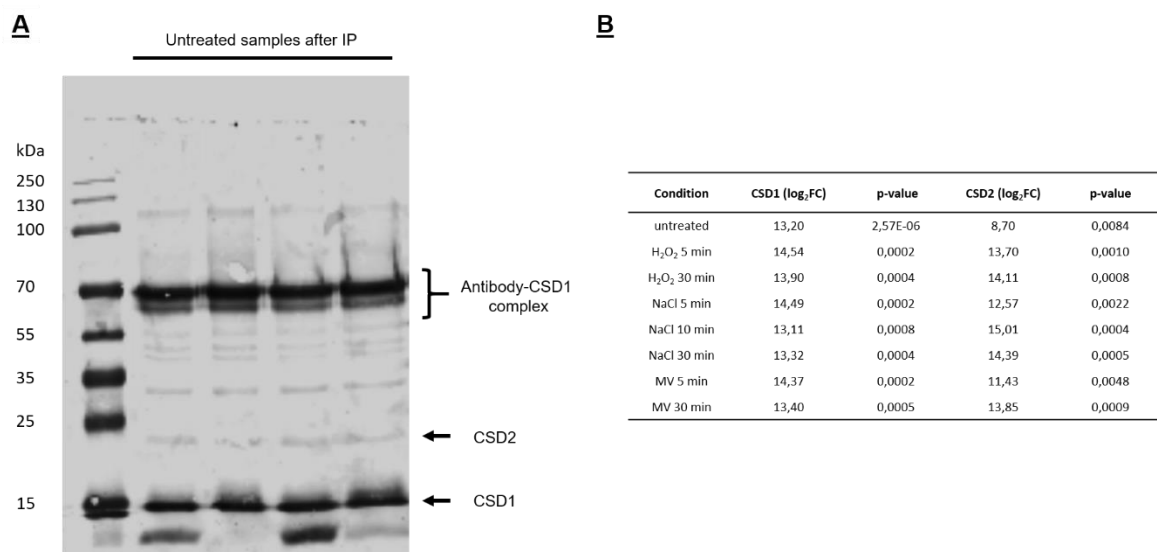


**Figure 22:** CSD1 and CSD2 pulldown from total protein extracts of Arabidopsis. **(A)** The western blot of the immunoprecipitated protein complexes with the magnetic beads is shown. Immunoprecipitation and western blot were performed with the CSD1-specific antibody. Results for an immunoprecipitation on total protein extracts of untreated 12 days old Arabidopsis seedlings is shown. **(B)** The average enrichment (log<sub>2</sub>(FC)) of CSD1 and CSD2 in all different conditions is shown as compared to immunoprecipitation with an mCherry-specific antibody (rabbit) as negative control. For all conditions, four biological replicates were used.

The western blot analysis showed additional bands that might represent the CSD1 dimer or the CSD1 protein bound to different complexes. The western blot confirmed the ability to pulldown the CSD1 and CSD2 protein from total protein extracts of Arabidopsis plants.



Within 5 minutes of salt stress, CSD1 moves to the nucleus which was shown before by FRAP analysis (**Figure 2**). The mechanism of this process is unknown. To gain further insights into the molecular function of CSD1 during the early stress response, the pulldown experiment was performed with Arabidopsis wild type seedlings stressed with H<sub>2</sub>O<sub>2</sub>, methyl viologen/paraquat (MV) and sodium chloride (NaCl) which were harvested at different time points (5-minutes and 30-minutes). The bead-antibody-protein complexes were shipped to the group of Prof. Dr. Iris Finkemeier (University of Münster, Germany) to perform mass-spectrometry analyses. As negative control, and to determine the enrichment of peptides, the pulldown was in parallel performed with an anti mCherry-antibody that was also synthesised in rabbits. By mass-spectrometry analysis, a strong and significant enrichment of CSD1 and CSD2 in all four replicates of the distinct stress conditions was found (**Figure 22 B**). This confirmed successful enrichment of CSD proteins in the different pulldown samples. Subsequently, the identified peptides of potential interaction partners were analysed, quantified and sorted based on their peptide enrichment, p-value and presence in at least 50% of the replicates for each condition. The analysis settings resulted in the overall identification of 515 unique interactors for CSD1 and CSD2 (**Supplementary data 1**). These 515 interactors were sorted based on their subcellular localisation within the SUBA4 database (<https://suba.live/>, Hooper et al., 2017). Hereby, it was found that 38% are localised to the cytosol, 30% to plastids, 11% to the mitochondrion and 8% to the nucleus (**Figure 23 A**).

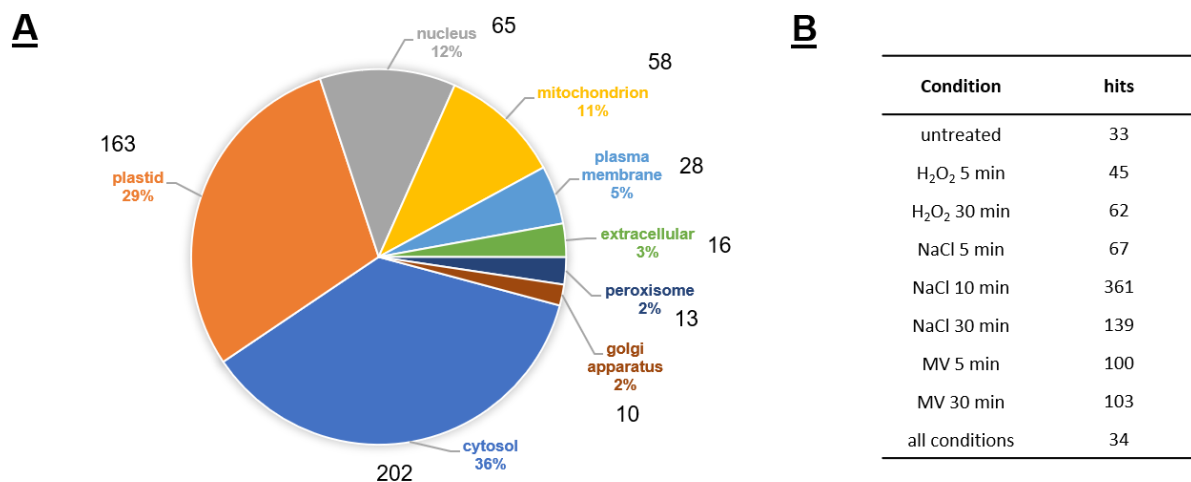


**Figure 23:** Identification of a plethora of CSD1 and CSD2 interaction partners. **(A)** Based on the SUBA4 database, the identified interaction partners were sorted for their subcellular localisation. In total, 515 interactors were identified. As several interactors have dual localisation the number increased to 555. **(B)** The number and distribution of enriched interaction partners are shown for each conditions analysed. Enriched interactions partners that were present in all conditions were excluded from the distribution and considered separately. An interaction partner was considered to be enriched based on the p-value ( $p < 0.05$ ) and the presence in  $>50\%$  of the replicates.

Based upon the subcellular localisation of the identified hits, 267 proteins potentially interact with CSD1 in the cytosol and/or nucleus. 163 plastidial proteins potentially interact with the chloroplastic CSD2 protein. Furthermore, 125 hits belong to proteins which are predicted to localise to the mitochondrion, Golgi apparatus, peroxisome and extracellular space which do not contain the CSD1 or the CSD2 protein. This crude analysis resulted in a total of 555 hits as certain proteins are localised to more than one subcellular compartment and will need further validation regarding the subcellular localisation of the complex formation.

The identified hits were sorted by conditions to link the interactors to the stress conditions (**Supplementary data 2**). Here, the hits were based on the p-value ( $< 0.05$ ) and the presence in at least 50% of the replicates. Through all conditions, 34 hits were identified and considered to be the “core”-interactome. Two out of these 34 hits were CSD1 and CSD2, therefore 32 novel hits were identified (**Table 5**). These hits were mostly ribosomal proteins which were correlated with the 30S, 40S, 50S and 60S subunits of the ribosome in cytosol and chloroplast.

**Table 5:** The 32 hits identified in all conditions (untreated and treated) are shown.

Annotation	Abbreviation	Description	Annotation	Abbreviation	Description
AT5G55070	E2-OGDH2	Dihydrolipoamide succinyltransferase	AT2G47610	Ribosomal protein	Ribosomal protein
AT5G23740	RPS11C	Ribosomal protein (40S)	AT5G20290	RPS8A	Ribosomal protein (40S)
AT2G36160	RPS14A	Ribosomal protein (40S)	AT1G54220	mtE2-3	Dihydrolipoamide acetyltransferase
AT5G14320	EMB3137, RPS13	Ribosomal protein (30S)	AT5G02450	RPL36C	Ribosomal protein (60S)
AT1G18540	RPL6A	Ribosomal protein (60S)	AT3G60770	Ribosomal protein	Ribosomal protein
AT2G19730	RPL28A	Ribosomal protein (60S)	AT3G55280	RPL23aB	Ribosomal protein (60S)
AT3G52200	mtE2-1, LTA3	Dihydrolipoamide acetyltransferase	ATCG00770	RPS8	Ribosomal protein (30S)
AT3G25920	RPL15	Ribosomal protein (50S)	AT3G04840	RPS3aA	Ribosomal protein (40S)
AT3G53020	RPL24B	Ribosomal protein (60S)	ATCG01310	RPL2.2	Ribosomal protein (50S)
AT4G17390	Ribosomal protein	Ribosomal protein	AT4G00100	RPS13B	Ribosomal protein (40S)
AT2G41840	RPS2C	Ribosomal protein (40S)	ATCG01230	RPS12	Ribosomal protein (30S)
ATCG00380	RPS4	Ribosomal protein (30S)	AT3G07110	RPL13aA	Ribosomal protein (60S)
AT2G18020	RPL8A	Ribosomal protein (60S)	AT2G31610	RPS3A	Ribosomal protein (40S)
AT3G24830	RPL13aB	Ribosomal protein (60S)	AT1G67430	RPL17B	Ribosomal protein (60S)
AT5G15200	RPS9B	Ribosomal protein (40S)	AT3G62870	RPL7aB	Ribosomal protein (60S)
AT5G62300	RPS20C	Ribosomal protein (40S)	AT3G13930	mtE2-2	Dihydrolipoamide acetyltransferase

Combined with 33 hits that were identified in the untreated samples, the interactome of CSD1 and CSD2 consisted of 65 proteins under untreated conditions (**Figure 23 B**). In comparison, 107 hits were identified for the two H<sub>2</sub>O<sub>2</sub> time points, 567 hits were identified for the three NaCl time points and 203 hits for the two MV time points. Interestingly, especially the 10 min NaCl time points resulted in the identification of a plethora of interaction partners. It remained elusive if this is related to an efficient pulldown compared to other samples or to the time point and stress condition. Nevertheless, the amount of identified hits highlights the stress and time point specific complex formation of the CSD proteins. By treatment with different stresses and harvesting at different time points the dynamics of the interactome of CSD1 and CSD2 became visible. To further highlight the dynamics of the interactome, the log<sub>2</sub>FC enrichment of peptides upon treatment with 30 minutes of H<sub>2</sub>O<sub>2</sub>, MV and NaCl was visualised in relation to the log<sub>2</sub>FC enrichment of these peptides in the untreated samples, indicated by the line corridor in **Figure 24 A**.

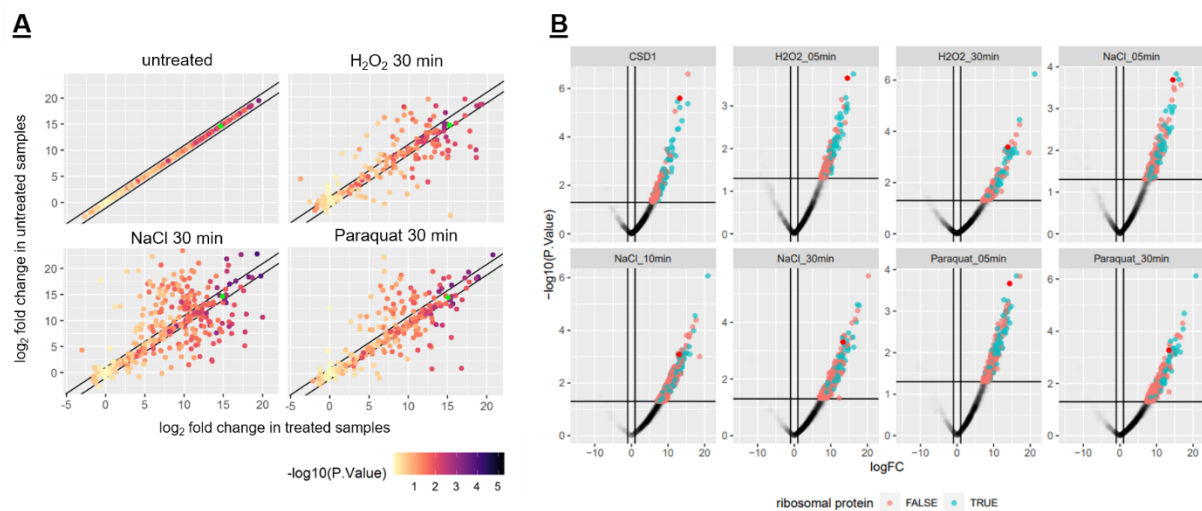


**Figure 24:** CSD interactome is dynamic. **(A)** A scatter plot highlighted the enrichment changes ( $\log_2(\text{FC})$ ) between untreated and treated samples is shown. The corridor (black lines) indicates the enrichment in the untreated samples. The CSD1 protein is highlighted in light green. Colour code represents the p-value. **(B)** The enrichment of all identified peptides in relation to the p-value is represented through all conditions as volcano plot. Ribosomal proteins are highlighted in cyan and non-ribosomal proteins in red. The threshold is shown by black lines. The CSD1 protein is highlighted with a dark red dot.

Of note, the CSD1 peptide is highlighted in light green and shows no change between untreated and treated samples, indicating that the pulldown was performed with the same efficiency. However, CSD1 interacting proteins showed an altered enrichment between untreated and treated conditions. The visualisation reveals that specifically the 30 min NaCl treatment increased the complexity of the CSD1 and CSD2 interactome. Overall, the complex formation of the CSD1 and CSD2 protein was found to be highly dynamic, depending on the type of stress applied and the time point at which the samples were analysed after the stress application.

In the interactome dataset, several ribosomal proteins were identified as strongly enriched proteins. Distinct ribosomal proteins were identified within the “core”-interactome of CSD1 and CSD2 (**Supplementary data 2**), but also changes in the enrichment of ribosomal proteins between the individual stress conditions were observed. To highlight the enrichment of ribosomal proteins (coloured in blue), the  $\log_2\text{FC}$  enrichment of peptide counts was visualised in relation to the p-value (**Figure 24 B**). The CSD1 protein is highlighted with a dark red dot. The visualisation revealed that ribosomal proteins were strongly enriched in all conditions and represent one major class of CSD interacting proteins. Interestingly, the ribosomal proteins showed an overall higher  $\log_2\text{FC}$  than other proteins through all conditions as highlighted by a density plot (**Figure 25**).

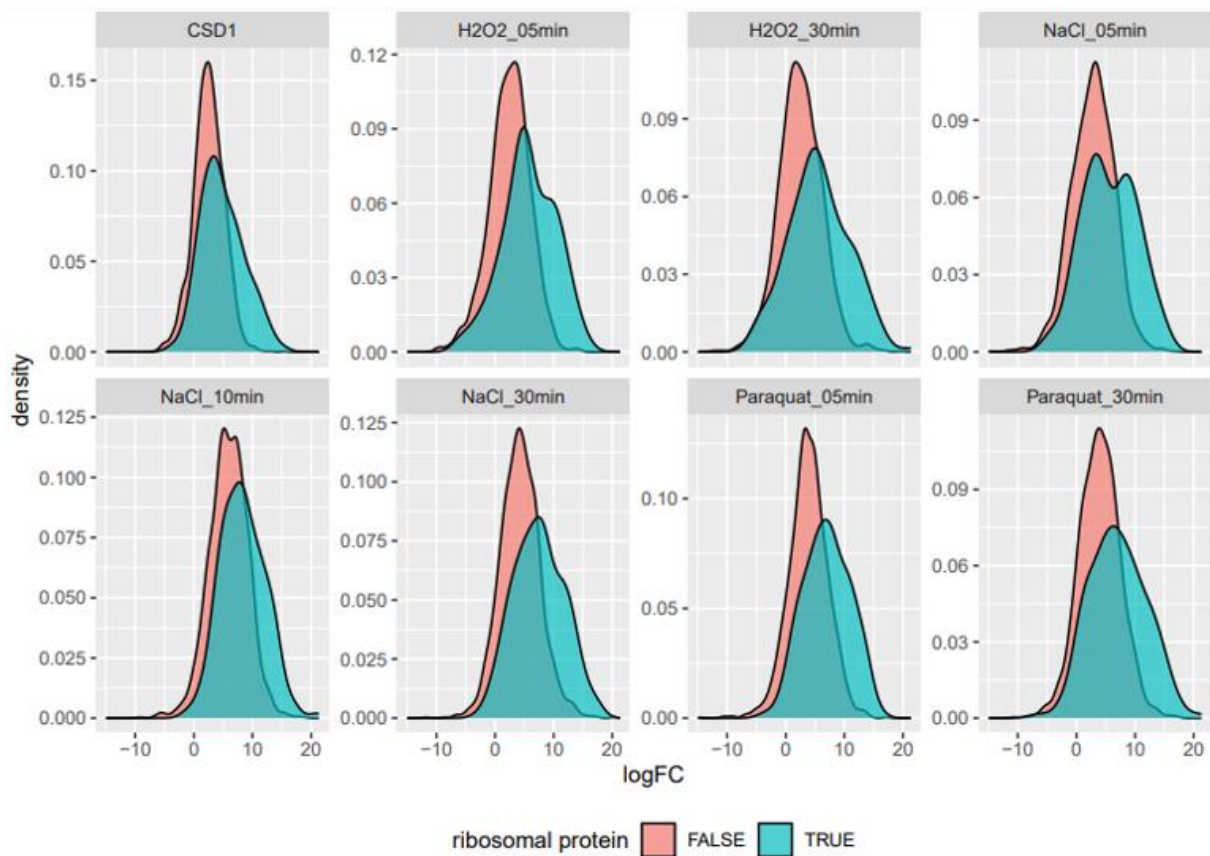


**Figure 25:** Ribosomal proteins are the strongest enriched fraction of identified interactions partners. The enrichment ( $\log_2(\text{FC})$ ) of all identified peptides is represented in a density plot for all conditions. Density of ribosomal proteins is highlighted in cyan and density of non-ribosomal proteins in red. The enrichment of ribosomal proteins is high through all conditions and increasing with stress.

The density plot describes the distribution of all peptides in relation to the  $\log_2(\text{FC})$  and thereby gives an overview if the strength of enrichment is increasing or decreasing between the conditions. Especially, the density of ribosomal proteins for high  $\log_2(\text{FC})$ s increased in the early 5-minute stress treatments. This might indicate a specific complex formation between ribosomes and the CSD proteins. **Figure 25** shows in general that the density of high FCs increased in the stress treatments. The increased number of peptides with high FCs indicates a stronger complex formation of CSD proteins upon stress.

### 3.3.4 Complex formation of CSD1 and CSD2 depends on the timing rather than the stress

To further understand the complex formation of the CSD1 and CSD2 protein upon stress, the hits identified at different time points were compared (**Figure 26**). Here, the focus was to explore if the CSD proteins were present in the same complex at different time points during the response towards for example H<sub>2</sub>O<sub>2</sub> (**Figure 26 A**).

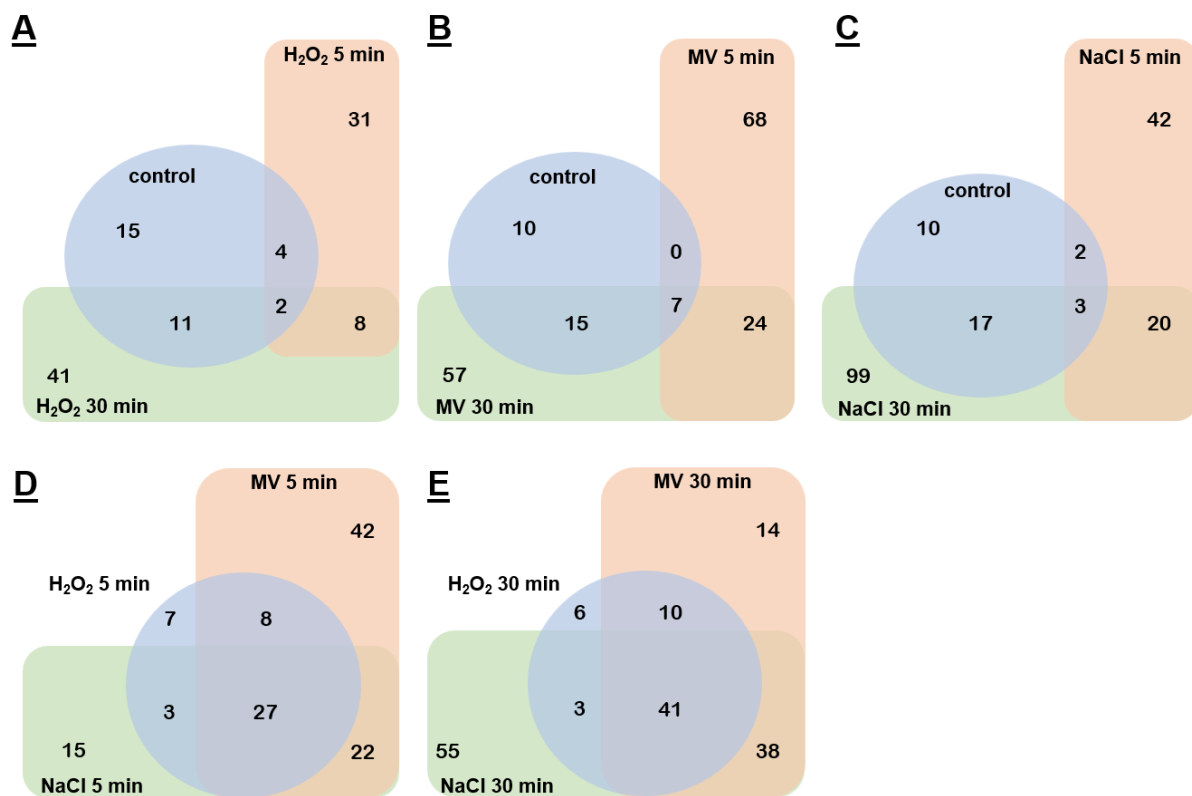


**Figure 26:** CSD complex formation depends on the stress condition and the time point. (A-C) The overlap of interaction partners between control, 5-minutes and 30-minutes time point for the H<sub>2</sub>O<sub>2</sub>, MV and NaCl treatment is shown in a Venn diagram from left to right, respectively. (D-E) The overlap of interaction partners between the different stress conditions at the same time point is shown in a Venn-diagram.

The overlap between untreated, 5-minutes of H<sub>2</sub>O<sub>2</sub> and 30-minutes of H<sub>2</sub>O<sub>2</sub> stress were two hits: the RPL4A/SAC56 (*AT3G09630*) and the plastidic RPL17 (*AT3G54210*) protein. Comparing the 5-minutes and 30-minutes time point of H<sub>2</sub>O<sub>2</sub> stress resulted in an overlap of eight hits: RH37 (*AT2G42520*), EIF3E (*AT3G57290*), Ribosomal protein (*AT2G20450*), RPL24 (*AT5G54600*), NAI2 (*AT3G15950*), RPL19 (*AT1G02780*), TPL6 (*AT1G47270*) and RPL13D (*AT5G23900*). A similar observation was made when comparing the MV and NaCl treatments with the control situation (Figure 26 B-C). The control and MV time points showed an overlap of 7 hits: RPL4A/SAC56 (*AT3G09630*), E1-OGDH1 (*AT3G55410*), MAB1 (*AT5G50850*), RPS11 (*AT3G52580*), plastidic RPL3 (*AT2G43030*), RPS6 (*AT4G31700*) and a Ribosomal protein (*AT3G53740*). The control and NaCl time points showed an overlap of 3 hits: RPS11 (*AT3G52580*), plastidic RPL3 (*AT2G43030*) and RPS6 (*AT4G31700*). It was found that between these three treatments, the CSD protein shared a minimal overlap of interaction partners under stress conditions as compared to the different time points and the control situation. This small overlap was surprising as it indicates that rather the time point than the

stress defines the CSD protein complexes. To understand if the time point was important, the hits for all three treatments at the 5-minutes time point were compared (**Figure 26 D-E**). These comparisons revealed an overlap of 27 hits between the three different stresses. At the 30-minutes time point the three stresses showed an overlap of 41 hits. Furthermore, in this comparison large overlaps between two out of three treatments were found as 5-minutes of MV and 5-minutes of NaCl shared 22 hits and 30-minutes of MV and 30-minutes of NaCl shared 38 hits. This overlap between the three treatments at the same time point, compared to the minimal overlap within a treatment (**Figure 26 A-C**), highlighted that the complex formation of the CSD proteins depends rather on the time point of the treatment than the individual treatment. Still, each condition and time point had a unique fingerprint of identified hits indicating a complex spatiotemporal interaction network of the CSD proteins.

The 27 hits that were identified in the overlap of the three different treatments at the 5-minute time point are highlighted in the **Table 6**.

**Table 6:** The 27 hits overlapping at the 5-minute time point between the H<sub>2</sub>O<sub>2</sub>, MV and NaCl treatment are shown.

Annotation	Abbreviation	Description	Annotation	Abbreviation	Description
AT3G57290	EIF3E	Eukaryotic translation initiation factor	AT1G02780	RPL19A	Ribosomal protein
AT1G70600	RPL27aC	Ribosomal protein	AT4G34670	RPS3aB	Ribosomal protein
AT3G09630	RPL4A, SAC56	Suppressor of ACAULIS 56	AT3G04920	RPS24A	Ribosomal protein
AT3G60245	RPL37aC	Ribosomal protein	AT3G18740	RPL30C	Ribosomal protein
AT4G02230	RPL19C	Ribosomal protein	AT5G54550	ATDOB12	Protein of unknown function
AT2G04865	MAIL2	MAIN-LIKE 2, aminotransferase-like	AT4G12310	CYP706A5	Cytochrome P450 oxidase
AT3G02660	FAC31, EMB2768	Tyrosyl-tRNA-synthetase	AT5G28060	RPS24B	Ribosomal protein
AT1G59359	RPS2B	Ribosomal protein	AT5G23900	RPL13D	Ribosomal protein
AT1G48380	RHL1, HYP7	ROOT HAIRLESS 1, HYPOCOTYL 7	AT3G52580	RPS14C	Ribosomal protein
AT2G20450	RPL14A	Ribosomal protein	AT5G45390	CLPP4	Caseinolytic protease P4
AT3G56340	RPS26C	Ribosomal protein	ATCG00130	ATPF	ATPase F0 complex
AT4G31700	RPS6A	Ribosomal protein	ATCG00750	RPS11	Ribosomal protein
AT5G54600	RPL24B	Ribosomal protein	AT2G20784	NA	Hypothetical protein
AT4G18100	RPL32A	Ribosomal protein			

Most of these identified hits were ribosomal proteins indicating that CSD1 might impact the translation in the early stress response towards these three treatments. The 41 hits that were identified in the overlap at the 30-minute time point represent less ribosomal proteins indicating that the CSD protein complexes changed between these two time points (**Table 7**).

**Table 7:** The 41 hits overlapping at the 30-minute time point between the H<sub>2</sub>O<sub>2</sub>, MV and NaCl treatment are shown.

Annotation	Abbreviation	Description	Annotation	Abbreviation	Description
AT2G42520	RH37	RNA helicase	AT2G45710	RPS27A	Ribosomal protein
AT4G23100	CAD2, PAD2	Glutamate-cysteine ligase	AT4G35110	PEARL4	Phospholipase-like protein
AT3G55410	E1-OGDH1	2-oxoglutarate dehydrogenase	AT3G08590	iPGAM2	Phosphoglycerate mutase
AT1G13930	NA	Nodulin-related protein 1	AT2G44640	NA	Trigalactosyldiacylglycerol-like protein
AT1G04780	NA	Ankyrin repeat family protein	AT3G22230	RPL27B	Ribosomal protein
AT1G74060	Ribosomal protein	Ribosomal protein	AT2G43030	RPL3 related	Ribosomal protein
AT1G11860	GLDT	Glycine-cleavage T-protein family	AT2G20450	RPL14A	Ribosomal protein
AT4G32470	NA	Cytochrom bd ubiquinol oxidase	AT3G55750	RPL35aD	Ribosomal protein
AT5G02960	RPS23B	Ribosomal protein	AT4G01050	TROL	Thylakoid rhodanese-like
AT3G09840	CDC48A	Cell division cycle protein 48A	AT5G54600	RPL24B	Ribosomal protein
AT1G02780	RPL19A	Ribosomal protein	AT5G51380	NA	RNI-like superfamily protein
AT1G27400	RPL17A	Ribosomal protein	AT3G15950	NAI2	DNA topoisomerase-related
AT4G02520	GSTF2, GST2	Glutathione S-transferase PHI 2	AT4G26910	E2-OGDH1	Dihydrolipoamide succinyltransferase
AT3G54210	RPL17	Ribosomal protein	AT3G53740	Ribosomal protein	Ribosomal protein
AT5G50850	MAB1	Transketolase family protein	AT4G19191	NA	TPR-like superfamily protein
AT1G47270	TPL6	Tubby like protein 6	AT4G27370	VIIIB	Myosin VIII B
AT5G23900	RPL13D	Ribosomal protein	AT2G21330	FBA1	Fructose-bisphosphate aldolase 1
AT3G27530	GC6, MAIGO4	Golgin candidate 6	AT1G01320	REC1, FLL2	Reduced chloroplast coverage 1
AT1G26910	RPL10B	Ribosomal protein	ATCG00810	RPL22	Ribosomal protein
AT1G14320	RPL10A	Ribosomal protein	AT2G01720	OST1A	Oligosaccharyltransferase 1A
AT1G77120	ADH1	Alcohol dehydrogenase 1			

Several interesting proteins were identified at these time points: the CELL-DIVISION CYCLE 48A (CDC48A) protein which is involved in the turn-over of an immune receptor (Copeland et al., 2016) and the ubiquitin-dependent degradation of intra-chloroplast proteins (Li et al., 2022) or the NAI2 protein which is involved in ER body formation (Yamada et al., 2008). It will be a future task to resolve the molecular role of the complex formation of CSD proteins with the identified proteins. As the complex formation was rather time point specific than treatment specific, the biological role might be part of a general stress response.

### 3.3.5 The complex formation of CSD1 and CSD2 is time- and stress-specific

To further highlight the temporal and condition-specific dynamics of the CSD complex formation, ten identified interacting proteins were analysed for their enrichment between the different stress conditions through a heatmap representation (**Figure 27 A**).



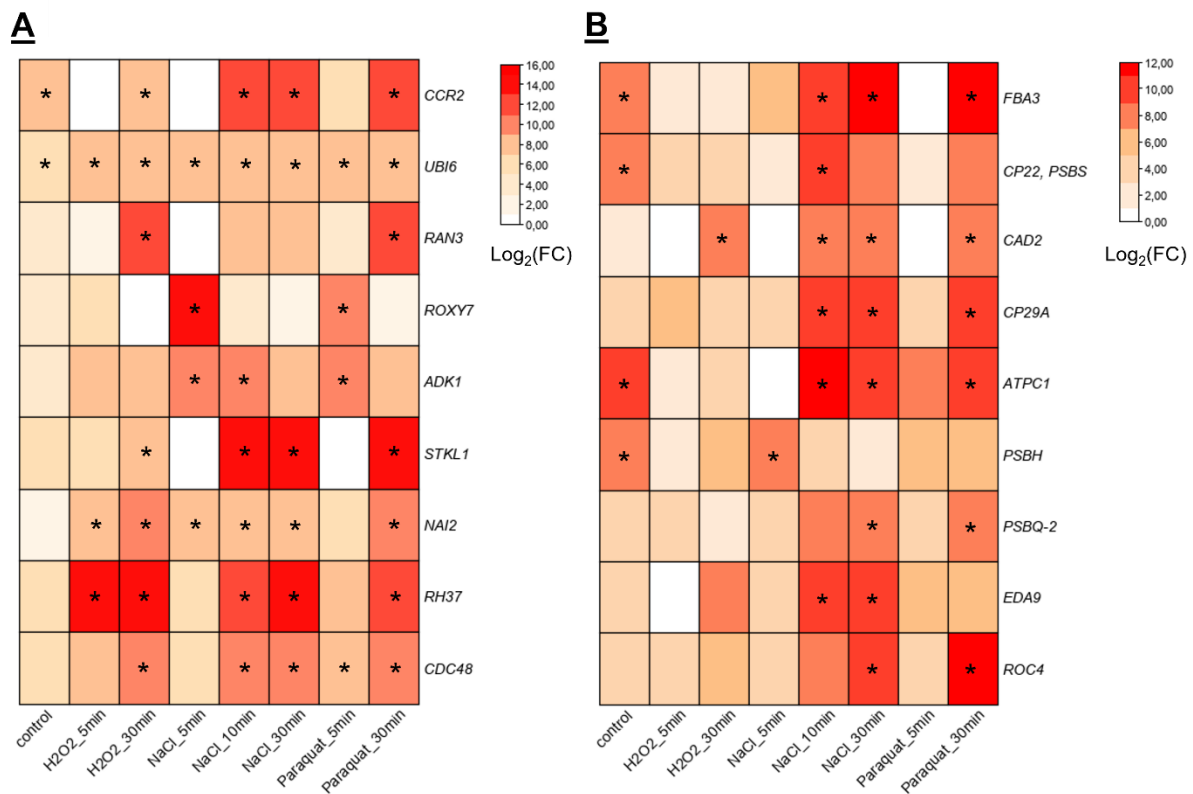


**Figure 27:** CSD1 and CSD2 interaction partners show stress and time point specific enrichment dynamics. The enrichment ( $\log_2(\text{FC})$ ) of selected interaction partners of CSD1 (**A**) and CSD2 (**B**) through the stress treatments and time points are shown in a heatmap. Each data point is the mean enrichment of four biological replicates. Statistical significance of individual enrichments is shown with an asterisk (p-value < 0.05).

In untreated samples, the CIRCADIAN RHYTHM AND RNA BINDING 2 (CCR2) and the UBIQUITIN 6 (UBI6) protein showed a significant enrichment indicating that they were present in the same complex as CSD1. The UBI6 protein was significantly enriched in all conditions indicating that the complex of UBI6-CSD1 was independent of the treatment and time point. The CCR2 protein was enriched in untreated and the 30-minute treatment time points. At the 5-minute time points, the CCR2 protein was not enriched in the pulldown samples indicating the CCR2-CSD1 complex was dynamic and dissociated during the early phase of the stress response. The enrichment of the RAN GTPASE 3 (RAN3) was significant at 30 minutes of H<sub>2</sub>O<sub>2</sub> and 30 minutes of MV treatment implying that the RAN3-CSD1 complex only forms under prolonged stress conditions. Opposing to RAN3, the CC-TYPE GLUTAREDOXIN 7 (ROXY7) was significantly enriched at 5 minutes of NaCl and 5 minutes of MV treatment. Furthermore, the complex formation of CSD1 with the STOREKEEPER-LIKE TRANSCRIPTION FACTOR 1 (STKL1) and CDC48A was specific for the 30-minute time point in all three different treatments while it was not present in the 5-minute time points, except

for CDC48A at 5 minutes of MV treatment. Stress-specific enrichment was also observed for the ADENOSINE KINASE 1 (ADK1) in the 5- and 10-minute NaCl treatment and 5-minute MV treatment. As the ADK1 is the homolog of the human adenosine kinase which was shown to interact with the human SOD1 counterpart (BioGRID, Stark et al., 2008; Wan et al., 2015), this cross-species complex formation will be a point for future research. These results showed that the complex formation of CSD1 with proteins like RAN3, ROXY7, CDC48A, STKL1 and ADK1 followed individual patterns with time point-related dynamics indicating a specific molecular fine-tuning for these complexes.

Similar to CSD1, dynamic complex formation was also observed for potential CSD2 interaction partners (**Figure 27 B**). For example, the FRUCTOSE-BISPHOSPHATE ALDOLASE 3 (FBA3) was enriched in the untreated samples and 30-minutes treatments of NaCl and MV, however it was not enriched in the 5-minutes time point or the H<sub>2</sub>O<sub>2</sub> treatment. This trend was also observed for CINNAMYL ALCOHOL DEHYDROGENASE HOMOLOG 2 (CAD2), CHLOROPLAST RNA-BINDING PROTEIN 29A (CP29A) and ATP SYNTHASE COMPLEX C1 (ATPC1). Oppositely, the enrichment of ROTAMASE CYP 4 (ROC4) was significant in the 30-minutes time point of NaCl and MV treatment. Interestingly, only CAD2 showed a significant enrichment upon H<sub>2</sub>O<sub>2</sub> treatment while the other 9 proteins only showed specific enrichment under control, NaCl or MV treatment. Taken together, these results showed that the CSD2 complex formation was, similar to CSD1, individual and highly dynamic. In an ongoing experiment, the interaction of CSD1 and CSD2 with the highlighted proteins is tested with another experimental setup to elucidate if the CSD proteins interact directly or indirectly with the identified protein partners.

Within the peptide dataset, a substantial amount of ribosomal proteins was identified. As the mCherry-antibody was used a negative control to clear the background noise of peptides in the dataset, the identified peptides which managed to pass the sorting filter (p-value <0.05, >50% of replicates) were considered as significant enriched hits. The observation that the density and enrichment of ribosomal proteins changed upon the different stress treatments (**Figure 25**) provoked the question if the CSD proteins were present in different ribosomal protein complexes upon stress treatment. To answer this question, the dataset was screened for ribosomal proteins and the enrichment of these ribosomal proteins was visualised in a heatmap (**Figure 28 A-B**).

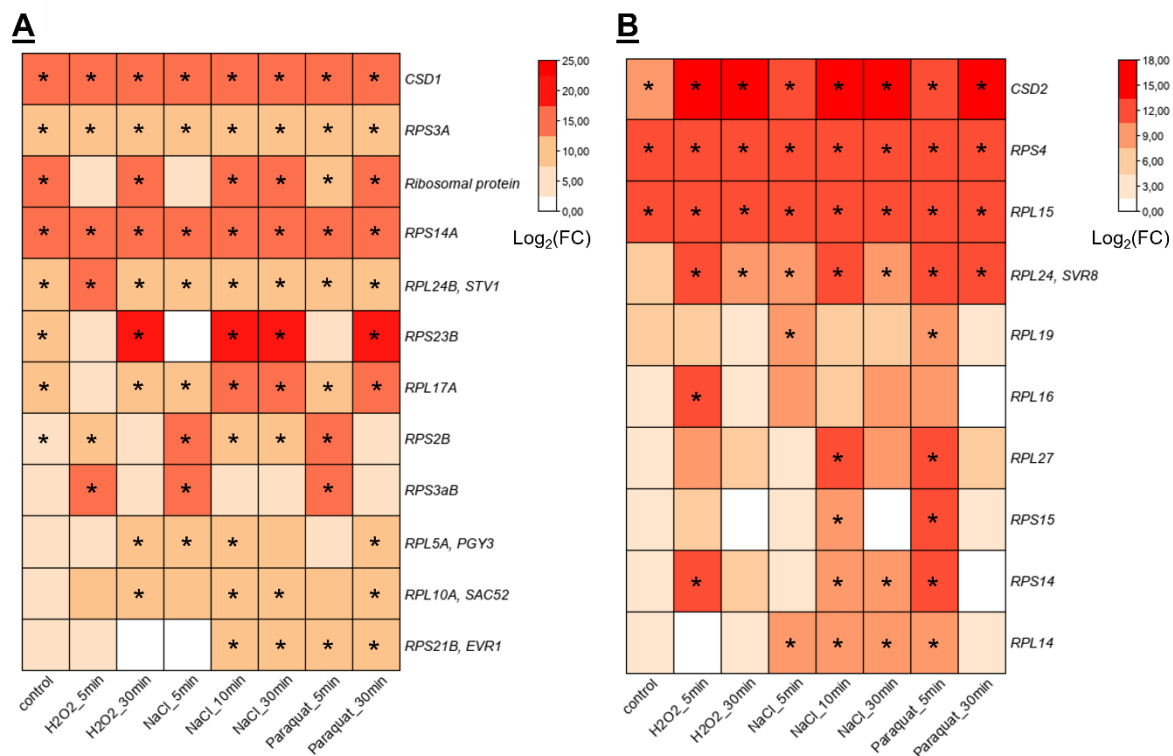


**Figure 28:** Complex formation with ribosomal proteins is partially time- and stress-specific. The enrichments ( $\log_2(\text{FC})$ ) of the CSD proteins and several ribosomal proteins through the different stress treatments and time points are shown in a heatmap. These ribosomal proteins are either interaction partners of CSD1 (**A**) or CSD2 (**B**). Each data point is the mean enrichment of four biological replicates. Statistical significance of individual enrichments is shown with an asterisk ( $p$ -value  $< 0.05$ ).

Two individual heatmaps were generated based on the subcellular localisation of the 60S/40S cytosolic and 50S/30S plastidic ribosomal proteins to discriminate between CSD1 and CSD2. In **Figure 28** (Panel A) the enrichment of CSD1 was visualised in comparison to a set of ribosomal proteins. Several ribosomal proteins constitutively interact with CSD1, as they were found under control conditions and all stress conditions tested (RPS3A, RPS14A and RPL24B). Other ribosomal proteins, like RPS23B, were strongly enriched after 30-minutes of stress as compared to the untreated samples but showed no enrichment in the 5-minutes time points. Opposingly, RPS3aB showed only a strong enrichment in the 5-minutes time point in all three treatments. Overall, the enrichment of the selected ribosomal proteins was highly dynamic indicating that CSD1 associates with different ribosomal proteins or complexes under control and stress conditions.

Similar to CSD1, the complex formation with different ribosomal proteins was also observed for CSD2 (**Figure 28 B**). Plastidial ribosomal proteins like RPS4 and RPL15 showed a constant enrichment through untreated and treated samples while ribosomal proteins like RPL27 and

RPS15 showed a specific enrichment pattern. RPL19 was enriched in the 5-minutes NaCl and MV time point, while RPL16 was only significantly enriched in the 5-minutes H<sub>2</sub>O<sub>2</sub> time point. Overall, the visualised enrichments of ribosomal proteins highlighted that CSD2 associates with certain ribosomal protein complexes through all conditions but seems to also associate with stress-specific and time point-specific ribosomal protein complexes.

### 3.3.6 Summary

In this chapter the N-terminal acetylation of CSD1 at the  $\alpha$ -amino acid alanine was found. The structure of the N-terminus of CSD1 and the work of Linster *et al.* strongly indicate that the acetylation is facilitated by the NatA complex (Linster *et al.*, 2015). An *in-silico* analysis suggests that several SOD isoforms in Arabidopsis might also be targets for NTA. Furthermore, the CSD1 counterparts in human, yeast, barley and Marchantia shared the conserved  $\alpha$ -amino acid alanine indicating that the N-terminal acetylation is conserved in the green lineage.

Furthermore, 515 interactors of CSD1 or CSD2 were identified in wild type Arabidopsis seedlings. Based on subcellular localisation information, 267 interactors were related to CSD1 and 163 to CSD2. Among the 515 interacting proteins, many ribosomal proteins were detected. By using Arabidopsis seedlings treated with different stresses for different time intervals, changes in the complex formation of the CSD proteins were explored. It was found that the complex formation of CSD proteins is highly dynamic and depends rather on the time point of the stress response than the response towards a specific treatment. Nevertheless, each individual stress treatment had a unique fingerprint of CSD interactors at a specific time point. Several CSD1 interacting proteins like CCR2, STKL1, CDC48A, RAN3, ROXY7 or ADK1 showed a time- and stress-specific complex formation with CSD1. Similarly, CSD2 interactors like FBA3, CP22, CAD2 or ROC4 showed a time- and stress-specific complex formation. Furthermore, several ribosomal proteins showed a time- and stress-specific complex formation with the CSD proteins. Combined, these results revealed that the CSD proteins are involved in the initial stress response through temporally restricted protein complex formation. The identification of the interaction partners and the dynamic of their complex formation with the CSD proteins provides novel insights that will help to understand the molecular function of CSD proteins during the stress response in Arabidopsis.

## 4 DISCUSSION

This work aimed to explore the moonlighting function of the *Arabidopsis* superoxide dismutase protein CSD1. Especially the recent advances on the role of SOD1 from human and yeast in transcriptional regulation urged for exploration of this novel function in plants (Tsang et al., 2014; Li et al., 2019). Here it was found that CSD1 in plants localised both to the cytosol and the nucleus. In the nucleus, CSD1 is able to bind DNA, and acts as a transcriptional regulator during the initial response to salt stress. Moreover, the protein interactome of CSD1 was explored by a unique experimental setup, revealing that CSD1 forms highly dynamic protein complexes that occur in a temporal manner upon stress. Furthermore, the exploration of the nuclear interaction partner HIPP20 indicates that CSD1 and HIPP20 form a transcriptional complex. The discovery that HIPP proteins act as transcriptional regulators grants an unknown plant protein family a novel and important molecular function. Here the major advances and follow-up research questions will be addressed and discussed.

### 4.1 Chapter 1: CSD1 acts as a transcriptional regulator in the early salt stress response

In this chapter, the moonlighting function of CSD1 as a transcriptional regulator during the early salt stress response in *Arabidopsis thaliana* was established. Upon salt stress, cytosolic CSD1 translocates to the nucleus where it binds specifically to DNA by recognising a TGCTTT *cis*-element in the promoter of here uncovered target genes. During the early salt stress response, CSD1 affects the transcriptional response of stress-related genes like *NCED3*, *HSFA6B* and *TAT3* through binding to their promoter and regulating their transcription. The impact of these discoveries and the potential for novel research lines will be addressed.

The SOD protein family was discovered more than 50 years ago by McCord and Fridovich and seen exclusively as pivotal antioxidant enzyme by the dismutation of superoxide to hydrogen peroxide (McCord & Fridovich, 1969). This fixed textbook view has dramatically changed within the last years by the discovery of the moonlighting function of SOD1 as transcriptional regulator in yeast and human cells. Tsang et al. (2014) found that SOD1 translocates to the nucleus and regulates the expression of stress-related genes upon oxidative stress in yeast. In

2019, Li et al. found that also in human cells SOD1 translocates to the nucleus and regulates the expression of stress-related genes upon oxidative stress. The initial discovery that SOD1 acts as a transcriptional regulator revolutionised and shifted the view on the CuZnSOD protein family (Tsang et al., 2014). Due to the causative link between SOD1 and ALS (Franklin et al., 2020), SOD1 has always been extensively studied, thus these novel discoveries are especially astonishing. To date, SOD1 is known to be a regulator in cancer development (Salem et al., 2015; Li et al., 2018), starvation/nutrient sensing (Tsang et al., 2018) and ribosome biogenesis (Wang et al., 2021). Highlighted in a review by Xu and co-authors, all these individual discoveries are specifically linked to the molecular function of the nuclear fraction of SOD1 (Xu et al., 2022). However, a clear separation between these two molecular functions of SOD1, as enzyme and as transcriptional regulator, remains open and will be a major research question to be entangled.

The recent findings are mostly connected to yeast and human research. My research work now translates and advances this knowledge into the plant kingdom by the identification of CSD1's role as transcriptional regulator during salt stress in Arabidopsis and is therefore a crucial contribution to further understanding the role of SODs in all kingdoms of life. Also, in plants SOD proteins are described as basic and pivotal antioxidant enzymes which now will be seen in a different light with the here uncovered novel function of CSD1 as transcriptional regulator during salt stress in Arabidopsis (Kliebenstein et al., 1998). It will be an important task to elucidate if the role of CSD1 as transcriptional regulator is also conserved within the eclectic SOD protein family in plants, especially in crops.

Several experimental aspects open new research opportunities in Arabidopsis. For example, the stress-induced movement of CSD1/SOD1 to the nucleus is conserved between Arabidopsis, yeast and human cells (Tsang et al., 2014; Li et al., 2019). The translocation of SOD1 in yeast and human depends on two stress-induced phosphorylation events facilitated by a conserved module of kinases (Tsang et al., 2014, Li et al., 2019). The phosphorylatable residues on the SOD1/CSD1 protein are conserved between yeast, human and Arabidopsis, however no obvious homologous kinases are present in Arabidopsis. Here, it will be illuminating to understand the interactome of CSD1 that might contain candidate protein kinases. To understand the mechanism that triggers the stress-induced nuclear movement of CSD1, will close a knowledge gap for the molecular function of CSD1 and might also provide a link to the upstream stress signal that is currently missing. Furthermore, it needs to be determined if the

enrichment of the SOD1/CSD1 protein is controlled by an active transport mechanism. The protein surface does not contain an obvious nuclear-localisation-signal (NLS). Of note, the described experimental evidence was based on the use of the transgenic *35S:CSD1-GFP* overexpression line that does not resemble the wild type protein level. To date it remains elusive how much CSD1 is present in the nucleus under control conditions. Therefore, it will be interesting to study how the nuclear fraction of CSD1 is controlled as the FRAP results strongly indicate an active transport mechanism.

In the nucleus, CSD1 associates with specific DNA motifs in the promoter of salt stress-related genes thereby regulating their transcription by acting as a transcriptional regulator during the initial response to salt stress. Here, the transcriptional role of CSD1 is not only linked to oxidative stress as shown in yeast and human cells but also to a natural stress like salt stress in *Arabidopsis*. The early salt stress response in *Arabidopsis* is comprised of osmotic stress whereas the “later” response is characterised by ion accumulation (Munns & Tester, 2008). Rapid growth reduction within the first minutes and hours in response to salt stress are connected to the osmotic phase (Rajendran et al., 2009; Adem et al., 2014; Tilbrook et al., 2017). Within the osmotic phase, growth reduction is based on altered cell cycle activity (West et al., 2004), cell expansion (Niu et al., 1996; Neves-Piestun & Bernstein, 2005), leaf emergence (James et al., 2002; Fricke et al., 2006) and cell wall rigidity (Byrt et al., 2018; Feng et al., 2018).

A molecular characteristic of the osmotic phase is the rapid accumulation of ROS, a so-called ROS burst (Jiang et al., 2012; Schmidt et al., 2013). This ROS burst is necessary for the adaptation of plants to salt stress (Ben Rejeb et al., 2015). However, the molecular sensors and facilitators of the ROS burst remain elusive. Here, the elucidation of a novel mechanism involved in the early salt stress response, and potentially involved in the growth reduction in the osmotic phase is reported. This novel mechanism provides a link between the initial ROS burst, the ABA accumulation and subsequently salt stress tolerance. It was found that CSD1 regulates the expression of salt-stress related genes like *NCED3* that represents the rate-limiting enzyme in the biosynthesis of ABA (Tan et al., 2003). ABA biosynthesis is dynamically regulated during salt stress (Fricke et al., 2006), however peak levels of ABA are correlated with the early phase (Geng et al., 2013) and might be induced by the rapid ROS signaling. As CSD1 dismutates superoxide to hydrogen peroxide it might be able to act as signal integrator of the initial ROS burst. In a future experiment, it will be interesting to study if CSD1 links the

ROS burst with the ABA peak in the osmotic phase by regulating the expression of *NCED3*. The expression of *NCED3* peaks at 1 and 3 hours suggesting that *NCED3* is the major factor to control the ABA content. The accumulation of ABA correlates with a growth quiescence in the primary root (Geng et al., 2013), something that also happens in the response to drought stress (Iuchi et al., 2001). Therefore, the transcriptional induction of *NCED3* by *CSD1* might represent an output signal of the initial ROS burst resulting in an initial growth reduction within the osmotic phase of the early salt stress response. With other words, *CSD1* might translate the ROS signal into an alteration of ABA levels for short term stress adaptation.

Another target gene of *CSD1* is *HSFA6B*. Heat shock transcription factors (HSFs) are known to control the expression of heat shock proteins (HSPs) which are important to respond and cope towards stress with their role as molecular chaperones (Guan et al., 2014). In a previous study, *HSFA6B* was shown to be induced during salt and osmotic stress, while other HSFs respond at later stages of the stress (Swindell et al., 2007). Furthermore, acquired thermotolerance and root elongation are regulated by *HSFA6B* in an ABA-dependent manner (Huang et al., 2016; Wenjing et al., 2020). Also, it is proposed that both *HSFA6A* and *HSFA6B* are involved in abiotic stress tolerance through regulation of ROS homeostasis in plants (Wenjing et al., 2020). This suggests that ABA and *HSFA6B* act upstream of ROS, however, here it is shown that the regulation of *HSFA6B* expression by *CSD1* acts upstream of ABA and is induced after the initial ROS burst. This suggests that the initial observation of ABA regulation of ROS homeostasis is rather a downstream feedback mechanism (Wenjing et al., 2020). In the future, it will be interesting to further tackle the hierarchy of the transcriptional regulation of *HSFA6B* expression and interconnection of ABA and ROS leading to abiotic stress and thermotolerance.

With *TAT3*, another target gene of *CSD1* was discovered. The *TAT* genes encode tyrosine aminotransferases that catalyze the reversible transamination between Tyr and 4-hydroxyphenylpyruvate representing the entry point in plants for the biosynthesis of secondary metabolites like plastoquinone and tocopherol (Vitamin E) while also enabling Tyr degradation in the recycling process of energy and nutrients (Wang et al., 2016d). The homologous *TAT1* and *TAT2* function together in tocopherol biosynthesis and *TAT1* plays the dominant role in Tyr degradation in planta with *TAT2* having a lesser role (Wang et al., 2019). The affinity for the Tyr substrate differs between both *TAT* enzymes indicating a functional difference (Wang et al., 2016d). Tocopherols are antioxidants that deactivate photosynthesis-derived ROS and



thereby prevent the propagation of lipid peroxidation (Munne-Bosch, 2005). So far, little is known about the molecular and biological function of *TAT3*, but a QTL analysis indicates that *TAT3* is involved in the metabolism and/or regulation of tocopherol biosynthesis (Gilliland et al., 2006). Therefore, by regulating the transcription of the *TAT3* gene, CSD1 might affect the detoxification of ROS within the chloroplast through tocopherol accumulation upon abiotic stress.

A T-DNA insertion line (*csd1-3*) and an overexpression line of the FLAG-CSD1 fusion protein (*35S:FLAG-CSD1*) resulted in plants virtually devoid of CSD1. The exact mechanism that caused the *35S:FLAG-CSD1* line to be virtually devoid is not known. Still, one reasonable explanation for the phenotype and genotype might be co-suppression. Co-suppression describes the introduction of a gene by transformation into a cell, that causes neither the resident nor the transgene copies of the same gene to get expressed (Napoli et al., 1990; Hamilton & Baulcombe, 1999). In a future work it will be interesting to understand if the observed phenomena is linked to the potential impact of the novel PTM for CSD1, the N-terminal acetylation of the  $\alpha$ -amino acid alanine. Potentially, the N-terminal FLAG tag stabilises CSD1, which results in the accumulation of CSD1 that promotes the co-suppression response. Both transgenic plants, *csd1-3* and *35S:FLAG-CSD1*, showed an early senescence and salt stress sensitive phenotype. Further, the transgenic *35S:FLAG-CSD1* plants were affected in their embryogenesis as several plants showed a cup-shape like phenotype. Both transgenic backgrounds strongly indicate that CSD1 is an important regulator during abiotic stress and development. These results are in line with identified target genes of CSD1. *NCED3*, *HSFA6B* and *TAT3* are salt-stress related genes and *SPL2* and *TTG1* are developmental regulators (Wang et al., 2016c; Xu et al., 2016; Airoidi et al., 2019). In future experiments, the major task will be to entangle the moonlighting function as transcriptional regulator from the enzymatic function of CSD1 and link the individual functions to the observed phenotypes. To this end, complementation assays can be performed with an enzyme-dead CSD1 mutant. That said, DNA binding assays with enzymatically inhibited CSD1 still allowed for efficient DNA binding, suggesting that the two functions do not depend on each other.

In this chapter, transcriptional targets of CSD1 in the early salt stress response in Arabidopsis were identified and three specific target genes were validated in detail: *NCED3*, *HSFA6B* and *TAT3*. The expression of all three genes is affected in transgenic Arabidopsis plants with altered CSD1 protein levels and the binding and activation of their promoter by CSD1 has been

confirmed by EMSA and TA assays. As the promoter sequence of a gene is always a competitive landscape for many different transcription factors, the sole impact of CSD1 on the expression of these target genes remains unclear. Several transcription factors have been identified to regulate *NCED3* and *HSFA6b*. For example, *NCED3* is regulated by transcription factors like ATAF1 (Jensen et al., 2013), SRM1 (Wang et al., 2015), NGATHA1 (Sato et al., 2018) and HAT1 (Tan et al., 2018), while NAC019 binds to the promoter of *HSFA6B* (Guan et al., 2014). It will be of interest to entangle the precise mechanism by which CSD1 regulates the expression of its target's genes and if cooperation or competition with other transcription factors is involved.

The new concept of CSD1 as nuclear localised protein raised the question if CSD1 is interacting with any protein that might impact CSD1's ability to activate transcription or affect the enzymatic function. Therefore, a pivotal point of research was to understand and explore the option for potential interactors. In the next chapter, a novel interactor of CSD1, HIP20, that represents a member of a rather uncharacterised plant-specific protein family was explored. This discovery resulted in new findings to understand the regulation of transcription by CSD1 and furthermore explored a specific function of this new protein family.

The experiments to understand the ability of CSD1 to activate the transcription of its target's genes using the TA assay in protoplasts revealed that the FLAG-CSD1 fusion protein is the strongest activator of promoter activity. This initial finding and the knowledge about plenty post-translational modifications to the yeast and human SOD1 protein raised the hypothesis that the Arabidopsis CSD1 protein is also post-translationally modified. Within a following chapter, it will be delineated how an initial experimental observation resulted in the identification of a novel post-translation modification with surprising biological impact.

In the first chapter of this thesis, the novel function of CSD1 as transcriptional regulator in Arabidopsis was explored. This complements and extends the knowledge about CSD1/SOD1 as transcriptional regulator in all major kingdoms of life. These groundbreaking findings provoked several new research avenues of which some will be highlighted below.

## 4.2 Chapter 2: CSD1-interacting protein HIPP20 belongs to a novel class of transcriptional co-activators

In this chapter a family of putative metallochaperones, the so called HIPP proteins, have been characterised as some of them can interact with CSD1. HIPP proteins contain one or more HMA domains and an isoprenylation motif and are suggested to be required for the safe transport of metallic ions inside the cell (de Abreu-Neto et al., 2013). Still the few characterised HIPP proteins reveal a role for these protein in abiotic and biotic stress pathways; however, the molecular mechanism through which they act are unknown. Here, the localisation of HIPP20/21/22 as mainly nuclear localised proteins was found. Moreover, in plant cells CSD1 specifically interact with HIPP20 inside the nucleus. The interaction of CSD1 with HIPP21 and HIPP22 was identified through heterologous expression in a Y2H assay. In addition, it was found that several HIPP proteins with distinct structure act as transcriptional activators, revealing a novel molecular function of HIPP proteins. These advances and the impact of these discoveries will be discussed below.

The here identified CSD1-interacting HIPP proteins, HIPP20, HIPP21 and HIPP22, are mainly nuclear localised proteins, except for HIPP21 which also resides in the cytosol. Furthermore, these three HIPP proteins show a specific subnuclear localisation to structures that might represent the nucleolus. As ribosome biogenesis occurs in the nucleolus (Weis et al., 2015), HIPP proteins might have a function in that which is in line with the identification of ribosomal proteins as CSD1-interacting proteins in results Chapter 3. The identified localisations fit to previous reports that show an exclusive localisation to the nucleus of HIPP3 (Zschiesche et al., 2015) and HIPP26 (Barth et al., 2009). Both proteins also show specific subnuclear localisation to the nucleolus. The homolog of AtHIPP26 in *Oryza sativa*, OsHIPP41, shows a nuclear and cytosolic localisation (de Abreu-Neto et al., 2013). A recent study discovered the cytosolic and nuclear localisation of HIPP1 and the cytosolic and nuclear envelope localisation of HIPP6 and HIPP7 (Guo et al., 2021). Summarised, the findings that HIPP20, HIPP21 and HIPP22 are mostly nuclear localised proteins complements previous reports. It will be curious to understand if this localisation is conserved between all five clades of the HIPP protein family. Furthermore, the effect of the isoprenylation or farnesylation on the localisation will be a future aspect to

research. Initial findings surrounding the HIPP26 protein suggest that this modification directly impacts the subcellular cytosol-nuclear equilibrium (Cowan et al., 2018).

The loss of the HIPP20 protein and its homologs did not have a direct impact on the vegetative growth of *Arabidopsis* under standard growth conditions. Also, double knockouts of either *hipp20/21* and *hipp20/22* did not show a direct impact (data not shown). Plants overexpressing *HIPP20* by a *35S:HIPP20-GFP* construct were indistinguishable from the wild type (data not shown), which is in line with the overexpression of *CSD1*. Still, what was not yet tested here is whether the loss or overexpression of *HIPPs* affects abiotic stress tolerance. That said, a previous investigation on cadmium induced oxidative stress found that *HIPP20/21/22* triple mutants are impaired in their tolerance (Tehseen et al, 2010). Recently, the clade I HIPP proteins *HIPP6* and *HIPP7* have been shown to interact with the FAD-containing cytokinin oxidase/dehydrogenase (CKX) enzymes in *Arabidopsis* (Guo et al., 2021). By regulating the endoplasmic reticulum-associated degradation of CKX proteins, the HIPP proteins directly affect the cytokinin response in *Arabidopsis* (Guo et al., 2021). Overexpression of *HIPP6* and *HIPP7* altered leaf development and the response to cytokinin. Interestingly, the authors highlight the use of a *35S:GFP-HIPP6/7* construct and indicate that a C-terminal tag does not have the same effect on the phenotype. This might explain why plants overexpressing the *35S:HIPP20-GFP* construct were indistinguishable from the wild type. For future transgenic approaches, it will be important to consider that the C-terminus harbours the isoprenylation motif that might be affected through a C-terminal-based overexpression. Combined with the need to generate a *hipp20/hipp21/hipp22* triple mutant the effect of the HIPP protein level on the phenotype of *Arabidopsis* plants demands future research.

The identification of the nuclear interaction of *CSD1* and *HIPP20* is a key-finding within this chapter. For both proteins, the identification of an interaction partner represents an exciting step forward to understand the molecular function as only a limited number of interactors are known in *Arabidopsis*. Interestingly, the HMA domain of HIPP proteins shows a high degree of similarity to the HMA domain of the CCS protein (de Abreu-Neto et al., 2013). As the CCS proteins is required to deliver copper metal ions to the CSD proteins and thereby inducing the conformational change towards the active form in *Arabidopsis* (Chu et al., 2005), it is reasonable to speculate that HIPP proteins could also affect the enzymatic function of *CSD1*. The *HIPP3* protein has been reported to bind zinc ions (Zschiesche et al., 2015), which is to date the only characterisation of a bound metal ion to HIPP proteins. The mode of action of HIPP proteins

remain elusive to date. Here, it is not hypothesised that HIPP20 delivers a Cu or Zn metal ion to CSD1 as it is expected that CSD1 already contains both metal ions while translocating to the nucleus. Based on the structural similarity of the HMA domain of CCS and HIPP20, one hypothesis might be that the HIPP20 protein can inactivate the enzymatic function of CSD1 by binding at the position of the Cu-binding pocket and thereby blocking the active site of CSD1. This hypothesis is founded on the rationale that the presence of hydrogen peroxide in the nucleus can cause direct harm to the genetic information. To date, experiments are ongoing and preliminary data indicate that indeed HIPP20 can inhibit the enzymatic function of CSD1.

The role as transcriptional activators is the first discovery that grants the HIPP protein family a molecular function. Here, it was found that HIPP5, HIPP20, HIPP21, HIPP22 and OsHIPP42 act as transcriptional activators. For now, members of two out of five clades within the protein family have been characterised as transcriptional activators. In the future, it will be interesting to study the subcellular localisation of HIPP proteins of the clades III, IV and V and if they can also act as transcriptional activators. This will clarify if the function as transcriptional activators is shared between all five clades. Nevertheless, as HIPP proteins are plant-specific proteins it indicates that transcriptional regulators evolved specifically in plants.

Reported interaction data indicate that HIPP proteins are commonly part of transcriptional complexes, underlying their novel function as transcriptional co-activators. For example, HIPP20 is reported to interact with transcription factors like the ZINC FINGER HOMEODOMAIN 1 (ZFHD1, AT1G69600), BASIC HELIX-LOOP-HELIX 145 (bHLH145, AT5G50010) and an uncharacterised SEQUENCE-SPECIFIC DNA BINDING TRANSCRIPTION FACTOR (AT3G54390) (Braun et al., 2011). Neither the exact mechanism that allows HIPP proteins to act as transcriptional activators nor the role of HIPP proteins in transcriptional complexes is yet understood. As HIPP proteins are thought to manage the safe transport of metal ions to target proteins (Tehseen et al., 2010), it is speculated to be the mode of action by which HIPP proteins control the activity of transcription factors. However, this is contradicted by the fact that HIPP20 interacts with bHLH145 that does not contain a metal ion. To understand the interaction of HIPP proteins with distinct transcription factors, ongoing experiments are performed with combinations of transcription factors and HIPP proteins to elucidate the effect of HIPP proteins in specific transcriptional complexes.

### 4.3 Chapter 3: Co-IP reveals novel PTM of CSD1 and temporal and stress-dependent interactome of CSD1 and CSD2

In other organisms it has been found that SOD1 interacts with hundreds of different proteins and undergoes a multitude of PTMs, suggesting that SOD1 is involved in a great number of cellular processes. As in plants virtually no CSD1 interacting proteins are known, nor the protein complexes with which it associates, here the CSD1-specific antibody was used to perform several independent Co-IP experiments to identify potential PTMs and PPIs of CSD1. The search for PTMs led to the discovery that CSD1 undergoes NTA at the  $\alpha$ -amino acid alanine. Initial evidence suggests that the N-terminal acetylation is facilitated by the NatA complex. Furthermore, an *in-silico* analysis indicates that several SOD proteins are potential targets for a N-terminal acetylation with unknown implication for their biological function. Secondly, 515 (in-)direct interaction partners for CSD1 and CSD2 were found. For CSD1, 267 putative cytosolic and/or nuclear interacting proteins were identified. For CSD2, 163 plastid-localised interactors were identified. These experiments have revealed novel interactors for CSD1 and CSD2 indicating that they act in diverse molecular pathways and processes. One of the main findings is that CSD1 and CSD2 associated with ribosomal complexes, suggesting a role in protein translation. Further it was found that the complex formation of CSD1 and CSD2 with most of the identified interactors is dynamic and depends on the environmental condition and timing after stress application. The presented work has resulted in a conclusive and important dataset that will help to understand the complex molecular function of CSD proteins. The major advances and novelties will be discussed.

To date PTMs for CSD1 have been elusive and therefore were a major focus in the here presented project. Studies in yeast and especially human cells discovered a plethora of PTMs with direct implications for the biological function of CSD1 (Banks & Andersen, 2019). For example, phosphorylation of two conserved amino acid residues is crucial for the nuclear translocation of SOD1 to the nucleus upon oxidative stress in yeast (Tsang et al., 2014). Here, a CSD1-specific antibody was used to immunopurify CSD1 from wild type Arabidopsis plants. However, the downstream MS analysis indicated that phosphorylation of CSD1 occurs (data not shown), but failed to specifically pinpoint the amino acids at which this occurs. Nevertheless, the experimental setup resulted in the discovery of the N-terminal acetylation,

which to date is the first identification of a PTM for CSD1 in plants. Interestingly, the N-terminal acetylation of CSD1 at the  $\alpha$ -amino acid alanine has also been identified for human SOD1 (Hallewell et al., 1987), representing therefore another point of conservation. However, also for SOD1, the impact of the NTA on the biological function remains elusive.

N-terminal acetylation of proteins is conducted by different NAT complexes (Giglione & Meinel, 2021). The structure of the CSD1 N-terminus suggests that the NatA complex facilitates the N-terminal acetylation. Experimental evidence that the acetylation yield of CSD1 is reduced in the *amiNaa15* background is another indication for this hypothesis (**Figure 20 D**). Furthermore, the CSD1-interactome indicates that the NatA complex is responsible for the N-terminal acetylation as peptides of NAA10 and NAA15 were detected. The impact of the N-terminal acetylation on the CSD1 protein and subsequently its biological function remains elusive.

The impact of NTAs on the protein fate was long enigmatic. Recently, Linster *et al.* discovered that the imprinting of the Arabidopsis proteome with acetylation marks is essential for coordinating proteome stability (Linster et al., 2022). The absence of NTAs triggers protein destabilisation by a conserved nonAc/N-degron. Interestingly, the protein level of CSD1 was significantly downregulated in the NatA depleted *amiNAA10* line indicating a destabilisation of CSD1 (Supplementary Data 5 of Linster *et al.*, 2022). These new findings indicate that the NTA might stabilise CSD1 by protection of the nonAc/N-degron. This might also explain the FLAG-CSD1 results observed in the transactivation assays (**Figure 12, Figure 13**), where the co-expression of target promoters with the FLAG-CSD1 protein results in stronger activation of the reporter gene compared to co-expression with the untagged CSD1 protein.

Also, the potential NTA of several other SOD proteins will be of interest. The  $\alpha$ -amino acid alanine is conserved between most SOD proteins within Arabidopsis but also between species. This strong conservation indicates a functional relevance. In plants, the NTA of certain chloroplast proteins was suggested to be necessary for the efficient accumulation inside the chloroplast (Pesaresi et al., 2003). If CSD2 also receives an NTA *in-vivo*, it will be a point of future research. As the misfolding and altered stability of SOD1 is linked to ALS it will also be of interest to test if the human SOD1 protein receives an NTA *in-vivo* and if it has a direct implication for the stability of SOD1. Summarised, a novel PTM for CSD1 was identified and

might also be conserved in SOD1 proteins of other organisms. So far, the precise molecular function remains elusive, however it represents a fruitful point for future research.

To identify protein-protein-interactions (PPIs) *in-vivo* several methods are available including the yeast two-hybrid assay (Y2H), co-immunoprecipitation (Co-IP), bimolecular fluorescence complementation (BiFC) and fluorescence resonance energy transfer (FRET) (Xing et al., 2016). Here, the Co-IP approach was chosen based on the availability of the CSD1-specific antibody and while it represents an *in planta* method. Using the mCherry-antibody (synthesised like the CSD1-specific antibody) to calculate the background noise increases the confidence in the detected protein interaction partners. The performed experiment showed that the combination of Co-IP and mass spectrometry is a powerful tool for discovering novel interactors and establishing interaction maps for proteins of interest (Miernyk and Thelen, 2008). However, transient and weak interactions might be difficult to detect using the Co-IP without cross-linking (Avila et al., 2015) and therefore the interactome of CSD1 and CSD2 is likely still incomplete. The transient nature of individual identified interactors might contribute to the differences in the number of interactors found between the different conditions and timings. For example, approximately 360 interactors were found in the 10 min time point of the salt stress treatment which exceeded the number of identified interactors of all other treatments. Interestingly, here also the catalytic subunit of the NatA complex was identified indicating that the NatA complex is responsible for the NTA of CSD1. This interaction is likely transient and an example why the number of identified interactors can vary between treatments and timings on top of the biological explanation.

Interactions identified via the Co-IP approach could result from a protein complex of multiple interactors where a binary interaction is facilitated by another cofactor. This comes as a blessing in disguise, as it allows the identification of multimeric protein complexes that is impossible with other methods like BiFC or FRET (Xing et al., 2016). To validate the direct interaction of CSD1 and CSD2 with the novel interactors a BiFC experiment will be performed.

Here, the Co-IP and MS combination was taken to another level by not only discovering the ability to interact with other proteins and form a protein complex in the wild type background, but also the dependence on timing and condition. These additional dimensions were used to create elaborate information about the CSD1/2 interaction network. The used approach represents and should set a new standard for the identification of PPI networks as the



information density is increased with the additional dimensions. Future work that adds the dimension of individual cell-types or plant-age can further increase the information of the CSD1/2 PPI network.

Many new interaction partners for the CSD1 and CSD2 protein were found within this work. Previously, only the interaction of CSD1 and CSD2 with CCS and the interaction of CSD1 with DJ-1a were known (Huang et al., 2012; Xu et al., 2010). Here, the interaction of CSD1 with 267 proteins was found. This number resembles the number of identified interaction partners in yeast and human cells, once again an indication for the strong conservation in structure and mostly likely also in function of SOD1/CSD1. For CSD2, 163 interactors were found. For both proteins this represents a point of new research, strongly indicating that CSD protein might be involved in many developmental and stress responsive pathways. Several identified interaction partners for CSD1 suggest a role in processes like regulation of circadian rhythm (CCR2; Schmal et al., 2013; Meyer et al., 2017), ER body formation (NAI2; Yamada et al., 2008), redox homeostasis and nitrogen starvation (ROXY7; Jung et al., 2018), sucrose metabolism (STKL1; Chung et al., 2016), nucleotide metabolism (ADK1; Zhang et al., 2009) and protein degradation (CDC48A; Copeland et al., 2016; Li et al., 2022). CSD2 might be involved in similar processes in the chloroplasts as it interacts with FBA3 (glycolysis, gluconeogenesis; Carrera et al., 2021; Kleffmann et al., 2004), CAD2 (glutathione biosynthesis; Cobbet et al., 1998), and ROC4 (redox homeostasis and sulfur assimilation; Dominguez-Solis et al., 2008; Park et al., 2013). The function of the CSD proteins in these processes might be directly related to the dismutation of superoxide to hydrogen peroxide by protecting these processes from toxic by-products. With other words, CSDs might protect enzymes from superoxide, especially those that contain Fe-S clusters as they are rapidly inactivated by superoxide (Keyer & Imlay, 1996; Imlay, 2006). However, they could also directly act as signaling molecules for altered ROS homeostasis in these processes. The second assumption is supported by the dynamic complex formation of CSD1 and CSD2 with individual interactors. For example, the interaction of CSD1 with CCR2 was devoid during the first minutes of the stress response towards H<sub>2</sub>O<sub>2</sub>, MV and NaCl while it was present in all other treatments and time points. Tackling these assumptions experimentally will be an exciting future task.

Interestingly, a majority of identified interaction partners are ribosomal proteins, for both CSD1 as well as CSD2. Up to now it remains elusive why such a high number of ribosomal proteins were found. The use of the negative control (mCherry antibody) and the dynamic changes of

individual ribosomal proteins during stress allows to be confident in these findings and to exclude potential artefacts. Most of the identified ribosomal proteins correlate with the 60S/40S subunits of the cytoplasmic and 50S/30S subunits of the chloroplastic ribosome, respectively (Firmino et al., 2020). The association of CSD with ribosome-related protein complexes indicates a role in protein translation. This fits to the observation that several of the identified proteins are RNA-binding proteins (RBPs) (Köster et al., 2020). For example, CCR2 is an RBP (Meyer et al., 2017). Overall, the view of ribosomes as passive and steady cellular machine is shifting towards a more dynamic macromolecular complex with specialised roles in the cell (Genuth & Barna, 2018). The obtained results strongly support this shifted view as especially the dynamic changes of the ribosome-related interactors of CSD1 and CSD2 was observed.

As the modulation of translation is an important adaptation during an early stress response, CSD1 and CSD2 might be involved in the process of adapting the machinery upon a change in ROS homeostasis. The link between ROS homeostasis and the early stress response is commonly known (Nadarajah et al., 2020) and the CSD proteins might be regulators connecting these two processes. This might also explain the dynamic complex formation of CSD1 and CSD2 with ribosomal proteins as the composition of ribosomes might change in the early stress response indicated by changes in the transcript levels of ribosomal proteins upon stress (Martinez-Seidel et al., 2020). Nevertheless, the dynamic complex formation of CSD1 and CSD2 confirm the heterogenous composition of ribosome complexes (Genutz & Barna, 2018; Martinez-Seidel et al., 2020). It will be fascinating to explore the function of CSD proteins in heterogenous ribosome complexes.

The dynamics of the interactome must be highlighted specifically. So far, many interaction studies only focussed on the binary approach of a PPI, yes or no. Here the study was extended with the dimension of the condition and timing. Based on the literature, this approach sets a new standard. This chapter has resulted in an important new resource for plant biology. First, many new interaction partners of CSD1 and CSD2 were found. Second, the condition of interaction as well as timing of interaction was determined. This approach discovered that CSD1 and CSD2 were present in different complexes at different time points and indicates the presence of heterogenous ribosome complexes upon stress. Future research needs to explore the biological function of this dynamic complex formation.

## 5 SUMMARY

Superoxide dismutase 1 (SOD1) has been regarded for more than 50 years as an important, pivotal antioxidant enzyme. Recently, it was found that SOD1 acts as regulator in several molecular pathways in yeast and human cells. Here, the textbook view for SOD1 in Arabidopsis, CSD1, is drastically adjusted by discovering the moonlighting function of CSD1 as transcriptional regulator.

It was found that CSD1 features a novel molecular function as a transcriptional regulator in the early salt stress response by binding and regulating the expression of salt-stress responsive genes. Within the first 5 minutes of salt stress CSD1 translocates to the nucleus in a concentration-dependent manner. In a combinatorial approach with different experimental methods, it could be shown that CSD1 binds DNA in a sequence-specific manner and hundreds of potential target genes were identified by ChIP-seq. The A/T-rich DNA binding motif AGCTTT was confirmed independently. The binding of CSD1 to the promoter sequence of salt-stress responsive genes like *NCED3*, *TAT3* and *HSFA6B* was validated. Furthermore, it was found that CSD1 activates the transcription of these salt-stress responsive genes. Thereby, CSD1 acts as a moonlighting protein by regulating the initial transcriptional response upon salt stress.

A nuclear interaction between CSD1 and HIPP20 was found that might result in the formation of a transcriptional complex. It was found that HIPP20, HIPP21 and HIPP22 are mostly nuclear localised protein, except HIPP21 that is also localised in the cytosol. Furthermore, it was found that HIPP5, HIPP20, HIPP21 and HIPP22 act as transcriptional activators revealing a molecular function for the HIPP protein family.

Finally, PTMs for CSD1 and its interactome was resolved. The NTA of CSD1 was found in Col-0 wild type plants which represents the first PTM identified for CSD1. It indicates that the protein fate of CSD1 is controlled post-translationally. A Co-IP experiment followed by mass spectrometry identified 515 (in-)direct interactors of CSD1 and CSD2 in Arabidopsis. Based on subcellular localisation databases, 267 interactors were related to CSD1 and 163 to CSD2. Several, including CCR2, STKL1, CDC48A, RAN3, ROXY7 or ADK1 showed a time- and stress-specific complex formation with CSD1 indicating that the complex formation of CSD

proteins is highly dynamic and depends rather on the time point of the stress response than the response towards a specific treatment.

The discoveries made, and the new research avenues opened will move CSD1 to a focal point of research in the future. Understanding the novel function and the regulation of CSD1 will have major implications on our understanding of plant development and stress tolerance, which is expected to contribute to future breeding strategies.

## 6 ZUSAMMENFASSUNG

Superoxide Dismutase 1 (SOD1) wird seit mehr als 50 Jahren als bedeutendes und lebenswichtiges Antioxidans-Enzym betrachtet. Neue Erkenntnisse, die hauptsächlich in Hefe- und menschlichen Zellen gemacht wurden, stellten fest, dass SOD1 ein wichtiger Regulator verschiedener molekularer Prozesse ist. Dies resultierte in einer veränderten Sicht auf SOD1. In dieser Arbeit wurde die Sicht auf das SOD1 komplementär in Arabidopsis, CSD1, grundlegend verändert, indem die „Moonlighting“ Funktion der CSD1 als transkriptioneller Regulator entdeckt wurde.

Die neue molekulare Funktion von CSD1 als transkriptioneller Regulator in der frühen Salzstressantwort durch die Bindung und Regulierung der Expression von Salzstress-sensiblen Genen wurde entdeckt. Innerhalb der ersten fünf Minuten der Salzstressantwort transloziert CSD1 in einer konzentrations-abhängigen Art und Weise in den Zellkern. Durch eine Kombination verschiedener Methoden wurden gezeigt, dass CSD1 innerhalb des Zellkerns DNA in einer sequenz-abhängigen Art und Weise bindet. Darüber hinaus wurden mithilfe der ChIP-seq Methode unzählige potenzielle Zielgene von CSD1 entdeckt. Die A/T-reiche Bindesequenz AGCTTTT wurde unabhängig bestätigt. Die Bindung CSD1s an die Promotoren Salzstress-sensibler Gene wie z.B. *NCED3*, *TAT3* und *HSFA6B* wurde mithilfe von EMSA nachgewiesen. Außerdem wurde gezeigt, dass CSD1 die Transkription dieser genannten Gene aktivieren kann. Damit wurde gezeigt, dass CSD1 ein „Moonlighting“ Protein ist, indem es als transkriptioneller Regulator innerhalb der frühen Saltstressantwort agiert.

Eine nukleare Interaktion zwischen HIPP20 und CSD1, die zur Bildung eines transkriptionellen Komplexes führen könnte, wurde entdeckt. Des Weiteren wurde die nukleare Lokalisation von HIPP20, HIPP21 und HIPP22 entdeckt, wobei HIPP21 zusätzlich auch cytosolisch lokalisiert ist. Es wurde gezeigt, dass HIPP5, HIPP20, HIPP21 und HIPP22 als transkriptionelle Aktivatoren agieren, was der HIPP Protein Familie eine molekulare Funktion verleiht.

Außerdem wurden PTMs der CSD1 und ihr Interaktom entschlüsselt. Die NTA von CSD1 wurde entdeckt und ist damit die erste Entdeckung einer PTM von CSD1 in Arabidopsis. Es deutet an, dass CSD1 post-translational kontrolliert wird. Ein Co-IP Experiment hat zur Entdeckung von 515 Interaktoren der CSD1 und CSD2 geführt. Dabei können aufgrund der subzellulären Lokalisation 267 Interaktoren CSD1 und 163 Interaktoren CSD2 zugeordnet werden. Mehrere interessante Interaktoren wie z.B. CCR2, STKL1, CDC48A, RAN3, ROXY7

und ADK1 zeigten eine dynamische und eher vom Zeitpunkt als des Stresses abhängige Komplexformierung mit CSD1.

Die Entdeckungen und die daraus resultierenden neuen Forschungsfragen machen CSD1 zu einem interessanten Forschungsobjekt in der Zukunft. Das Verständnis der neuen Funktion und der Regulierung der CSD1 könnten zu großen Fortschritten im Verständnis des Pflanzenwachstums und der abiotischen Stresstoleranz führen.

## 7 REFERENCES

- Abercrombie JM, Halfhill MD, Ranjan P, et al. Transcriptional responses of *Arabidopsis thaliana* plants to As (V) stress. *BMC Plant Biol.* 2008;8:87. Published 2008 Aug 6. doi:10.1186/1471-2229-8-87
- Adem GD, Roy SJ, Zhou M, Bowman JP, Shabala S. Evaluating contribution of ionic, osmotic and oxidative stress components towards salinity tolerance in barley. *BMC Plant Biol.* 2014;14:113. Published 2014 Apr 28. doi:10.1186/1471-2229-14-113
- Aida M, Ishida T, Fukaki H, Fujisawa H, Tasaka M. Genes involved in organ separation in *Arabidopsis*: an analysis of the cup-shaped cotyledon mutant. *Plant Cell.* 1997;9(6):841-857. doi:10.1105/tpc.9.6.841
- Airoldi CA, Hearn TJ, Brockington SF, Webb AAR, Glover BJ. TTG1 proteins regulate circadian activity as well as epidermal cell fate and pigmentation. *Nat Plants.* 2019;5(11):1145-1153. doi:10.1038/s41477-019-0544-3
- Aksnes H, Drazic A, Marie M, Arnesen T. First Things First: Vital Protein Marks by N-Terminal Acetyltransferases. *Trends Biochem Sci.* 2016;41(9):746-760. doi:10.1016/j.tibs.2016.07.005
- Arvidsson S, Kwasniewski M, Riaño-Pachón DM, Mueller-Roeber B. QuantPrime--a flexible tool for reliable high-throughput primer design for quantitative PCR. *BMC Bioinformatics.* 2008;9:465. Published 2008 Nov 1. doi:10.1186/1471-2105-9-465
- Avila JR, Lee JS, Torii KU. Co-Immunoprecipitation of Membrane-Bound Receptors. *Arabidopsis Book.* 2015;13:e0180. Published 2015 Jun 3. doi:10.1199/tab.0180
- Babior BM, Kipnes RS, Curnutte JT. Biological defense mechanisms. The production by leukocytes of superoxide, a potential bactericidal agent. *J Clin Invest.* 1973;52(3):741-744. doi:10.1172/JCI107236
- Balparda M, Elsässer M, Badia MB, et al. Acetylation of conserved lysines fine-tunes mitochondrial malate dehydrogenase activity in land plants. *Plant J.* 2022;109(1):92-111. doi:10.1111/tbj.15556

- Banks CJ, Rodriguez NW, Gashler KR, et al. Acylation of Superoxide Dismutase 1 (SOD1) at K122 Governs SOD1-Mediated Inhibition of Mitochondrial Respiration. *Mol Cell Biol.* 2017;37(20):e00354-17. Published 2017 Sep 26. doi:10.1128/MCB.00354-17
- Banks CJ, Andersen JL. Mechanisms of SOD1 regulation by post-translational modifications. *Redox Biol.* 2019;26:101270. doi:10.1016/j.redox.2019.101270
- Barber SC, Shaw PJ. Oxidative stress in ALS: key role in motor neuron injury and therapeutic target. *Free Radic Biol Med.* 2010;48(5):629-641. doi:10.1016/j.freeradbiomed.2009.11.018
- Barrero JM, Rodríguez PL, Quesada V, Piqueras P, Ponce MR, Micol JL. Both abscisic acid (ABA)-dependent and ABA-independent pathways govern the induction of NCED3, AAO3 and ABA1 in response to salt stress. *Plant Cell Environ.* 2006;29(10):2000-2008. doi:10.1111/j.1365-3040.2006.01576.x
- Bartels, D. and Sunkar, R. Drought and salt tolerance in plants. *Critical Reviews in Plant Sciences.* 2015;24(23-58). doi: 10.1080/07352680590910410.
- Barth O, Vogt S, Uhlemann R, Zschiesche W, Humbeck K. Stress induced and nuclear localized HIP26 from Arabidopsis thaliana interacts via its heavy metal associated domain with the drought stress related zinc finger transcription factor ATHB29. *Plant Mol Biol.* 2009;69(1-2):213-226. doi:10.1007/s11103-008-9419-0
- Bartlett A, O'Malley RC, Huang SC, et al. Mapping genome-wide transcription-factor binding sites using DAP-seq. *Nat Protoc.* 2017;12(8):1659-1672. doi:10.1038/nprot.2017.055
- Ben Rejeb K, Benzarti M, Debez A, Bailly C, Savouré A, Abdely C. NADPH oxidase-dependent H<sub>2</sub>O<sub>2</sub> production is required for salt-induced antioxidant defense in Arabidopsis thaliana. *J Plant Physiol.* 2015;174:5-15. doi:10.1016/j.jplph.2014.08.022
- Bienvenut WV, Giglione C, Meinnel T. Proteome-wide analysis of the amino terminal status of Escherichia coli proteins at the steady-state and upon dephosphorylation inhibition. *Proteomics.* 2015;15(14):2503-2518. doi:10.1002/pmic.201500027
- Bonnet E, Wuyts J, Rouzé P, Van de Peer Y. Detection of 91 potential conserved plant microRNAs in Arabidopsis thaliana and Oryza sativa identifies important target genes [published correction appears in Proc Natl Acad Sci U S A. 2005 Mar 22;102(12):4655]. *Proc Natl Acad Sci U S A.* 2004;101(31):11511-11516. doi:10.1073/pnas.0404025101



- Borsani O, Zhu J, Verslues PE, Sunkar R, Zhu JK. Endogenous siRNAs derived from a pair of natural cis-antisense transcripts regulate salt tolerance in Arabidopsis. *Cell*. 2005;123(7):1279-1291. doi:10.1016/j.cell.2005.11.035
- Bowler, C., Van Montagu, M. and Inzé, D. Superoxide Dismutase and Stress Tolerance. *Annual Review of Plant Physiology and Plant Molecular Biology*. 1992;43(83-116). doi:10.1146/annurev.pp.43.060192.000503
- Braun et al., Arabidopsis Interactome Mapping Consortium. Evidence for network evolution in an Arabidopsis interactome map. *Science*. 2011;333(6042):601-607. doi:10.1126/science.1203877
- Breiman A, Fieulaine S, Meinnel T, Giglione C. The intriguing realm of protein biogenesis: Facing the green co-translational protein maturation networks. *Biochim Biophys Acta*. 2016;1864(5):531-550. doi:10.1016/j.bbapap.2015.11.002
- Broom HR, Vassall KA, Rumfeldt JA, et al. Combined Isothermal Titration and Differential Scanning Calorimetry Define Three-State Thermodynamics of fALS-Associated Mutant Apo SOD1 Dimers and an Increased Population of Folded Monomer. *Biochemistry*. 2016;55(3):519-533. doi:10.1021/acs.biochem.5b01187
- Byrt CS, Munns R, Burton RA, Gilliham M, Wege S. Root cell wall solutions for crop plants in saline soils. *Plant Sci*. 2018;269:47-55. doi:10.1016/j.plantsci.2017.12.012
- Carrera DÁ, George GM, Fischer-Stettler M, et al. Distinct plastid fructose bisphosphate aldolases function in photosynthetic and non-photosynthetic metabolism in Arabidopsis. *J Exp Bot*. 2021;72(10):3739-3755. doi:10.1093/jxb/erab099
- Castro B, Citterico M, Kimura S, Stevens DM, Wrzaczek M, Coaker G. Stress-induced reactive oxygen species compartmentalization, perception and signalling. *Nat Plants*. 2021;7(4):403-412. doi:10.1038/s41477-021-00887-0
- Chattopadhyay M, Nwadibia E, Strong CD, Gralla EB, Valentine JS, Whitelegge JP. The Disulfide Bond, but Not Zinc or Dimerization, Controls Initiation and Seeded Growth in Amyotrophic Lateral Sclerosis-linked Cu,Zn Superoxide Dismutase (SOD1) Fibrillation. *J Biol Chem*. 2015;290(51):30624-30636. doi:10.1074/jbc.M115.666503

- Chao LM, Liu YQ, Chen DY, Xue XY, Mao YB, Chen XY. Arabidopsis Transcription Factors SPL1 and SPL12 Confer Plant Thermotolerance at Reproductive Stage. *Mol Plant*. 2017;10(5):735-748. doi:10.1016/j.molp.2017.03.010
- Cho YH, Yoo SD, Sheen J. Regulatory functions of nuclear hexokinase1 complex in glucose signaling. *Cell*. 2006;127(3):579-589. doi:10.1016/j.cell.2006.09.028
- Choudhury FK, Rivero RM, Blumwald E, Mittler R. Reactive oxygen species, abiotic stress and stress combination. *Plant J*. 2017;90(5):856-867. doi:10.1111/tpj.13299
- Chu CC, Lee WC, Guo WY, et al. A copper chaperone for superoxide dismutase that confers three types of copper/zinc superoxide dismutase activity in Arabidopsis. *Plant Physiol*. 2005;139(1):425-436. doi:10.1104/pp.105.065284
- Chung, M.-S., Lee, S., Min, J.-H., Huang, P., Ju, H.-W., Soo Kim, C., Regulation of Arabidopsis thaliana plasma membrane glucose-responsive regulator (AtPGR) expression by A. thaliana storekeeper-like transcription factor, AtSTKL, modulates glucose response in Arabidopsis, *Plant Physiology and Biochemistry*. 2016;104:155-164. doi:10.1016/j.plaphy.2016.03.029.
- Clough SJ, Bent AF. Floral dip: a simplified method for Agrobacterium-mediated transformation of Arabidopsis thaliana. *Plant J*. 1998;16(6):735-743. doi:10.1046/j.1365-313x.1998.00343.x
- Cobbett CS, May MJ, Howden R, Rolls B. The glutathione-deficient, cadmium-sensitive mutant, cad2-1, of Arabidopsis thaliana is deficient in gamma-glutamylcysteine synthetase. *Plant J*. 1998;16(1):73-78. doi:10.1046/j.1365-313x.1998.00262.x
- Coelho FR, Iqbal A, Linares E, et al. Oxidation of the tryptophan 32 residue of human superoxide dismutase 1 caused by its bicarbonate-dependent peroxidase activity triggers the non-amyloid aggregation of the enzyme. *J Biol Chem*. 2014;289(44):30690-30701. doi:10.1074/jbc.M114.586370
- Copeland C, Woloshen V, Huang Y, Li X. AtCDC48A is involved in the turnover of an NLR immune receptor. *Plant J*. 2016;88(2):294-305. doi:10.1111/tpj.13251

- Cowan GH, Roberts AG, Jones S, et al. Potato Mop-Top Virus Co-opts the Stress Sensor HIP26 for Long-Distance Movement. *Plant Physiol.* 2018;176(3):2052-2070. doi:10.1104/pp.17.01698
- Crowell DN. Functional implications of protein isoprenylation in plants. *Prog Lipid Res.* 2000;39(5):393-408. doi:10.1016/s0163-7827(00)00010-2
- Culotta VC. Superoxide dismutase, oxidative stress, and cell metabolism. *Curr Top Cell Regul.* 2000;36:117-132. doi:10.1016/s0070-2137(01)80005-4
- Dalle-Donne I, Rossi R, Colombo G, Giustarini D, Milzani A. Protein S-glutathionylation: a regulatory device from bacteria to humans. *Trends Biochem Sci.* 2009;34(2):85-96. doi:10.1016/j.tibs.2008.11.002
- de Abreu-Neto JB, Turchetto-Zolet AC, de Oliveira LF, Zanettini MH, Margis-Pinheiro M. Heavy metal-associated isoprenylated plant protein (HIP26): characterization of a family of proteins exclusive to plants. *FEBS J.* 2013;280(7):1604-1616. doi:10.1111/febs.12159
- Devic M. The importance of being essential: EMBRYO-DEFECTIVE genes in Arabidopsis. *C R Biol.* 2008;331(10):726-736. doi:10.1016/j.crv.2008.07.014
- Dhindsa, R.S. and Matowe, W. Drought tolerance in two mosses: correlated with enzymatic defence against lipid peroxidation. *Journal of Experimental Botany.* 1981; 32(1):79-91. doi: 10.1093/jxb/32.1.79.
- Diaz-Vivancos P, Faize M, Barba-Espin G, et al. Ectopic expression of cytosolic superoxide dismutase and ascorbate peroxidase leads to salt stress tolerance in transgenic plums. *Plant Biotechnol J.* 2013;11(8):976-985. doi:10.1111/pbi.12090
- Doke, N. Involvement of superoxide anion generation in the hypersensitive response of potato tuber tissues to infection with an incompatible race of *Phytophthora infestans* and to the hyphal wall components. *Physiological Plant Pathology.* 1983; 23(3):345-357. doi: 10.1016/0048-4059(83)90019-X.
- Dominguez-Solis JR, He Z, Lima A, Ting J, Buchanan BB, Luan S. A cyclophilin links redox and light signals to cysteine biosynthesis and stress responses in chloroplasts [published correction appears in Proc Natl Acad Sci U S A. 2009 Jan 27;106(4):1292]. *Proc Natl Acad Sci U S A.* 2008;105(42):16386-16391. doi:10.1073/pnas.0808204105

- Dunand C, Crèvecoeur M, Penel C. Distribution of superoxide and hydrogen peroxide in Arabidopsis root and their influence on root development: possible interaction with peroxidases. *New Phytol.* 2007;174(2):332-341. doi:10.1111/j.1469-8137.2007.01995.x
- Eastmond PJ. MONODEHYDROASCORBATE REDUCTASE4 is required for seed storage oil hydrolysis and postgerminative growth in Arabidopsis. *Plant Cell.* 2007;19(4):1376-1387. doi:10.1105/tpc.106.043992
- Elchuri S, Oberley TD, Qi W, et al. CuZnSOD deficiency leads to persistent and widespread oxidative damage and hepatocarcinogenesis later in life. *Oncogene.* 2005;24(3):367-380. doi:10.1038/sj.onc.1208207
- Faize M, Burgos L, Faize L, et al. Involvement of cytosolic ascorbate peroxidase and Cu/Zn-superoxide dismutase for improved tolerance against drought stress. *J Exp Bot.* 2011;62(8):2599-2613. doi:10.1093/jxb/erq432
- Fay JM, Zhu C, Proctor EA, et al. A Phosphomimetic Mutation Stabilizes SOD1 and Rescues Cell Viability in the Context of an ALS-Associated Mutation. *Structure.* 2016;24(11):1898-1906. doi:10.1016/j.str.2016.08.011
- Feng X, Lai Z, Lin Y, Lai G, Lian C. Genome-wide identification and characterization of the superoxide dismutase gene family in *Musa acuminata* cv. Tianbaojiao (AAA group). *BMC Genomics.* 2015;16:823. Published 2015 Oct 20. doi:10.1186/s12864-015-2046-7
- (a) Feng K, Yu J, Cheng Y, et al. The SOD Gene Family in Tomato: Identification, Phylogenetic Relationships, and Expression Patterns. *Front Plant Sci.* 2016;7:1279. Published 2016 Aug 30. doi:10.3389/fpls.2016.01279
- (b) Feng J, Li R, Yu J, et al. Protein N-terminal acetylation is required for embryogenesis in Arabidopsis. *J Exp Bot.* 2016;67(15):4779-4789. doi:10.1093/jxb/erw257
- (c) Feng J, Ma L. NatA is required for suspensor development in Arabidopsis. *Plant Signal Behav.* 2016;11(10):e1231293. doi:10.1080/15592324.2016.1231293
- Feng W, Kita D, Peaucelle A, et al. The FERONIA Receptor Kinase Maintains Cell-Wall Integrity during Salt Stress through Ca<sup>2+</sup> Signaling. *Curr Biol.* 2018;28(5):666-675.e5. doi:10.1016/j.cub.2018.01.023

- Firmino AAP, Gorka M, Graf A, et al. Separation and Paired Proteome Profiling of Plant Chloroplast and Cytoplasmic Ribosomes. *Plants (Basel)*. 2020;9(7):892. Published 2020 Jul 14. doi:10.3390/plants9070892
- Foyer, C.H., Lelandais, M., and Kunert, K.L. Photooxidative stress in plants. *Physiologia Plantarum*. 1994;92:696–717. doi:10.1111/j.1399-3054.1994.tb03042.x
- Foyer, C.H. and Noctor, G. Oxidant and antioxidant signalling in plants: a re-evaluation of the concept of oxidative stress in a physiological context. *Plant, Cell & Environment*, 2005;28: 1056-1071. doi:10.1111/j.1365-3040.2005.01327.x
- Franklin, J. P., Azzouz, M., & Shaw, P. J. SOD1-targeting therapies for neurodegenerative diseases: a review of current findings and future potential. *Expert Opinion on Orphan Drugs*, 2020;8(10), 379-392. doi:10.1080/21678707.2020.1835638
- Fricke W, Akhiyarova G, Wei W, et al. The short-term growth response to salt of the developing barley leaf. *J Exp Bot*. 2006;57(5):1079-1095. doi:10.1093/jxb/erj095
- Fridovich I. The biology of oxygen radicals. *Science*.1978;201(4359):875-880. doi:10.1126/science.210504
- Fujita S, De Bellis D, Edel KH, et al. SCHENGEN receptor module drives localized ROS production and lignification in plant roots. *EMBO J*. 2020;39(9):e103894. doi:10.15252/embj.2019103894
- Fujita S. CASPARIAN STRIP INTEGRITY FACTOR (CIF) family peptides - regulator of plant extracellular barriers. *Peptides*. 2021;143:170599. doi:10.1016/j.peptides.2021.170599
- Geng Y, Wu R, Wee CW, et al. A spatio-temporal understanding of growth regulation during the salt stress response in Arabidopsis. *Plant Cell*. 2013;25(6):2132-2154. doi:10.1105/tpc.113.112896
- Genuth NR, Barna M. The Discovery of Ribosome Heterogeneity and Its Implications for Gene Regulation and Organismal Life. *Mol Cell*. 2018;71(3):364-374. doi:10.1016/j.molcel.2018.07.018

- Gietz RD, Woods RA. Transformation of yeast by lithium acetate/single-stranded carrier DNA/polyethylene glycol method. *Methods Enzymol.* 2002;350:87-96. doi:10.1016/s0076-6879(02)50957-5
- Giglione C, Meinnel T. Evolution-Driven Versatility of N Terminal Acetylation in Photoautotrophs. *Trends Plant Sci.* 2021;26(4):375-391. doi:10.1016/j.tplants.2020.11.012
- Gilliland LU, Magallanes-Lundback M, Hemming C, et al. Genetic basis for natural variation in seed vitamin E levels in *Arabidopsis thaliana*. *Proc Natl Acad Sci U S A.* 2006;103(49):18834-18841. doi:10.1073/pnas.0606221103
- Gottfredsen RH, Larsen UG, Enghild JJ, Petersen SV. Hydrogen peroxide induce modifications of human extracellular superoxide dismutase that results in enzyme inhibition. *Redox Biol.* 2013;1(1):24-31. Published 2013 Jan 11. doi:10.1016/j.redox.2012.12.004
- Guan Q, Yue X, Zeng H, Zhu J. The protein phosphatase RCF2 and its interacting partner NAC019 are critical for heat stress-responsive gene regulation and thermotolerance in *Arabidopsis*. *Plant Cell.* 2014;26(1):438-453. doi:10.1105/tpc.113.118927
- Guan Q, Liao X, He M, et al. Tolerance analysis of chloroplast OsCu/Zn-SOD overexpressing rice under NaCl and NaHCO<sub>3</sub> stress. *PLoS One.* 2017;12(10):e0186052. Published 2017 Oct 11. doi:10.1371/journal.pone.0186052
- Gupta AS, Heinen JL, Holaday AS, Burke JJ, Allen RD. Increased resistance to oxidative stress in transgenic plants that overexpress chloroplastic Cu/Zn superoxide dismutase. *Proc Natl Acad Sci U S A.* 1993;90(4):1629-1633. doi:10.1073/pnas.90.4.1629
- Guo T, Weber H, Niemann MCE, et al. *Arabidopsis* HIPP proteins regulate endoplasmic reticulum-associated degradation of CKX proteins and cytokinin responses. *Mol Plant.* 2021;14(11):1918-1934. doi:10.1016/j.molp.2021.07.015
- Gralla EB, Valentine JS. Null mutants of *Saccharomyces cerevisiae* Cu,Zn superoxide dismutase: characterization and spontaneous mutation rates. *J Bacteriol.* 1991;173(18):5918-5920. doi:10.1128/jb.173.18.5918-5920.1991
- Hafidh S, Breznenová K, Růžička P, Feciková J, Capková V, Honys D. Comprehensive analysis of tobacco pollen transcriptome unveils common pathways in polar cell expansion and

underlying heterochronic shift during spermatogenesis. *BMC Plant Biol.* 2012;12:24. Published 2012 Feb 16. doi:10.1186/1471-2229-12-24

Hallewell, R., Mills, R., Tekamp-Olson, P. *et al.* Amino Terminal Acetylation of Authentic Human Cu,Zn Superoxide Dismutase Produced in Yeast. *Nat Biotechnol* **5**, 363–366 (1987). <https://doi.org/10.1038/nbt0487-363>

Hamilton AJ, Baulcombe DC. A species of small antisense RNA in posttranscriptional gene silencing in plants. *Science.* 1999;286(5441):950-952. doi:10.1126/science.286.5441.950

Hashizume K, Hirasawa M, Imamura Y, et al. Retinal dysfunction and progressive retinal cell death in SOD1-deficient mice. *Am J Pathol.* 2008;172(5):1325-1331. doi:10.2353/ajpath.2008.070730

Hasson A, Plessis A, Blein T, et al. Evolution and diverse roles of the CUP-SHAPED COTYLEDON genes in Arabidopsis leaf development. *Plant Cell.* 2011;23(1):54-68. doi:10.1105/tpc.110.081448

He L, Shi X, Wang Y, Guo Y, Yang K, Wang Y. Arabidopsis ANAC069 binds to C[A/G]CG[T/G] sequences to negatively regulate salt and osmotic stress tolerance. *Plant Mol Biol.* 2017;93(4-5):369-387. doi:10.1007/s11103-016-0567-3

Hentze MW, Kühn LC. Molecular control of vertebrate iron metabolism: mRNA-based regulatory circuits operated by iron, nitric oxide, and oxidative stress. *Proc Natl Acad Sci U S A.* 1996;93(16):8175-8182. doi:10.1073/pnas.93.16.8175

Hirling H, Henderson BR, Kühn LC. Mutational analysis of the [4Fe-4S]-cluster converting iron regulatory factor from its RNA-binding form to cytoplasmic aconitase. *EMBO J.* 1994;13(2):453-461. doi:10.1002/j.1460-2075.1994.tb06280.x

Hooper CM, Castleden IR, Tanz SK, Aryamanesh N, Millar AH. SUBA4: the interactive data analysis centre for Arabidopsis subcellular protein locations. *Nucleic Acids Res.* 2017;45(D1):D1064-D1074. doi:10.1093/nar/gkw1041

Huang CH, Kuo WY, Weiss C, Jinn TL. Copper chaperone-dependent and -independent activation of three copper-zinc superoxide dismutase homologs localized in different cellular compartments in Arabidopsis. *Plant Physiol.* 2012;158(2):737-746. doi:10.1104/pp.111.190223

- Huang YC, Niu CY, Yang CR, Jinn TL. The Heat Stress Factor HSFA6b Connects ABA Signaling and ABA-Mediated Heat Responses. *Plant Physiol.* 2016;172(2):1182-1199. doi:10.1104/pp.16.00860
- Huberts DH, van der Klei IJ. Moonlighting proteins: an intriguing mode of multitasking. *Biochim Biophys Acta.* 2010;1803(4):520-525. doi:10.1016/j.bbamcr.2010.01.022
- Hung IH, Casareno RL, Labesse G, Mathews FS, Gitlin JD. HAH1 is a copper-binding protein with distinct amino acid residues mediating copper homeostasis and antioxidant defense. *J Biol Chem.* 1998;273(3):1749-1754. doi:10.1074/jbc.273.3.1749
- Imlay JA. Iron-sulphur clusters and the problem with oxygen. *Mol Microbiol.* 2006;59(4):1073-1082. doi:10.1111/j.1365-2958.2006.05028.x
- Inoue E, Tano K, Yoshii H, et al. SOD1 Is Essential for the Viability of DT40 Cells and Nuclear SOD1 Functions as a Guardian of Genomic DNA. *J Nucleic Acids.* 2010;2010:795946. Published 2010 Aug 5. doi:10.4061/2010/795946
- Iuchi S, Kobayashi M, Taji T, et al. Regulation of drought tolerance by gene manipulation of 9-cis-epoxycarotenoid dioxygenase, a key enzyme in abscisic acid biosynthesis in Arabidopsis [published correction appears in Plant J. 2002 Jun;30(5):611]. *Plant J.* 2001;27(4):325-333. doi:10.1046/j.1365-313x.2001.01096.x
- Iuchi Y, Okada F, Onuma K, et al. Elevated oxidative stress in erythrocytes due to a SOD1 deficiency causes anaemia and triggers autoantibody production. *Biochem J.* 2007;402(2):219-227. doi:10.1042/BJ20061386
- James RA, Rivelli AR, Munns R, Caemmerer SV. Factors affecting CO<sub>2</sub> assimilation, leaf injury and growth in salt-stressed durum wheat. *Funct Plant Biol.* 2002;29(12):1393-1403. doi:10.1071/FP02069
- Janků M, Luhová L, Petřivalský M. On the Origin and Fate of Reactive Oxygen Species in Plant Cell Compartments. *Antioxidants (Basel).* 2019;8(4):105. Published 2019 Apr 17. doi:10.3390/antiox8040105
- Jeffery CJ. Moonlighting proteins. *Trends Biochem Sci.* 1999;24(1):8-11. doi:10.1016/s0968-0004(98)01335-8



- Jeffery CJ. Moonlighting proteins: old proteins learning new tricks. *Trends Genet.* 2003;19(8):415-417. doi:10.1016/S0168-9525(03)00167-7
- Jeffery CJ. An introduction to protein moonlighting. *Biochem Soc Trans.* 2014;42(6):1679-1683. doi:10.1042/BST20140226
- Jeffery CJ. Multitalented actors inside and outside the cell: recent discoveries add to the number of moonlighting proteins. *Biochem Soc Trans.* 2019;47(6):1941-1948. doi:10.1042/BST20190798
- Jensen MK, Lindemose S, de Masi F, et al. ATAF1 transcription factor directly regulates abscisic acid biosynthetic gene NCED3 in *Arabidopsis thaliana*. *FEBS Open Bio.* 2013;3:321-327. Published 2013 Jul 29. doi:10.1016/j.fob.2013.07.006
- Jethva J, Schmidt RR, Sauter M, Selinski J. Try or Die: Dynamics of Plant Respiration and How to Survive Low Oxygen Conditions. *Plants (Basel).* 2022;11(2):205. Published 2022 Jan 13. doi:10.3390/plants11020205
- Jia X, Wang WX, Ren L, et al. Differential and dynamic regulation of miR398 in response to ABA and salt stress in *Populus tremula* and *Arabidopsis thaliana*. *Plant Mol Biol.* 2009;71(1-2):51-59. doi:10.1007/s11103-009-9508-8
- Jiang C, Belfield EJ, Mithani A, et al. ROS-mediated vascular homeostatic control of root-to-shoot soil Na delivery in *Arabidopsis* [published correction appears in *EMBO J.* 2013 Mar 20;32(6):914]. *EMBO J.* 2012;31(22):4359-4370. doi:10.1038/emboj.2012.273
- Jing X, Hou P, Lu Y, et al. Overexpression of copper/zinc superoxide dismutase from mangrove *Kandelia candel* in tobacco enhances salinity tolerance by the reduction of reactive oxygen species in chloroplast. *Front Plant Sci.* 2015;6:23. Published 2015 Jan 22. doi:10.3389/fpls.2015.00023
- Jung JY, Ahn JH, Schachtman DP. CC-type glutaredoxins mediate plant response and signaling under nitrate starvation in *Arabidopsis*. *BMC Plant Biol.* 2018;18(1):281. Published 2018 Nov 13. doi:10.1186/s12870-018-1512-1
- Kanaoka MM, Torii KU. FERONIA as an upstream receptor kinase for polar cell growth in plants. *Proc Natl Acad Sci U S A.* 2010;107(41):17461-17462. doi:10.1073/pnas.1013090107

- Karimi M, Depicker A, Hilson P. Recombinational cloning with plant gateway vectors. *Plant Physiol.* 2007;145(4):1144-1154. doi:10.1104/pp.107.106989
- Kasai, T., Suzuki, T., Ono, K. et al. Pea extracellular Cu/Zn-superoxide dismutase responsive to signal molecules from a fungal pathogen. *Journal of General Plant Pathology.* 2006;72:265-272. doi: 10.1007/s10327-006-0283-y.
- Kaufmann K, Muiño JM, Østerås M, Farinelli L, Krajewski P, Angenent GC. Chromatin immunoprecipitation (ChIP) of plant transcription factors followed by sequencing (ChIP-SEQ) or hybridization to whole genome arrays (ChIP-CHIP). *Nat Protoc.* 2010;5(3):457-472. doi:10.1038/nprot.2009.244
- Keyer K, Imlay JA. Superoxide accelerates DNA damage by elevating free-iron levels. *Proc Natl Acad Sci U S A.* 1996;93(24):13635-13640. doi:10.1073/pnas.93.24.13635
- Kim J, Lee H, Lee JH, et al. Dimerization, oligomerization, and aggregation of human amyotrophic lateral sclerosis copper/zinc superoxide dismutase 1 protein mutant forms in live cells. *J Biol Chem.* 2014;289(21):15094-15103. doi:10.1074/jbc.M113.542613
- Kleffmann, T., Russenberger, D., Zychlinski, A., Christopher, W., Sjölander, K., Gruissem, W., Baginsky, S., The Arabidopsis thaliana Chloroplast Proteome Reveals Pathway Abundance and Novel Protein Functions, *Current Biology*, Volume 14, Issue 5, 2004, <https://doi.org/10.1016/j.cub.2004.02.039>.
- Kliebenstein DJ, Monde RA, Last RL. Superoxide dismutase in Arabidopsis: an eclectic enzyme family with disparate regulation and protein localization. *Plant Physiol.* 1998;118(2):637-650. doi:10.1104/pp.118.2.637
- Kliebenstein DJ, Dietrich RA, Martin AC, Last RL, Dangl JL. LSD1 regulates salicylic acid induction of copper zinc superoxide dismutase in Arabidopsis thaliana. *Mol Plant Microbe Interact.* 1999;12(11):1022-1026. doi:10.1094/MPMI.1999.12.11.1022
- Köster T, Reichel M, Staiger D. CLIP and RNA interactome studies to unravel genome-wide RNA-protein interactions in vivo in Arabidopsis thaliana. *Methods.* 2020;178:63-71. doi:10.1016/j.ymeth.2019.09.005

- Kreps JA, Wu Y, Chang HS, Zhu T, Wang X, Harper JF. Transcriptome changes for *Arabidopsis* in response to salt, osmotic, and cold stress. *Plant Physiol.* 2002;130(4):2129-2141. doi:10.1104/pp.008532
- Lee SH, Ahsan N, Lee KW, et al. Simultaneous overexpression of both CuZn superoxide dismutase and ascorbate peroxidase in transgenic tall fescue plants confers increased tolerance to a wide range of abiotic stresses. *J Plant Physiol.* 2007;164(12):1626-1638. doi:10.1016/j.jplph.2007.01.003
- Lee YJ, Yang Z. Tip growth: signaling in the apical dome. *Curr Opin Plant Biol.* 2008;11(6):662-671. doi:10.1016/j.pbi.2008.10.002
- Li S, Fu L, Tian T, et al. Disrupting SOD1 activity inhibits cell growth and enhances lipid accumulation in nasopharyngeal carcinoma. *Cell Commun Signal.* 2018;16(1):28. Published 2018 Jun 11. doi:10.1186/s12964-018-0240-3
- Li X, Qiu S, Shi J, et al. A new function of copper zinc superoxide dismutase: as a regulatory DNA-binding protein in gene expression in response to intracellular hydrogen peroxide. *Nucleic Acids Res.* 2019;47(10):5074-5085. doi:10.1093/nar/gkz256
- Li Z, Han X, Song X, et al. Overexpressing the *Sedum alfredii* Cu/Zn Superoxide Dismutase Increased Resistance to Oxidative Stress in Transgenic *Arabidopsis*. *Front Plant Sci.* 2017;8:1010. Published 2017 Jun 13. doi:10.3389/fpls.2017.01010
- Li J, Yuan J, Li Y, et al. The CDC48 complex mediates ubiquitin-dependent degradation of intra-chloroplast proteins in plants. *Cell Rep.* 2022;39(2):110664. doi:10.1016/j.celrep.2022.110664
- Licausi F, Kosmacz M, Weits DA, et al. Oxygen sensing in plants is mediated by an N-end rule pathway for protein destabilization. *Nature.* 2011;479(7373):419-422. Published 2011 Oct 23. doi:10.1038/nature10536
- Lightfoot DJ, Mcgrann GR, Able AJ. The role of a cytosolic superoxide dismutase in barley-pathogen interactions. *Mol Plant Pathol.* 2017;18(3):323-335. doi:10.1111/mpp.12399
- Lin SJ, Pufahl RA, Dancis A, O'Halloran TV, Culotta VC. A role for the *Saccharomyces cerevisiae* ATX1 gene in copper trafficking and iron transport. *J Biol Chem.* 1997;272(14):9215-9220.

- Linster E, Stephan I, Bienvenut WV, et al. Downregulation of N-terminal acetylation triggers ABA-mediated drought responses in Arabidopsis. *Nat Commun.* 2015;6:7640. Published 2015 Jul 17. doi:10.1038/ncomms8640
- Linster E, Forero Ruiz FL, Miklankova P, et al. Cotranslational N-degron masking by acetylation promotes proteome stability in plants. *Nat Commun.* 2022;13(1):810. Published 2022 Feb 10. doi:10.1038/s41467-022-28414-5
- Luchinat E, Barbieri L, Rubino JT, Kozyreva T, Cantini F, Banci L. In-cell NMR reveals potential precursor of toxic species from SOD1 fALS mutants. *Nat Commun.* 2014;5:5502. Published 2014 Nov 27. doi:10.1038/ncomms6502
- Malan, C., Greyling, M.M., and Gressel, J. Correlation between CuZn superoxide dismutase and glutathione reductase, and environmental and xenobiotic stress tolerance in maize inbreds. *Plant Science.* 1990;69(2):157-166. doi: 10.1016/0168-9452(90)90114-4.
- Mallikarjuna G, Mallikarjuna K, Reddy MK, Kaul T. Expression of OsDREB2A transcription factor confers enhanced dehydration and salt stress tolerance in rice (*Oryza sativa* L.). *Biotechnol Lett.* 2011;33(8):1689-1697. doi:10.1007/s10529-011-0620-x
- Martinez-Seidel F, Beine-Golovchuk O, Hsieh YC, Kopka J. Systematic Review of Plant Ribosome Heterogeneity and Specialization. *Front Plant Sci.* 2020;11:948. Published 2020 Jun 25. doi:10.3389/fpls.2020.00948
- Matters, G.L. and Scandalios, J.G. (1986). Effect of the free radical-generating herbicide paraquat on the expression of the superoxide dismutase (Sod) genes in maize. *BBA - General Subjects.* 1986;882(1):29-38. doi: 10.1016/0304-4165(86)90051-6.
- McCord JM, Fridovich I. Superoxide dismutase. An enzymic function for erythrocyte hemocuprein. *J Biol Chem.* 1969;244(22):6049-6055.
- McCord JM, Fridovich I. Superoxide dismutases: you've come a long way, baby. *Antioxid Redox Signal.* 2014;20(10):1548-1549. doi:10.1089/ars.2013.5547
- McCord JM, Keele BB Jr, Fridovich I. An enzyme-based theory of obligate anaerobiosis: the physiological function of superoxide dismutase. *Proc Natl Acad Sci U S A.* 1971;68(5):1024-1027. doi:10.1073/pnas.68.5.1024

- Meyer K, Köster T, Nolte C, et al. Adaptation of iCLIP to plants determines the binding landscape of the clock-regulated RNA-binding protein AtGRP7. *Genome Biol.* 2017;18(1):204. Published 2017 Oct 31. doi:10.1186/s13059-017-1332-x
- Miernyk JA, Thelen JJ. Biochemical approaches for discovering protein-protein interactions. *Plant J.* 2008;53(4):597-609. doi:10.1111/j.1365-313X.2007.03316.x
- Mittler R. ROS Are Good. *Trends Plant Sci.* 2017;22(1):11-19. doi:10.1016/j.tplants.2016.08.002
- Moeder W, Del Pozo O, Navarre DA, Martin GB, Klessig DF. Aconitase plays a role in regulating resistance to oxidative stress and cell death in Arabidopsis and Nicotiana benthamiana. *Plant Mol Biol.* 2007;63(2):273-287. doi:10.1007/s11103-006-9087-x
- Moore B, Zhou L, Rolland F, et al. Role of the Arabidopsis glucose sensor HXK1 in nutrient, light, and hormonal signaling. *Science.* 2003;300(5617):332-336. doi:10.1126/science.1080585
- Moran PJ, Cheng Y, Cassell JL, Thompson GA. Gene expression profiling of Arabidopsis thaliana in compatible plant-aphid interactions. *Arch Insect Biochem Physiol.* 2002;51(4):182-203. doi:10.1002/arch.10064
- Mosa KA, El-Naggar M, Ramamoorthy K, et al. Copper Nanoparticles Induced Genotoxicity, Oxidative Stress, and Changes in Superoxide Dismutase (SOD) Gene Expression in Cucumber (*Cucumis sativus*) Plants. *Front Plant Sci.* 2018;9:872. Published 2018 Jul 16. doi:10.3389/fpls.2018.00872
- Munné-Bosch S. The role of alpha-tocopherol in plant stress tolerance. *J Plant Physiol.* 2005;162(7):743-748. doi:10.1016/j.jplph.2005.04.022
- Munns R, Tester M. Mechanisms of salinity tolerance. *Annu Rev Plant Biol.* 2008;59:651-681. doi:10.1146/annurev.arplant.59.032607.092911
- Nadarajah KK. ROS Homeostasis in Abiotic Stress Tolerance in Plants. *Int J Mol Sci.* 2020;21(15):5208. Published 2020 Jul 23. doi:10.3390/ijms21155208
- Nakayama T, Shinohara H, Tanaka M, Baba K, Ogawa-Ohnishi M, Matsubayashi Y. A peptide hormone required for Casparian strip diffusion barrier formation in Arabidopsis roots. *Science.* 2017;355(6322):284-286. doi:10.1126/science.aai9057

- Napoli C, Lemieux C, Jorgensen R. Introduction of a Chimeric Chalcone Synthase Gene into *Petunia* Results in Reversible Co-Suppression of Homologous Genes in trans. *Plant Cell*. 1990;2(4):279-289. doi:10.1105/tpc.2.4.279
- Neuser J, Metzen CC, Dreyer BH, et al. HBI1 Mediates the Trade-off between Growth and Immunity through Its Impact on Apoplastic ROS Homeostasis. *Cell Rep*. 2019;28(7):1670-1678.e3. doi:10.1016/j.celrep.2019.07.029
- Neves-Piestun BG, Bernstein N. Salinity-induced changes in the nutritional status of expanding cells may impact leaf growth inhibition in maize. *Funct Plant Biol*. 2005;32(2):141-152. doi:10.1071/FP04113
- Niu X, Damsz B, Kononowicz AK, Bressan RA, Hasegawa PM. NaCl-Induced Alterations in Both Cell Structure and Tissue-Specific Plasma Membrane H<sup>+</sup>-ATPase Gene Expression. *Plant Physiol*. 1996;111(3):679-686. doi:10.1104/pp.111.3.679
- Nounjan N, Nghia PT, Theerakulpisut P. Exogenous proline and trehalose promote recovery of rice seedlings from salt-stress and differentially modulate antioxidant enzymes and expression of related genes. *J Plant Physiol*. 2012;169(6):596-604. doi:10.1016/j.jplph.2012.01.004
- Ogawa, K., Kanematsu, S., and Asada, K. Intra- and extra-cellular localization of “cytosolic” CuZn-superoxide dismutase in spinach leaf and hypocotyl. *Plant and Cell Physiology*. 1996;37(6):790-799. doi: 10.1093/oxfordjournals.pcp.a029014.
- O'Malley RC, Huang SC, Song L, et al. Cistrome and Epicistrome Features Shape the Regulatory DNA Landscape [published correction appears in *Cell*. 2016 Sep 8;166(6):1598]. *Cell*. 2016;165(5):1280-1292. doi:10.1016/j.cell.2016.04.038
- Ouidir T, Jarnier F, Cosette P, Jouenne T, Hardouin J. Characterization of N-terminal protein modifications in *Pseudomonas aeruginosa* PA14. *J Proteomics*. 2015;114:214-225. doi:10.1016/j.jprot.2014.11.006
- Owusu-Ansah E, Banerjee U. Reactive oxygen species prime *Drosophila* haematopoietic progenitors for differentiation. *Nature*. 2009;461(7263):537-541. doi:10.1038/nature08313
- Ozfidan-Konakci C, Yildiztugay E, Kucukoduk M. Upregulation of antioxidant enzymes by exogenous gallic acid contributes to the amelioration in *Oryza sativa* roots exposed to salt and

- osmotic stress. *Environ Sci Pollut Res Int*. 2015;22(2):1487-1498. doi:10.1007/s11356-014-3472-9
- Park SW, Li W, Viehhauser A, et al. Cyclophilin 20-3 relays a 12-oxo-phytodienoic acid signal during stress responsive regulation of cellular redox homeostasis. *Proc Natl Acad Sci U S A*. 2013;110(23):9559-9564. doi:10.1073/pnas.1218872110
- Pasinelli P, Brown RH. Molecular biology of amyotrophic lateral sclerosis: insights from genetics. *Nat Rev Neurosci*. 2006;7(9):710-723. doi:10.1038/nrn1971
- Perl A, Perl-Treves R, Galili S, et al. Enhanced oxidative-stress defense in transgenic potato expressing tomato Cu,Zn superoxide dismutases. *Theor Appl Genet*. 1993;85(5):568-576. doi:10.1007/BF00220915
- Pertea M, Kim D, Pertea GM, Leek JT, Salzberg SL. Transcript-level expression analysis of RNA-seq experiments with HISAT, StringTie and Ballgown. *Nat Protoc*. 2016;11(9):1650-1667. doi:10.1038/nprot.2016.095
- Pesaresi P, Gardner NA, Masiero S, et al. Cytoplasmic N-terminal protein acetylation is required for efficient photosynthesis in Arabidopsis. *Plant Cell*. 2003;15(8):1817-1832. doi:10.1105/tpc.012377
- Pilon M, Ravet K, Tapken W. The biogenesis and physiological function of chloroplast superoxide dismutases. *Biochim Biophys Acta*. 2011;1807(8):989-998. doi:10.1016/j.bbabi.2010.11.002
- Pitcher LH, Zilinskas BA. Overexpression of Copper/Zinc Superoxide Dismutase in the Cytosol of Transgenic Tobacco Confers Partial Resistance to Ozone-Induced Foliar Necrosis. *Plant Physiol*. 1996;110(2):583-588. doi:10.1104/pp.110.2.583
- Proctor EA, Fee L, Tao Y, et al. Nonnative SOD1 trimer is toxic to motor neurons in a model of amyotrophic lateral sclerosis. *Proc Natl Acad Sci U S A*. 2016;113(3):614-619. doi:10.1073/pnas.1516725113
- Radakovic ZS, Anjam MS, Escobar E, et al. Arabidopsis HIPP27 is a host susceptibility gene for the beet cyst nematode *Heterodera schachtii* [published online ahead of print, 2018 Feb 22]. *Mol Plant Pathol*. 2018;19(8):1917-1928. doi:10.1111/mpp.12668

- Rajendran K, Tester M, Roy SJ. Quantifying the three main components of salinity tolerance in cereals. *Plant Cell Environ.* 2009;32(3):237-249. doi:10.1111/j.1365-3040.2008.01916.x
- Raju, T.S. Prenylation of Proteins. In *Co- and Post-Translational Modifications of Therapeutic Antibodies and Proteins*, T.S. Raju (Ed.). 2019;1:177-181. doi:10.1002/9781119053354.ch14
- Reddi AR, Culotta VC. SOD1 integrates signals from oxygen and glucose to repress respiration. *Cell.* 2013;152(1-2):224-235. doi:10.1016/j.cell.2012.11.046
- Redler RL, Wilcox KC, Proctor EA, Fee L, Caplow M, Dokholyan NV. Glutathionylation at Cys-111 induces dissociation of wild type and FALS mutant SOD1 dimers. *Biochemistry.* 2011;50(32):7057-7066. doi:10.1021/bi200614y
- Redler RL, Dokholyan NV. The complex molecular biology of amyotrophic lateral sclerosis (ALS). *Prog Mol Biol Transl Sci.* 2012;107:215-262. doi:10.1016/B978-0-12-385883-2.00002-3
- Redler RL, Fee L, Fay JM, Caplow M, Dokholyan NV. Non-native soluble oligomers of Cu/Zn superoxide dismutase (SOD1) contain a conformational epitope linked to cytotoxicity in amyotrophic lateral sclerosis (ALS). *Biochemistry.* 2014;53(14):2423-2432. doi:10.1021/bi500158w
- Rojas-Murcia N, Hématy K, Lee Y, et al. High-order mutants reveal an essential requirement for peroxidases but not laccases in Casparian strip lignification. *Proc Natl Acad Sci U S A.* 2020;117(46):29166-29177. doi:10.1073/pnas.2012728117
- Rossatto T, do Amaral MN, Benitez LC, et al. Gene expression and activity of antioxidant enzymes in rice plants, cv. BRS AG, under saline stress. *Physiol Mol Biol Plants.* 2017;23(4):865-875. doi:10.1007/s12298-017-0467-2
- Sairam, R.K., Srivastava, G.C., Agarwal, S. et al. Differences in antioxidant activity in response to salinity stress in tolerant and susceptible wheat genotypes. *Biologia Plantarum.* 2005;49(85). doi: 10.1007/s10535-005-5091-2.
- Salem K, McCormick ML, Wendlandt E, Zhan F, Goel A. Copper-zinc superoxide dismutase-mediated redox regulation of bortezomib resistance in multiple myeloma. *Redox Biol.* 2015;4:23-33. doi:10.1016/j.redox.2014.11.002



- Sarsour EH, Venkataraman S, Kalen AL, Oberley LW, Goswami PC. Manganese superoxide dismutase activity regulates transitions between quiescent and proliferative growth. *Aging Cell*. 2008;7(3):405-417. doi:10.1111/j.1474-9726.2008.00384.x
- Sato H, Takasaki H, Takahashi F, et al. *Arabidopsis thaliana* NGATHA1 transcription factor induces ABA biosynthesis by activating *NCED3* gene during dehydration stress. *Proc Natl Acad Sci U S A*. 2018;115(47):E11178-E11187. doi:10.1073/pnas.1811491115
- Schmal C, Reimann P, Staiger D. A circadian clock-regulated toggle switch explains AtGRP7 and AtGRP8 oscillations in *Arabidopsis thaliana*. *PLoS Comput Biol*. 2013;9(3):e1002986. doi:10.1371/journal.pcbi.1002986
- Schmidt R, Mieulet D, Hubberten HM, et al. Salt-responsive ERF1 regulates reactive oxygen species-dependent signaling during the initial response to salt stress in rice. *Plant Cell*. 2013;25(6):2115-2131. doi:10.1105/tpc.113.113068
- Schmidt R, Schippers JH. ROS-mediated redox signaling during cell differentiation in plants. *Biochim Biophys Acta*. 2015;1850(8):1497-1508. doi:10.1016/j.bbagen.2014.12.020
- Schütze K, Harter K, Chaban C. Bimolecular fluorescence complementation (BiFC) to study protein-protein interactions in living plant cells. *Methods Mol Biol*. 2009;479:189-202. doi:10.1007/978-1-59745-289-2\_12
- Shafi A, Chauhan R, Gill T, et al. Expression of SOD and APX genes positively regulates secondary cell wall biosynthesis and promotes plant growth and yield in *Arabidopsis* under salt stress. *Plant Mol Biol*. 2015;87(6):615-631. doi:10.1007/s11103-015-0301-6
- Shibata N, Hirano A, Kobayashi M, et al. Cu/Zn superoxide dismutase-like immunoreactivity in Lewy body-like inclusions of sporadic amyotrophic lateral sclerosis. *Neurosci Lett*. 1994;179(1-2):149-152. doi:10.1016/0304-3940(94)90956-3
- Shibata N, Asayama K, Hirano A, Kobayashi M. Immunohistochemical study on superoxide dismutases in spinal cords from autopsied patients with amyotrophic lateral sclerosis. *Dev Neurosci*. 1996;18(5-6):492-498. doi:10.1159/000111445
- Shiraya T, Mori T, Maruyama T, et al. Golgi/plastid-type manganese superoxide dismutase involved in heat-stress tolerance during grain filling of rice. *Plant Biotechnol J*. 2015;13(9):1251-1263. doi:10.1111/pbi.12314

- Sriram G, Martinez JA, McCabe ER, Liao JC, Dipple KM. Single-gene disorders: what role could moonlighting enzymes play? *Am J Hum Genet.* 2005;76(6):911-924. doi:10.1086/430799
- Stam M, Mol JNM, Kooter JM. Review Article: The Silence of Genes in Transgenic Plants, *Annals of Botany.* 1997;79(1):3-12. doi:10.1006/anbo.1996.0295
- Stark C, Breitkreutz BJ, Reguly T, Boucher L, Breitkreutz A, Tyers M. BioGRID: a general repository for interaction datasets. *Nucleic Acids Res.* 2006 Jan 1;34(Database issue):D535-9. doi: 10.1093/nar/gkj109. PMID: 16381927; PMCID: PMC1347471.
- Streller S, Wingsle G. *Pinus sylvestris* L. needles contain extracellular CuZn superoxide dismutase. *Planta.* 1994;192(2):195-201.
- Sunkar R, Kapoor A, Zhu JK. Posttranscriptional induction of two Cu/Zn superoxide dismutase genes in *Arabidopsis* is mediated by downregulation of miR398 and important for oxidative stress tolerance [published correction appears in *Plant Cell.* 2006 Sep;18(9):2415]. *Plant Cell.* 2006;18(8):2051-2065. doi:10.1105/tpc.106.041673
- Swindell WR, Huebner M, Weber AP. Transcriptional profiling of *Arabidopsis* heat shock proteins and transcription factors reveals extensive overlap between heat and non-heat stress response pathways. *BMC Genomics.* 2007;8:125. Published 2007 May 22. doi:10.1186/1471-2164-8-125
- Sytykiewicz H. Differential expression of superoxide dismutase genes in aphid-stressed maize (*Zea mays* L.) seedlings. *PLoS One.* 2014;9(4):e94847. Published 2014 Apr 10. doi:10.1371/journal.pone.0094847
- Tan BC, Joseph LM, Deng WT, et al. Molecular characterization of the *Arabidopsis* 9-cis epoxy-carotenoid dioxygenase gene family. *Plant J.* 2003;35(1):44-56. doi:10.1046/j.1365-313x.2003.01786.x
- Tan W, Zhang D, Zhou H, Zheng T, Yin Y, Lin H. Transcription factor HAT1 is a substrate of SnRK2.3 kinase and negatively regulates ABA synthesis and signaling in *Arabidopsis* responding to drought. *PLoS Genet.* 2018;14(4):e1007336. Published 2018 Apr 16. doi:10.1371/journal.pgen.1007336
- Tehseen M, Cairns N, Sherson S, Cobbett CS. Metallochaperone-like genes in *Arabidopsis thaliana*. *Metallomics.* 2010;2(8):556-564. doi:10.1039/c003484c

- Tepperman JM, Dunsmuir P. Transformed plants with elevated levels of chloroplastic SOD are not more resistant to superoxide toxicity. *Plant Mol Biol.* 1990;14(4):501-511. doi:10.1007/BF00027496
- Tilbrook J, Schilling RK, Berger B, et al. Variation in shoot tolerance mechanisms not related to ion toxicity in barley. *Funct Plant Biol.* 2017;44(12):1194-1206. doi:10.1071/FP17049
- Tran LS, Urao T, Qin F, et al. Functional analysis of AHK1/ATHK1 and cytokinin receptor histidine kinases in response to abscisic acid, drought, and salt stress in Arabidopsis. *Proc Natl Acad Sci U S A.* 2007;104(51):20623-20628. doi:10.1073/pnas.0706547105
- Tsang CK, Liu Y, Thomas J, Zhang Y, Zheng XF. Superoxide dismutase 1 acts as a nuclear transcription factor to regulate oxidative stress resistance. *Nat Commun.* 2014;5:3446. Published 2014 Mar 19. doi:10.1038/ncomms4446
- Tsang CK, Chen M, Cheng X, et al. SOD1 Phosphorylation by mTORC1 Couples Nutrient Sensing and Redox Regulation. *Mol Cell.* 2018;70(3):502-515.e8. doi:10.1016/j.molcel.2018.03.029
- Tseng MJ, Liu CW, Yiu JC. Enhanced tolerance to sulfur dioxide and salt stress of transgenic Chinese cabbage plants expressing both superoxide dismutase and catalase in chloroplasts. *Plant Physiol Biochem.* 2007;45(10-11):822-833. doi:10.1016/j.plaphy.2007.07.011
- Tsukagoshi H, Busch W, Benfey PN. Transcriptional regulation of ROS controls transition from proliferation to differentiation in the root. *Cell.* 2010;143(4):606-616. doi:10.1016/j.cell.2010.10.020
- Tsuzuki M, Futagami K, Shimamura M, et al. An Early Arising Role of the MicroRNA156/529-SPL Module in Reproductive Development Revealed by the Liverwort *Marchantia polymorpha*. *Curr Biol.* 2019;29(19):3307-3314.e5. doi:10.1016/j.cub.2019.07.084
- Turek I, Irving H. Moonlighting Proteins Shine New Light on Molecular Signaling Niches. *Int J Mol Sci.* 2021;22(3):1367. Published 2021 Jan 29. doi:10.3390/ijms22031367
- Ueda Y, Uehara N, Sasaki H, Kobayashi K, Yamakawa T. Impacts of acute ozone stress on superoxide dismutase (SOD) expression and reactive oxygen species (ROS) formation in rice leaves. *Plant Physiol Biochem.* 2013;70:396-402. doi:10.1016/j.plaphy.2013.06.009

Vroemen CW, Mordhorst AP, Albrecht C, Kwaaitaal MA, de Vries SC. The CUP-SHAPED COTYLEDON3 gene is required for boundary and shoot meristem formation in Arabidopsis. *Plant Cell*. 2003;15(7):1563-1577. doi:10.1105/tpc.012203

Wan C, Borgeson B, Phanse S, et al. Panorama of ancient metazoan macromolecular complexes. *Nature*. 2015;525(7569):339-344. doi:10.1038/nature14877

Wang T, Tohge T, Ivakov A, et al. Salt-Related MYB1 Coordinates Abscisic Acid Biosynthesis and Signaling during Salt Stress in Arabidopsis. *Plant Physiol*. 2015;169(2):1027-1041. doi:10.1104/pp.15.00962

(a) Wang W, Xia MX, Chen J, Yuan R, Deng FN, Shen FF. Gene Expression Characteristics and Regulation Mechanisms of Superoxide Dismutase and Its Physiological Roles in Plants under Stress. *Biochemistry (Mosc)*. 2016;81(5):465-480. doi:10.1134/S0006297916050047

(b) Wang X, Zhang H, Gao Y, Zhang W. Characterization of Cu/Zn-SOD enzyme activities and gene expression in soybean under low nitrogen stress. *J Sci Food Agric*. 2016;96(8):2692-2697. doi:10.1002/jsfa.7387

(c) Wang Z, Wang Y, Kohalmi SE, Amyot L, Hannoufa A. SQUAMOSA PROMOTER BINDING PROTEIN-LIKE 2 controls floral organ development and plant fertility by activating ASYMMETRIC LEAVES 2 in Arabidopsis thaliana. *Plant Mol Biol*. 2016;92(6):661-674. doi:10.1007/s11103-016-0536-x

(d) Wang M, Toda K, Maeda HA. Biochemical properties and subcellular localization of tyrosine aminotransferases in Arabidopsis thaliana. *Phytochemistry*. 2016;132:16-25. doi:10.1016/j.phytochem.2016.09.007

Wang W, Zhang X, Deng F, Yuan R, Shen F. Genome-wide characterization and expression analyses of superoxide dismutase (SOD) genes in Gossypium hirsutum. *BMC Genomics*. 2017;18(1):376. Published 2017 May 12. doi:10.1186/s12864-017-3768-5

Wang M, Toda K, Block A, Maeda HA. TAT1 and TAT2 tyrosine aminotransferases have both distinct and shared functions in tyrosine metabolism and degradation in Arabidopsis thaliana. *J Biol Chem*. 2019;294(10):3563-3576. doi:10.1074/jbc.RA118.006539

- Wang X, Zhang H, Sapio R, et al. SOD1 regulates ribosome biogenesis in KRAS mutant non-small cell lung cancer. *Nat Commun.* 2021;12(1):2259. Published 2021 Apr 15. doi:10.1038/s41467-021-22480-x
- Waszczak C, Carmody M, Kangasjärvi J. Reactive Oxygen Species in Plant Signaling. *Annu Rev Plant Biol.* 2018;69:209-236. doi:10.1146/annurev-arplant-042817-040322
- Weis BL, Kovacevic J, Missbach S, Schleiff E. Plant-Specific Features of Ribosome Biogenesis. *Trends Plant Sci.* 2015;20(11):729-740. doi:10.1016/j.tplants.2015.07.003
- Wenjing W, Chen Q, Singh PK, Huang Y, Pei D. CRISPR/Cas9 edited *HSFA6a* and *HSFA6b* of *Arabidopsis thaliana* offers ABA and osmotic stress insensitivity by modulation of ROS homeostasis. *Plant Signal Behav.* 2020;15(12):1816321. doi:10.1080/15592324.2020.1816321
- West G, Inzé D, Beemster GT. Cell cycle modulation in the response of the primary root of *Arabidopsis* to salt stress. *Plant Physiol.* 2004;135(2):1050-1058. doi:10.1104/pp.104.040022
- Wilcox KC, Zhou L, Jordon JK, et al. Modifications of superoxide dismutase (SOD1) in human erythrocytes: a possible role in amyotrophic lateral sclerosis. *J Biol Chem.* 2009;284(20):13940-13947. doi:10.1074/jbc.M809687200
- Wu FH, Shen SC, Lee LY, Lee SH, Chan MT, Lin CS. Tape-*Arabidopsis* Sandwich - a simpler *Arabidopsis* protoplast isolation method. *Plant Methods.* 2009;5:16. Published 2009 Nov 24. doi:10.1186/1746-4811-5-16
- Xu XM, Lin H, Maple J, et al. The *Arabidopsis* DJ-1a protein confers stress protection through cytosolic SOD activation. *J Cell Sci.* 2010;123(Pt 10):1644-1651. doi:10.1242/jcs.063222
- Xing Y, Cao Q, Zhang Q, Qin L, Jia W, Zhang J. MKK5 regulates high light-induced gene expression of Cu/Zn superoxide dismutase 1 and 2 in *Arabidopsis*. *Plant Cell Physiol.* 2013;54(7):1217-1227. doi:10.1093/pcp/pct072
- Xing S, Wallmeroth N, Berendzen KW, Grefen C. Techniques for the Analysis of Protein-Protein Interactions in Vivo. *Plant Physiol.* 2016;171(2):727-758. doi:10.1104/pp.16.00470
- Xu J, Yang J, Duan X, Jiang Y, Zhang P. Increased expression of native cytosolic Cu/Zn superoxide dismutase and ascorbate peroxidase improves tolerance to oxidative and chilling

- stresses in cassava (*Manihot esculenta* Crantz). *BMC Plant Biol.* 2014;14:208. Published 2014 Aug 5. doi:10.1186/s12870-014-0208-4
- Xu F, Huang Y, Li L, et al. Two N-terminal acetyltransferases antagonistically regulate the stability of a nod-like receptor in *Arabidopsis*. *Plant Cell.* 2015;27(5):1547-1562. doi:10.1105/tpc.15.00173
- Xu M, Hu T, Zhao J, et al. Developmental Functions of miR156-Regulated SQUAMOSA PROMOTER BINDING PROTEIN-LIKE (SPL) Genes in *Arabidopsis thaliana*. *PLoS Genet.* 2016;12(8):e1006263. Published 2016 Aug 19. doi:10.1371/journal.pgen.1006263
- Xu J, Su X, Burley SK, Zheng XFS. Nuclear SOD1 in Growth Control, Oxidative Stress Response, Amyotrophic Lateral Sclerosis, and Cancer. *Antioxidants (Basel).* 2022;11(2):427. Published 2022 Feb 21. doi:10.3390/antiox11020427
- Yalovsky S, Rodr Guez-Concepción M, Gruissem W. Lipid modifications of proteins - slipping in and out of membranes. *Trends Plant Sci.* 1999;4(11):439-445. doi:10.1016/s1360-1385(99)01492-2
- Yamada K, Nagano AJ, Nishina M, Hara-Nishimura I, Nishimura M. NAI2 is an endoplasmic reticulum body component that enables ER body formation in *Arabidopsis thaliana*. *Plant Cell.* 2008;20(9):2529-2540. doi:10.1105/tpc.108.059345
- Zeng J, Dong Z, Wu H, Tian Z, Zhao Z. Redox regulation of plant stem cell fate. *EMBO J.* 2017;36(19):2844-2855. doi:10.15252/embj.201695955
- Zhang Y, Primavesi LF, Jhurrea D, et al. Inhibition of SNF1-related protein kinase1 activity and regulation of metabolic pathways by trehalose-6-phosphate. *Plant Physiol.* 2009;149(4):1860-1871. doi:10.1104/pp.108.133934
- Zhang, W.B., Li, N.N., Qi, F. et al. Isolation and expression analysis of Cu/Zn superoxide dismutase genes from three *Caragana* species. *Russian Journal of Plant Physiology.* 2014;61:656-663. doi: 10.1134/S1021443714050185.
- Zhong Y, Wang J, Henderson MJ, et al. Nuclear export of misfolded SOD1 mediated by a normally buried NES-like sequence reduces proteotoxicity in the nucleus. *Elife.* 2017;6:e23759. Published 2017 May 2. doi:10.7554/eLife.23759

Zhou Y, Hu L, Wu H, Jiang L, Liu S. Genome-Wide Identification and Transcriptional Expression Analysis of Cucumber Superoxide Dismutase (SOD) Family in Response to Various Abiotic Stresses. *Int J Genomics*. 2017;2017:7243973. doi:10.1155/2017/7243973

Zschiesche W, Barth O, Daniel K, Böhme S, Rausche J, Humbeck K. The zinc-binding nuclear protein HIPP3 acts as an upstream regulator of the salicylate-dependent plant immunity pathway and of flowering time in *Arabidopsis thaliana*. *New Phytol*. 2015;207(4):1084-1096. doi:10.1111/nph.13419

## 8 CURRICULUM VITAE

### **Bernd Heinrich Dreyer, M. Sc.**

Born in Stadt Haren (Ems), 22.06.1994

#### **School:**

2000 – 2004 Grundschule St. Clemens (Wesuwe)

2004 – 2012 Gymnasium Marianum Meppen

**(Graduation: Abitur)**

#### **Education:**

2012 – 2015 **Bachelor's Degree** in Biology at the RWTH Aachen

**(Graduation: Bachelor of Science, Biology)**

Bachelor's thesis: "Ist die Rolle der Superoxide Dismutase als Transkriptionsfaktor konserviert in Pflanzen? "

2015 – 2018 **Master's Degree** in Biology at the RWTH Aachen

**(Graduation: Master of Science, Biology)**

Master's thesis: "The moonlighting function of superoxide dismutase in plants: Transcriptional complex formation with HIP20 proteins".

Since 2018 **PhD student** at the RWTH Aachen (until 2019) and the IPK Gatersleben



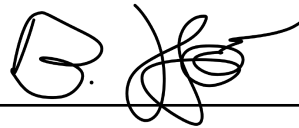
## 9 EIDESTATTLICHE ERKLÄRUNG/ DECLARATION UNDER OATH

Ich erkläre an Eides statt, dass ich die Arbeit selbstständig und ohne fremde Hilfe verfasst, keine anderen als die von mir angegebenen Quellen und Hilfsmittel benutzt und die den benutzten Werken wörtlich oder inhaltlich entnommenen Stellen als solche kenntlich gemacht habe.

I declare under the penalty of perjury that this thesis is my own work entirely and has been written without any help from other people. I used only the sources mentioned and included all the citations correctly both in word or content.

14.07.2023, Haren (Ems)

Datum/date



Unterschrift des Antragstellers/ Signature of the applicant


### **Erklärung über bestehende Vorstrafen und anhängige Ermittlungsverfahren/ Declaration concerning criminal record and pending investigations**

Hiermit erkläre ich, dass ich weder vorbestraft bin noch, dass gegen mich Ermittlungsverfahren anhängig sind.

I hereby declare that I have no criminal record and that no preliminary investigations are pending against me.

14.07.2023, Haren (Ems)

Datum/date



Unterschrift des Antragstellers/ Signature of the applicant

## 10 APPENDIX

### 10.1 Supplemental figures for Chapter 1



**Figure 29:** Growth phenotype of transgenic CSD1 plants grown under short day conditions. The phenotype of Col-0, *csd1-3* and *OxCSD1#2* plants which were grown for 8 weeks under short day conditions is shown.

## AT1G08830 – CSD1

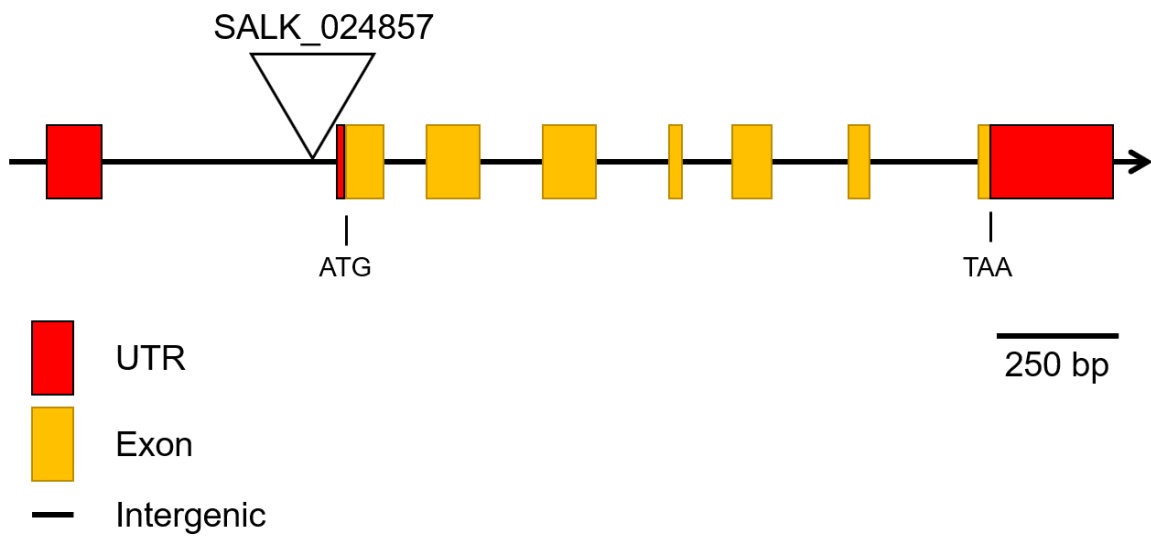


**Figure 30:** T-DNA insertion in genomic locus of AT1G08830 - CSD1. The position of the T-DNA insertion of line SALK\_024857 (*pROK2*) in the genomic locus of CSD1 is shown. A full-length coding sequence of CSD1 can still be formed.

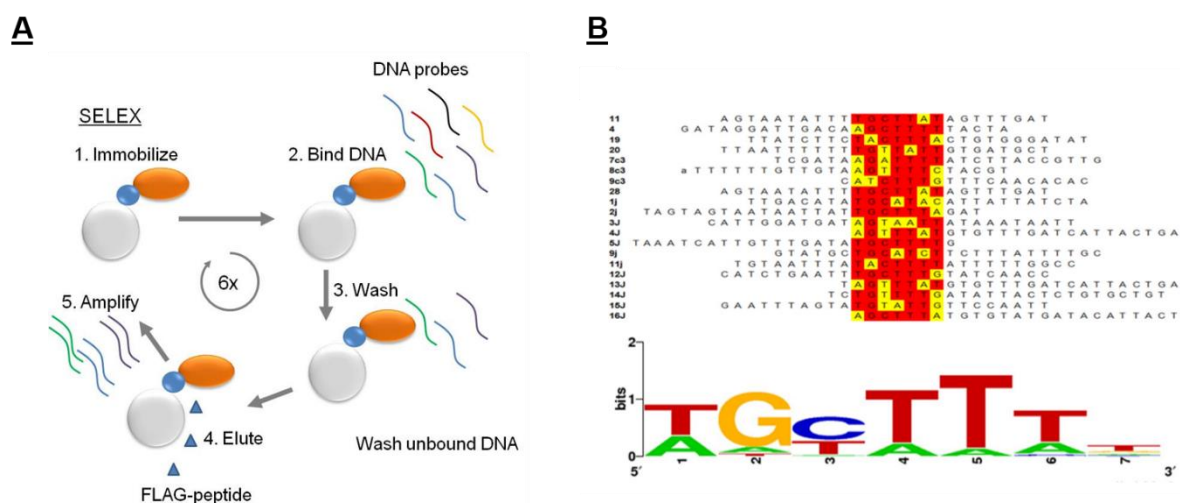


**Figure 31:** Overview of the systematic evolution of ligands by exponential enrichment (SELEX) experiment. **(A)** The individual steps of the SELEX experiment which include the immobilisation, the binding, the washing, the elution and the amplification step are visualised. These steps were performed six rounds and after the amplification step the sequences were cloned and sequenced. **(B)** The sequences derived after the amplification were aligned and the consensus sequence TGCTTT was identified.

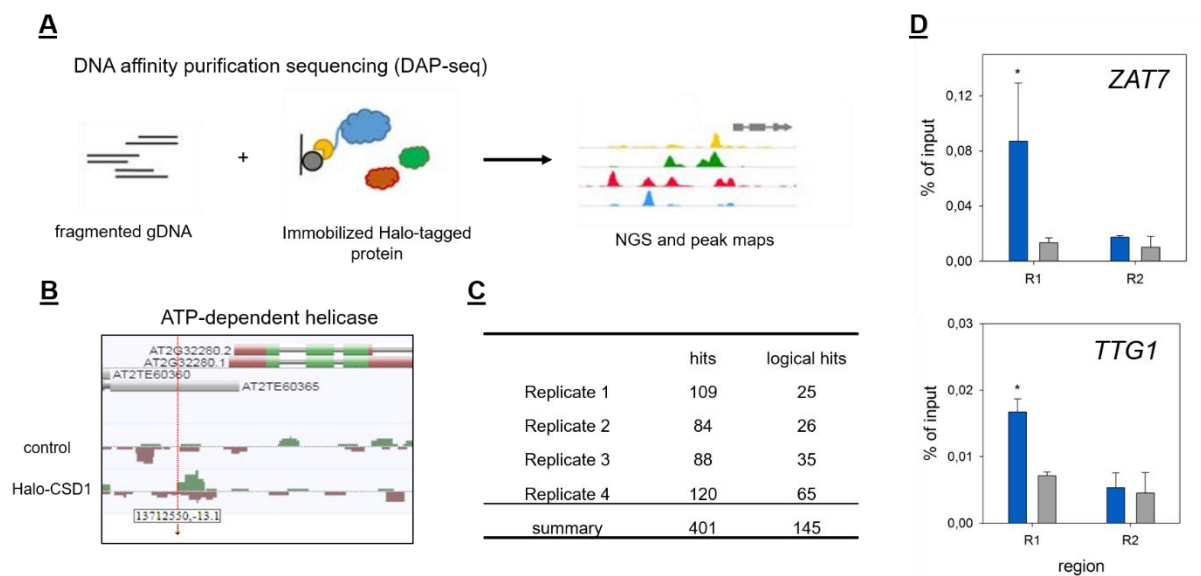


**Figure 32:** DNA-affinity purification sequencing (DAP-seq) and ChIP-qPCR confirmation experiment. The DAP-seq experiment was performed in collaboration with Anna Bartlett, Carol Huang and Joseph Ecker from the Salk Institute. **(A)** The schematic procedure of the DAP-seq analysis is visualised. Adapted from Bartlett *et al.*, 2017. **(B)** A peak visualised in a genome browser (Carol Huang) is shown. In green and red, the enrichment of the sequence is highlighted. Here, the peak is linked to an ATP-dependent helicase (AT2G32260) in Arabidopsis. **(C)** The number of peaks linked to the Arabidopsis genome is shown. Logical hits are defined as those sequences that can be linked to upstream or downstream sequences of genes. In total, 145 logical hits were identified. **(D)** A ChIP-qPCR experiment was performed for the *ZAT7* and *TTG1* gene which were linked to logical hits of the DAP-seq experiment. The enrichment of the sequence is visualised as percentage of the input sequence. Each data point represents at least three technical replicates and the statistical difference was determined by a Student's t-test ( $p < 0.05$ ).

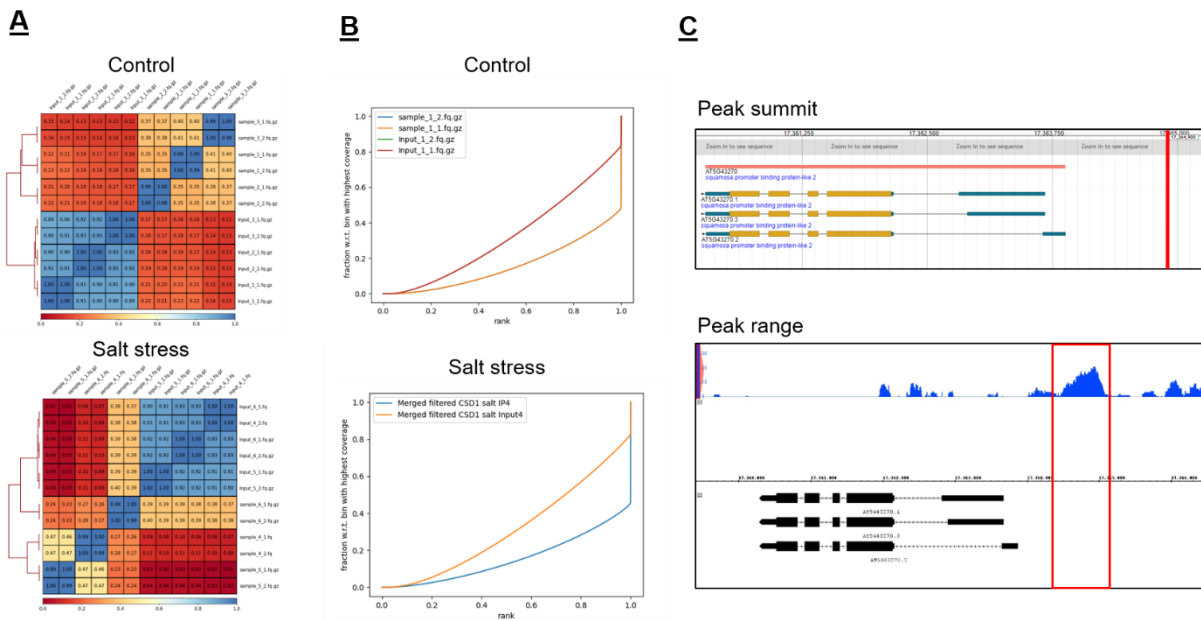


**Figure 33:** ChIP-seq analysis of untreated and treated (30 minutes, 150 mM NaCl) samples. **(A)** The correlation between the 12 samples (input and immunoprecipitated (IP)) is shown. In the upper part the overlap for the 12 input and IP control samples is shown, and in the lower panel the overlap for the salt stress samples. **(B)** A bin analysis for the input and IP samples is shown highlighting the specific enrichment in the IP samples. **(C)** As example for a ChIP-seq peak, the peak in the *SPL2* promoter is shown. In the lower panel, the blue graph indicates the location and intensity of the peak.

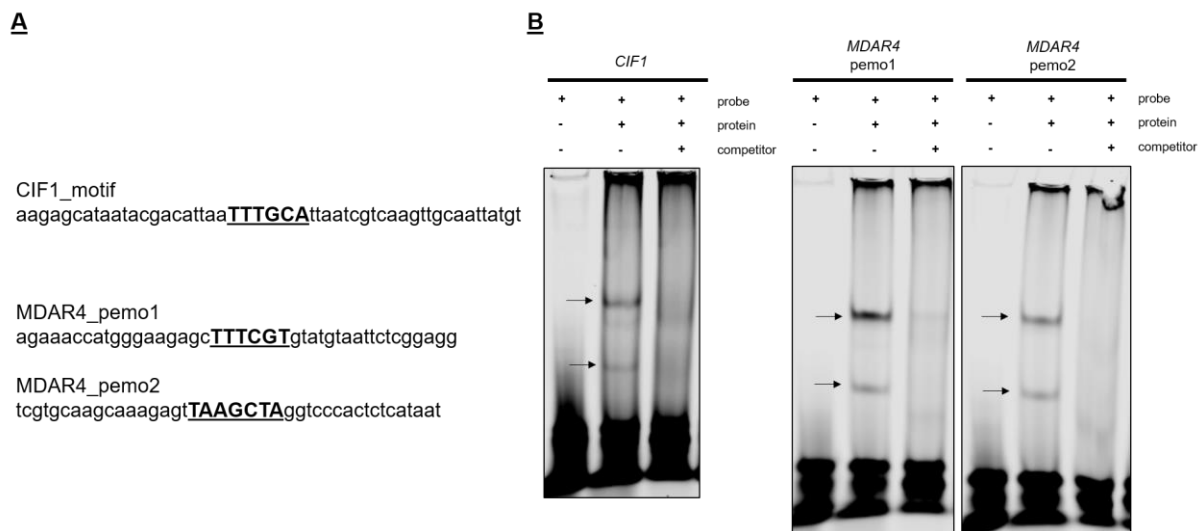


**Figure 34:** CSD1 binds to a sequence in the *CIF1* and *MDAR4* promoter. (A) Two ChIP-seq peaks were related to the *CIF1* and *MDAR4* promoter. The promoter sequences with a putative CSD1-binding motif are shown and used for the EMSA in Panel B. (B) The EMSA experiment is shown after visualisation. Band shifts show retention of the labeled probes and indicate the binding of CSD1 to these sequences, both as dimer and monomer. The less intense shift for *CIF1* indicates a weaker binding. 2000 ng of CSD1 protein was used. The competitor was used in 200-fold excess. The gel was analysed with a LI-COR Odyssey device.

## 10.2 Supplemental figures for Chapter 2

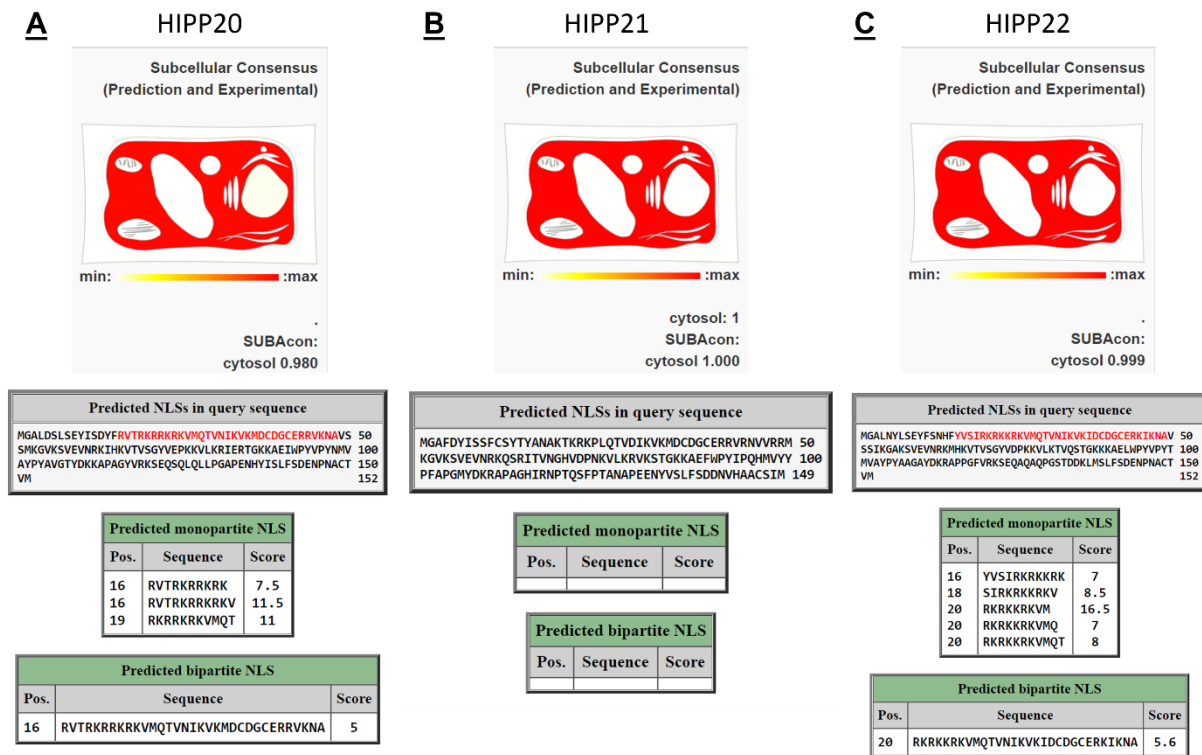


**Figure 35: Subcellular localisation and NLS of HIPP20, HIPP21 and HIPP22.** The predicted subcellular localisation and the predicted presence of a nuclear localisation signal (NLS) of the HIPP20 (A), HIPP21 (B) and HIPP22 (C) protein is shown. The SUBA4 database was used for the subcellular localisation (<https://suba.live>). To predict the presence of an NLS, the cNLS mapper was used ([https://nls-mapper.iab.keio.ac.jp/cgi-bin/NLS\\_Mapper\\_form.cgi](https://nls-mapper.iab.keio.ac.jp/cgi-bin/NLS_Mapper_form.cgi)).



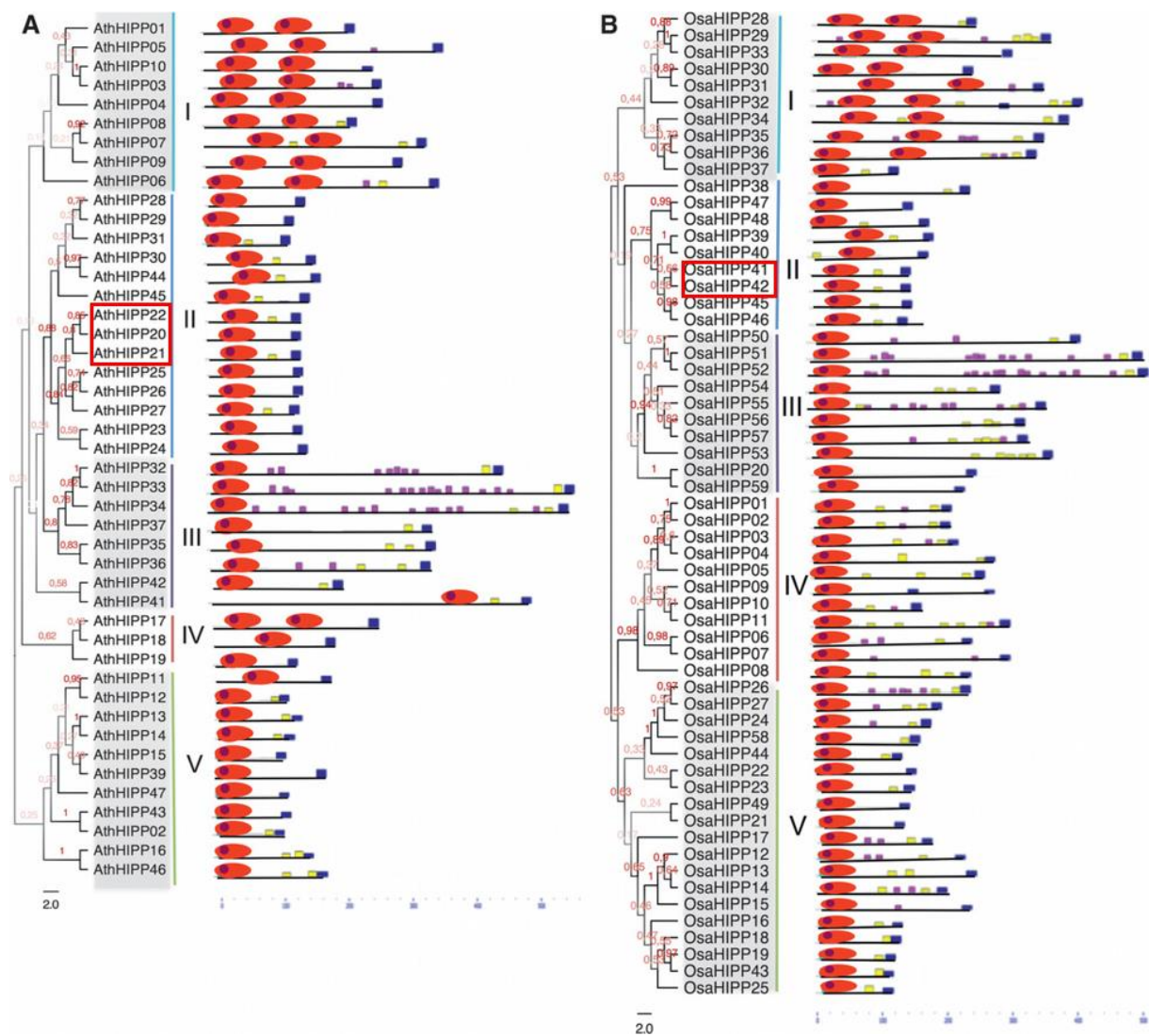


**Figure 36:** Phylogenetic tree of the HIPP protein family in *Arabidopsis* (A) and *Oryza sativa* (B). The figure was adapted from de Abreu-Neto *et al.*, 2013.

### 10.3 Supplementary data

The supplementary data is either available on the USB stick together with the electronic version of the PhD thesis or after publishing on the website of the Martin-Luther University.

**Supplementary data 1:** All identified interactors of CSD1 and CSD2. Filtered for the p-value (0.05) and the presence in >50% of the replicates.

**Supplementary data 2:** Interactor dataset of CSD1 and CSD2. After being filtered by the p-value and the presence in more than 50% of the replicate (2 out of 4), the interactors were sorted based on the conditions they were detected.